The Pennsylvania State University

The Graduate School

The College of Agricultural Sciences

EXCESS FEED CONSUMPTION DURING GROWTH CAUSES CHANGES IN EXPRESSION OF STEROIDOGENIC ENZYMES AND NEUROACTIVE RECEPTORS IN OVARIES OF PREPUBESCENT BROILER-BREEDER HENS

A Thesis in

Animal Science

by

Kate Lordan Anthony

Submitted in Partial Fulfillment
of the Requirements
for the Degree of

Master of Science

May 2017

The thesis of Kate Lordan Anthony was reviewed and approved* by the following:

Francisco Javier Diaz
Associate Professor of Reproductive Biology
Thesis Advisor

Alan Leslie Johnson
Walther H. Ott Professor in Avian Biology
Professor of Animal Science

Ramesh Ramachandran
Professor of Molecular Endocrinology

Terry D. Etherton
Distinguished Professor of Animal Nutrition
Head of the Department of Animal Science

*Signatures are on file in the Graduate School

ABSTRACT

Modern broiler chicken lines have been selected for high growth rate and increased feed consumption. The fast growth of the broiler chick is offset by poor breeding performance of the broiler breeders (parent lines). In the adult broiler breeder hen, excessive feed consumption causes severe ovarian dysfunction and results in superfluous follicle growth and double preovulatory hierarchies, leading to reduced fertility and egg production. Modern management practices involve severe restriction of feed to help minimize reproductive dysfunction and maintain productivity. However, little is known about the effects of overfeeding or feed restriction on ovarian function in the prepubescent hen. The objective of this thesis was to identify differences in morphology, gene and protein expression within the ovarian cortex that distinguish the follicular growth environments of full-fed (FF) and restricted-fed (RF) prepubescent hens. Current work was performed on ovaries of 10-and 16-week-old-hens. Results showed, at both ages, heavier ovaries in FF hens, with a shift towards greater proportion of larger (>0.3 mm) cortical follicles and fewer smaller (<0.1 mm) cortical follicles as compared to RF. Expression of proteins and mRNA of factors known to be involved in follicular development were measured. Increased follicular development seen in FF was not associated with changes in mRNA of TGF-β ligands (*AMH, BMP6, BMP15,* or *GDF9*) or protein of their signaling transcription factors (SMAD1/5/8 or SMAD2/3). Nor were there differences in immunolocalization of the modified histone proteins associated with transcription activity; trimethylated histone H3K4, acetylated histone H3K9, or trimethylated histone H3K27. However, serine phosphorylation, which localized to the oocyte cytoplasm, revealed vesicle-like structures in the RF hens, while

tyrosine phosphorylation localized more prominently to the surface of granulosa cells from RF hens. Exploration of possible pathways and genetic markers associated with follicle growth using microarray analysis of the ovarian cortex transcriptome of the 16-week-old hens uncovered differentially expressed genes (DEG) involved in steroidogenesis and neuroactive ligand-receptor interaction. Transcripts with greater abundance in the full-fed hens included those involved in cholesterol biosynthesis (*HMGCR* and *DHCR24*) and transport (*STAR* and *STARD4*), steroid biosynthesis (*CYP11A1, HSD3β2, HSD17β1* and *CYP19A1*), and G protein-coupled receptor *VIPR2*. Two transcripts with less abundance in FF at 16 weeks were adenylyl cyclase inhibitors *CHRM5* and *DRD4*. This pattern was also seen at 10 weeks but with less DEG represented in each group. DEG with greater abundance at 10 weeks included *DHCR24*, *STAR* and *STARD4*, *CYP11A1* and *CYP19A1*, as well as *VIPR2*. One adenylyl cyclase inhibitor, *DRD4*, had less abundance in FF at 10 weeks. Vasoactive intestinal polypeptide (VIP) and its receptors (VIPR1 and VIPR2) had become factors-of-interest in this thesis because of their role in steroidogenesis in mammalian ovaries and in larger follicles of adult hens. But little is known about the role of VIP in the chicken cortex. The final group of experiments in this thesis focused on cortical follicle culture to test effects of VIP on *STAR* mRNA expression. The results showed that *STAR* abundance was maintained in follicles treated with VIP equal to that of fresh samples, but follicles cultured with no steroidogenic activator could not maintain *STAR*. Unexpectedly, abundance of *VIPR2* also was not maintained, while that of *VIPR1* was 5 fold higher than that of fresh in the VIP-treated follicles. The roles of these receptors within the cortex have not been determined, and most likely the expression of

each changes as follicles develop, suggesting greater expression of *VIPR1* during proliferation and *VIPR2* during differentiation. But taken together, our observations suggest that excessive energy intake leads to increased follicle growth and abundance of transcripts involved in steroid biosynthesis and neuronal activity in ovaries of immature broiler breeder hens and that VIP promotes activation of steroidogenic transcripts in cortical follicles.

TABLE OF CONTENTS

LIST OF FIGURES

LIST OF TABLES

ACKNOWLEDGEMENTS

The time spent on this project, working and learning with the folks in Animal Science has been thoroughly enjoyable. It took me a long time to come to the decision to commit to earning a Master's Degree, but when I became part of this department, realized I was with the best group of people I have ever worked with, I knew I could do it. I will start with my advisor, Dr. Francisco Diaz. Thank you for your patience, and generosity with your time, knowledge and resources, and realistic goals. Thank you for supporting my decision to become a student while working as a technician. And thank you for being such a nice person to work with.

Extend that to my committee members; Dr. Alan Johnson, you made me realize I have a lot to learn about VIP and its receptors, and Dr. Ramesh Ramachandran you kept me focused-what can I do in the amount of time I have. I am grateful for your extensive knowledge of all things avian and for always being available when I have a question.

Funding to allow me to pursue this degree was generously provided by Dr. Terry Etherton and the Animal Science Department.

To my supportive and positive lab mates, Xi Tian and Tian Sun, who have graduated and are off becoming famous in their own right, and James Hester who is still building his knowledge foundation but will be successful no matter what he does. I'm excited for all of you and all that you have ahead.

Maria Horvat-Gordon, my exercise buddy. Getting the blood moving and clearing my brain for an hour absolutely improved my productivity.

Kahina Ghanem, my number one sounding board, I so enjoyed talking through concepts and pathways and ideas with you. You helped clear away the fog. I especially appreciated your enthusiasm and interest in the project.

Special thanks to Jill Hadley, who took care of the broiler breeder hens in PERC for me, wrestling with them weekly, calculating amount of feed. Thank you Jill! I would not have been able to do my thesis on the hens. And would not have learned about and appreciated these fascinating creatures...

Scott Kephart and Dave Witherite, your help and consideration at sacrifice time made the collecting of samples as smooth as possible for everyone.

Processing of the microarray by Dr. Craig Praul at the Penn State Genomics Core Facility produced the bulk of data in this thesis and pointed to new areas of research in the ovarian cortex.

I want to thank the collective group of energetic, enthusiastic students and the dedicated, generous, helpful, encouraging faculty that have pushed me out of my comfort zone and let me realize how much fun learning can be.

Two more thanks I have saved for last. One is to my husband, Craig. You know that the idea of pursuing this degree would never have been a gleam in my eye if not for your support and encouragement. You gave me the confidence to start and to finish this project.

The last thanks go to the chickens. They made the ultimate sacrifice so that we may learn a bit more about ovarian physiology.

I have learned so much from all of you and have become a better person for knowing you.

Chapter 1. Review of the Literature

1. Ovarian Development

The ovary is composed of cortex (which contains follicles) and medulla (which contains nerves and blood vessels) (Gilbert 1971), both of which are enclosed within stroma, tissue that makes up the bulk of the ovary (King 2013). The follicle is the functional unit specific to ovaries (reviewed in Lebbe and Woodruff 2013). Each follicle consists of an oocyte and supporting somatic cells (granulosa and theca), all surrounded by vascularized connective tissue (Hummel et al. 2004). Follicle growth and development is a continuous process marked by tremendous changes in size, first within the cortex (Ginsburg 1994; Leghari et al. 2015; Nitta et al. 1993), then after emergence from the cortex at puberty (Johnson et al. 2002; Gilbert et al. 1983). Vast changes in ability to produce steroids are also apparent as follicles develop, with emphasis on estrogen within the cortex and progestins after emergence (Nitta et al.1991; Nitta et al. 1993). Much of the mechanisms controlling follicle growth are still unknown. This project examined effects of excess feed on gene expression in ovaries of prepubertal broiler breeder hens and identified a role for vasoactive intestinal polypeptide in promoting steroidogenesis in cortical follicles.

a) Embryonic gonadal development

Progenitors of sperm or ovum are primordial germ cells (PGC) which develop very early in embryonic life (within two of days of incubation) in the yolk sac which is outside the embryo (Ginsburg 1994). PGCs migrate to the embryo through the

bloodstream (de Melo Bernardo et al. 2012), colonizing gonadal ridges asymmetrically, favoring the left side in both males and females (Nakamura et al. 2007). But in developing female embryos, gonadal asymmetry continues. At about embryonic day 10, the left ovary develops a cortex-like area rich in proliferating germ cells and a medulla-like area that contains few, less developed, germ cells. In contrast, the right gonad fails to form a cortex and is only composed of medulla-like tissue (Ukeshima and Fujimoto 1991). This distinction between the left and right ovary has been linked to differential cascades of gene expression (Ishimaru et al. 2008). Germ cells enter into meiosis through actions of retinoic acid (Yu et al. 2013). In the cortex of the left ovary, at about embryonic day 12, a meiotic wave occurs, beginning centrally and extending to extremities, so that just prior to hatching, germ cells in the cortex center are in a more advanced meiotic stage of Prophase I, that is zygotene/pachytene (homologous chromosomes fully synapse), versus early leptotene stage (no pairing) for germ cells at cortical extremities (de Melo Bernardo et al. 2015). At hatching, only the left ovary is functioning; the right gonad remains rudimentary (Smith and Sinclair 2004).

b) Follicle assembly and activation

Two essential processes, assembly and activation of primordial follicles, determine number of follicles available to a female in her reproductive lifetime and are critical to her reproductive success (Kezele et al. 2002). In humans, great variability exists in age at which a woman can become pregnant solely based on ovarian reserve (Broekmans et al. 1998). Mechanisms governing these processes are not known in chickens but have been well studied in mammals. In the first process, follicular

assembly, developing germ cells transition into oocytes; each germ cell is enclosed in a layer of granulosa cells (supporting steroidogenic somatic cells) to form primordial follicles (Kezele and Skinner 2003; Skinner 2005; Pepling 2012). Success of follicle assembly relies on coordination of many factors. Those involved in promoting follicle assembly include two growth factors acting through receptor tyrosine kinases; KitL (kit ligand)/ SCF (stem cell factor) which affects PGC migration and proliferation (Huang et al. 1993; Parrott and Skinner 1999), and NGF (nerve growth factor), a neurotropin involved in somatic cell organization of the follicle (Dissen et al. 2001). Factors that act as inhibitors in the procedure (by affecting rate of assembly) include hormones progesterone (Kezele and Skinner 2003) and anti-mullerian hormone (AMH) (Nilsson et al. 2011). The second process, activation, is the transition from primordial to primary follicles, known as initiation of folliculogenesis (Abir et al. 2006). Again, little is known in chickens regarding signals that activate follicles and why only some follicles activate while others remain quiescent in avian species. In mammals, the PI3K pathway controls follicle activation of primordial follicles (reviewed in Liu et al. 2006). In rodents, primordial follicle activation occurs via suppression of oocyte-specific transcription factor Foxo3 through PTEN-PI3K-Akt signaling (Castrillon et al. 2003; Reddy et al. 2005; John et al. 2008). Both PTEN and Foxo3 inhibit follicle activation in mice (John et al. 2008). Knocking out either PTEN (Reddy et al. 2008) or Foxo3 (Reddy et al. 2005) will similarly result in global follicle activation of primordial follicles and lead to premature ovarian failure. A known activator of primordial follicles in mammals is VIP (Chen et al. 2013) but the mechanism is not fully understood. VIP, a neurotransmitter, signals through a cyclic AMP-dependent pathway (Davoren and Hsueh 1985) and can increase cAMP

production (Heindell et al. 1996). A target of VIP may be KitL (kit ligand) because cAMP can promote synthesis of KitL mRNA in mouse granulosa cells (Packer et al. 1994) and VIP promotes KitL mRNA expression in neonatal rat ovaries (Chen et al. 2013). KitL is able to initiate activation of the PI3K-Akt pathway when bound to its cell-surface receptor in cultured rodent oocytes (Reddy et al. 2005). George and Ojeda (1987) demonstrated that VIP, through induction of KitL, may also promote synthesis of aromatase enzyme (CYP19) in cultured neonatal rat ovaries during primordial follicle development, which may increase estrogen production that may be important for follicle growth (Reiter et al. 1972). Problems associated with the short reproductive life observed in broiler breeder hens, relative to that of layers, may initiate during these very early processes and certainly requires future study.

c) Cortical follicle development

Primordial follicles are the basic unit in the ovary of neonatal chicks (Leghari et al. 2015), and can remain quiescent for months to years (reviewed in Johnson 2015), but upon activation (release of inhibition) begin to grow and develop, changing remarkably. First stage of activation is marked by formation of a theca cell layer (Johnson and Woods 2007). Theca cells (supporting steroidogenic somatic cells) originate from interfollicular stroma. Stromal cells make up much of ovarian connective tissue (King 2013) and those associated with growing follicles gain capacity to produce steroids (Boucek and Savard 1970; King 2013). Several proteins, some still unknown, are secreted from granulosa cells of growing follicles into the surrounding stroma, triggering differentiation of local unspecialized mesenchymal cells into theca cells

(Magoffin and Magarelli 1995). Stages of follicle development are not as well-defined in avian as they are in mammalian ovaries. Within the cortex, follicles maintain a continuous size distribution of <0.1 mm (before activation) to ~1 mm when they begin to emerge at puberty (Diaz et al. 2011) (Figure 1.1). But as they evolve within the cortex, follicles are also identified by increased development of somatic (granulosa and theca) cells surrounding the growing oocyte (Nitta et al. 1993). Granulosa cells change shape from flattened to cuboidal, and become surrounded by a single, then double theca layer (interna and externa). The theca layer, particularly the theca interna, contains blood vessels and neural tissue as well as steroidogenic interstitial cells (Nitta et al. 1991). Successful survival and growth of the follicle rely on mutual support of these somatic cells, for example, through secretion of paracrine and autocrine factors such as EGF and TGFα produced in theca that stimulate granulosa cell proliferation (Peddie et al. 1994). Significant changes in transcript abundance are evident as follicles grow within the cortex. Abundance of transcripts encoding steroidogenic enzymes such as STAR, CYP11A1, HSD3β and CYP19 increased 15-30 fold in 1 mm follicles compared to 0.5 mm follicles, while mRNA for KitL increased 3 fold (Diaz et al. 2011). Thus this early stage of follicular development is marked by likely increases in local steroidogenic capacity. These observations are in agreement with previous studies in birds showing significant expression of *HSD3β, CYP11A1* and *CYP19* mRNA in theca/interstitial cells of cortical follicles ~1 mm in diameter (Nitta et al. 1991, 1993).

d) Follicle development after emerging from cortex

In the pubertal avian ovary, follicles begin to emerge from the cortex at ~1 mm in diameter. At this time follicles develop a stalk to accommodate blood vessels and nerves necessary to sustain the phenomenal growth and development until ovulation, when the follicle has reached a diameter of >40 mm (Johnson 1999) (Figure 1.1). As follicles grow, they are arbitrarily characterized by size (continuous distribution from ~1 to >40 mm), and yolk color (white or yellow) into several stages of development (Gilbert et al. 1983). Pre-selection or pre-recruitment stages include 1-2 mm (small white), 3-5 mm (large white), and 6-8 mm (small yellow) (Gilbert et al. 1983, Perry et al. 1983, Johnson and Woods 2007). Granulosa cells from follicles 1-8 mm in size are unresponsive to FSH. But from the 6-8 mm pool, a single follicle will be selected (recruited) into the hierarchy of preovulatory follicles, increasing in size and becoming FSH responsive (Johnson et al. 2002; Johnson and Woods 2007).

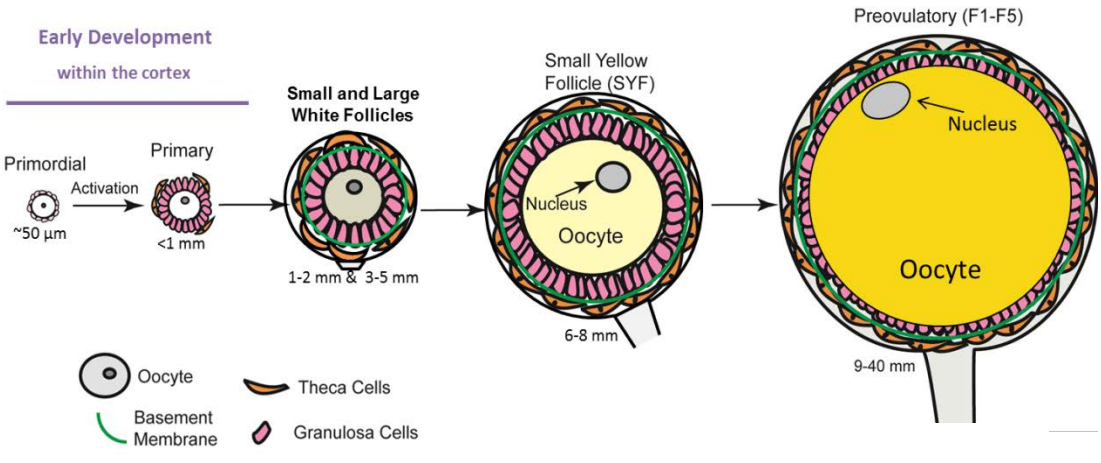

Figure 1.1. Model of avian follicular development depicting the stages of growth, from primordial (within the cortex) through slow growth phase into prehierarchy, and recruitment to hierarchy.

e) Follicle selection and recruitment

On a nearly daily basis in layer hens, one 6-8 mm follicle will become responsive to FSH through differentiation of its granulosa cells (Woods and Johnson 2005), grow to 9-12 mm (now identified as most-recently-recruited follicle), and enter the last stage of growing follicles, > 9 mm (large yellow follicles), a cohort known as hierarchical or preovulatory (Johnson 1990; Bahr 1991). The hierarchy is a well-organized group of follicles composed of five or six largest follicles, approximately 9-40 mm in diameter labeled F1- F5/6 by size (F1 is the largest) and are committed to ovulate within the next five to six ovulations (Johnson 1990; Bahr 1991). Hierarchical follicles have two distinctions over prehierarchical follicles. One is that steroid production emphasis switches from estrogens in prehierarchical to progestins in hierarchical (Bahr et al. 1983), and two is protection from atresia (Gilbert et al. 1983). A mechanism offering protection against apoptosis in these follicles is the PI3K/Akt pathway. Johnson et al. (2001), using cultured granulosa cells from F1-F3, showed that activation of Akt by IGF-1 (insulin-like growth factor 1) prevented oligonucleosome formation, an indicator of apoptosis. Indeed, prior to selection and recruitment, follicular atresia in the selectable pool of follicles is quite high (Tilly et al. 1991b; Johnson et al. 1996). Also, proliferative capacity of granulosa cells decreases as the follicle progresses through the hierarchy (Tilly et al. 1992; Tischkau and Bahr 1996; Yao and Bahr 2001; Wang et al. 2007). Mechanisms responsible for follicle selection and recruitment are proposed to involve an increase in FSH receptor mRNA expression and/or signaling and release from the inhibitory effects of MAPK signaling (Woods et al. 2005, 2007; Kim et al. 2013).

f) Ovulation

Growth and development of post emergent follicles occurs in response to gonadotropins, FSH and LH. FSH stimulates follicle development, causing increases in production of estrogens, progestins, and androgens, depending on follicle stage (Nitta et al. 1991). LH causes ovulation of the dominant follicle (F1). As F1 grows it produces progesterone (Johnson et al. 2002) which positively feeds back to the hypothalamus, increasing gonadotropin releasing hormone (GnRH) until a pituitary surge of LH causes the F1 follicle to ovulate (Etches et al. 1984) along the stigma, an area on the oocyte surface devoid of vasculature (Bahr 1991). Cycling gonadotropins, which increase at puberty, are under stimulatory control of GnRH in all vertebrates (reviewed in Parhar et al. 2016).

2. Puberty

Puberty in the domestic hen occurs when body weight is sufficient, with an appropriate amount of muscle and fat, and the ovary has developed to respond to photostimulation (Pishnamazi et al. 2014). In modern broiler breeder hens, puberty begins at approximately 20 weeks of age (Cobb-Vantress 2008). Photostimulation is activation, by light, of reproductive axis (hypothalamus – pituitary – ovary). Within the hypothalamus are gonadotropin releasing hormone (GnRH) and gonadotropin inhibitory hormone (GnIH) neurons (Bédécarrats et al. 2009). Light of appropriate wavelengths, duration, and intensity, increases GnRH secretion from the hypothalamus (Sharp et al. 1990) by activating hypothalamic photoreceptors that directly stimulate GnRH neurons (Saldanha 2001). Before puberty and during short day length, Bédécarrats et al. (2009)

proposed that increased melatonin binds to and activates GnIH neurons, blocking production of FSH and LH. But after puberty, with photostimulation, melatonin is decreased, and GnRH neurons become active. GnRH neuropeptides bind to their respective receptors in the anterior pituitary, FSH or LH is released into circulation to act on the gonads (Bédécarrats et al. 2009, 2016).

3. Steroidogenesis in the Ovary

Steroidogenesis is a major function of the ovary and is a well-studied process in both mammals (reviewed in Leung and Armstrong 1980; King and LaVoie 2012) and birds (Nitta et al. 1991; Johnson et al. 2002). Cells responsible for steroid biosynthesis are mainly somatic cells, theca and granulosa, that surround and support the oocyte. Androgens, estrogens and progestins are critical for growth and development of not only follicles, but the entire reproductive tract, and additionally promote reproductive behaviors (Johnson 1999). Sex steroids are synthesized from cholesterol that is either brought into the cell as low density lipid (LDL) or manufactured within the cell (Azhar et al. 2003). Multiple enzymes affect production of steroids; presence of the enzymes and capability of the cell to synthesize steroids depend on type of cell and stage of follicle (Nitta et al. 1991). Small cortical follicles and stromal tissue produce mainly estrogens (Armstrong 1984; Robinson and Etches 1986), while large preovulatory follicles mainly produce progestins (Bahr et al. 1983). Consequently, depending on stage of follicle development, steroidogenesis is initiated by different stimuli. This has been shown in follicles that have emerged from the cortex (Johnson and Bridgham 2001; Stocco et al. 2005). Steroid biosynthesis is a cAMP-dependent process that eventually increases

transcription of cAMP-dependent genes such as *STAR* and *CYP11A1.* STAR protein carries out the rate limiting step in the steroidogenic pathway, as it binds cholesterol at the mitochondrial membrane in preparation for cholesterol transfer to the inner membrane for conversion to pregnenolone by the enzyme CYP11A1 (reviewed in Stocco et al. 2005). Activators of steroidogenesis in cortical follicles are less studied, however VIP, identified in neurons and located in theca, affect steroidogenesis in granulosa cells (Johnson et al. 1994). VIP increases expression of *STAR* mRNA in cultured granulosa cells of rats (Davoren and Hsueh 1985) and chickens (Kim and Johnson 2016) and induces cAMP formation in granulosa cells of preovulatory follicles (Johnson and Tilly 1988).

4. Vasoactive Intestinal Polypeptide

Vasoactive Intestinal Polypeptide (VIP) is a neuropeptide, 28 amino acids long, first isolated from porcine small intestine and characterized by Said and Mutt (1970). When introduced into the blood stream of dogs it causes systemic vasodilation, hypotension, increased respiration and cardiac output, and hyperglycemia. Further characterization identified VIP as an octacosapeptide, related to secretin and glucagon (Said and Mutt 1972). VIP acts as a neurotransmitter inducing effects through its G protein-coupled receptors, VIPR1 and VIPR2. VIP stimulates adenylyl cyclase and cAMP production in many peripheral tissues (Fahrenkrug and Emson 1982; Vaudry et al. 2000 review). When VIP binds to its receptor, the stimulatory subunit of the G protein activates enzyme adenylyl cyclase which converts ATP to cAMP (a powerful second messenger involved in many processes with the cleaving of PPi and formation

of a phosphodiester bond (cyclization) (reviewed in Taussig and Gilman 1995). When sufficient cAMP accumulates, it activates a kinase which phosphorylates cAMP response element binding protein (CREB) which then binds to nuclear transcription factors to affect transcription. Protein kinase A (PKA) is the main kinase activated, but VIP and its receptors can also stimulate phospholipase C/PKC and mitogen-activated protein (MAP) kinase pathways (reviewed in Vaudry et al. 2000). Levels of cyclic AMP are controlled by phosphodiesterases that will convert cAMP to inactive AMP (reviewed in Taussig and Gilman 1995). Johnson and colleagues demonstrated that cAMP provides anti-apoptotic effects in cultured granulosa cells by increasing levels of Bcl-X (long), both mRNA (1996) and protein (1999). Activators of cAMP include LH and FSH (Chun et al. 1994), as well as VIP (Flaws et al. 1995). Davoren and Hsueh (1985**)** were able to increase both VIP-dependent progesterone production and cAMP levels in a dose-dependent manner from cultured rat granulosa cells with addition of a phosphodiesterase inhibitor.

a) VIP and receptors in the ovary

VIP, acting through its receptors, plays multiple roles in ovary. It participates in follicle growth, demonstrated by initiation of primordial follicle activation (Chen et al. 2013), maintenance of follicle growth in cultured neonatal rat ovaries, and involvement in mechanisms associated with cell differentiation that enable follicles to gain sensitivity to gonadotropins (Mayerhofer et al. 1997). VIP prevents granulosa cell apoptosis and follicle atresia in chickens and rats (Flaws et al. 1995) and may play a role in ovulation (Schultea et al. 1992; Hulshof et al. 1994). VIP also regulates steroidogenic activity

(Davoren and Hsueh 1985; Ahmed et al. 1986) and is the only known neuropeptide capable of initiating steroid synthesis in the ovary (Advis et al. 1989). Interestingly, VIP may act on a different set of granulosa cells than does FSH (Kasson et al. 1985).

Coincident with varied functions of VIP is the wide ovarian distribution of VIP-ergic fibers. Innervation occurs predominantly through two main routes: ovarian plexus, which supplies blood vessels, and superior ovarian nerve, which innervates both vascular and interstitial tissue (Lawrence et al. 1980). VIP reaches the ovary via the superior ovarian nerve (Dees et al. 1986) and VIP-containing nerve fibers have been identified in ovaries of the rat (Ahmed 1986) and the hen (Johnson et al. 1994). VIP fibers are localized around blood vessels suggesting an involvement with ovarian blood flow (Jørgensen 1991), in interstitial cells where VIP may regulate steroidogenesis (Davoren and Hsueh 1985), and surrounding primordial follicles where VIP stimulates follicle activation (Chen et al. 2013).

VIP and its receptors, VIPR1 and VIPR2 (also known as VPAC1 and VPAC2, respectively) have been characterized in ovarian follicles of many species (Schultea et al. 1992; Hulshof et al. 1994; Vaccari et al. 2006; Barberi et al. 2007; Zhou et al. 2011; Gabbay-Benziv et al. 2012; Kim and Johnson 2016). In monkeys (Schultea et al. 1992) and cows (Hulshof et al. 1994), number of VIP immunoreactive sites in the ovary increases with age through adulthood and may be associated with age-related developmental changes. In the bovine fetus, VIP immunostaining first appears at a few sites within the ovarian cortex at 4.5-6 months of gestation (Hulshof et al. 1994), a stage of development coinciding with initiation of folliculogenesis (Erickson 1966). VIP immunoreactivity increases again at 6-7.5 and 7.5-9 months of gestation with

appearance of secondary and tertiary follicles, respectively (Hulshof et al. 1994). Increased VIP staining through fetal life is also seen in humans, after first appearing in the ovary at 22 weeks of gestation (Gabbay-Benziv et al. 2012). In human fetal ovaries, primordial follicles form by 20 weeks and primary follicles are present by 24 gestational weeks (reviewed in McGee and Hsueh 2000). In rhesus monkey, the number of VIP fibers increases between 2 months and 3 years (puberty), remain constant through the reproductive years, then decline in numbers and remain constant through senescence (Shultea et al. 1992).

Both receptors have been identified in ovarian follicles of many species. From fully grown oocytes of rats and mice, *VIPR2* mRNA is present in both granulosa and theca/interstitial cells (Vaccari et al. 2006; Barberi et al. 2007), while *VIPR1* mRNA is found predominantly in theca/interstitial of mice (Barberi et al. 2007), and solely in theca of rats (Vaccari et al. 2006). Neither was identified in the oocyte of rats (Vaccari et al. 2006). By contrast, in zebrafish, *VIPR1* is expressed exclusively in the follicle layer (both granulosa and theca) and *VIPR2* expresses exclusively in the oocyte (Zhou et al. 2011). From prehierarchical and preovulatory follicles of chicken, *VIPR1* and *VIPR*2 mRNA are present in both granulosa and theca, but were not measured in oocytes (Kim and Johnson 2016). Expression and characterization of VIP and its receptors within the cortex of the immature remains largely unknown and is a main interest of this thesis.

5. Obesity in Reproduction

For decades, obesity has been a growing epidemic in many species including humans (Kopelman 2000) and companion animals, including dogs and cats (German

2006). Consuming calories in excess of the biological needs of an organism causes problems with fertility. For both sexes this has been shown in many species (Correa and Jacoby 1978). While every organism is capable of becoming obese, certain animals have a genetic predisposition, for example, Labrador Retriever dogs (Edney and Smith 1986) and strains of broiler chickens (Griffin and Goddard 1994; Heck et al. 2004; Decuypere et al. 2006). Obesity during the growing phase of a young animal will accelerate the time of puberty in humans (Adair and Gordon-Larsen 2001) and in chickens (Yu et al. 1992a; Onagbesan et al. 2006). In the young growing broiler breeder hen, consuming excess feed increases folliculogenesis so that at puberty, follicles are at an advanced stage of development when the hens are exposed to maximum day length (Pishnamazi et al. 2014). In adult rats, obesity accelerates follicle development and depletion of the primordial pool (Wang et al. 2014).

6. Reproductive Problems of the Broiler-Breeder Hen

Modern broiler species have been genetically selected for fast growth and large muscle deposition and, along with selection for increased feed consumption can reach market weight in 35 days (Clauer 2016). But these qualities are problematic for the parent breeding stock (broiler breeders). Large body size and muscle composition are a direct consequence of genetic selection but are negatively correlated with egg production (Kinney and Shoffner 1965), while being positively correlated with multiple ovulations (Reddy and Siegel 1976). Siegel and Dunnington (1985) had surmised that the mode of inheritance responsible for laying down muscle and fat in the growing chicken may also amplify yolk accumulation in the

adult ovary. When given free access to feed (full-fed), broiler breeder hens will overeat, far exceeding requirements for normal growth and development. Excess feed consumption during the growing/rearing period causes severe ovarian disorders during the laying period (Yu et al. 1992a; Yu et al. 1992b), such as erratic ovipositions and defective eggs attributed to excess follicle development (Hocking et al. 1987; Hocking et al. 1989) along with increased ovulations (Udale et al. 1972). The adult full-fed hen also suffers from poor heath, indicated by metabolic disease and shortened lifespan (Griffin and Goddard 1994), and research suggests that ovarian dysfunction in the full fed hen is the result of lipotoxicity caused by obesity (Chen et al. 2006). Full feeding clearly affects the welfare of the hen. However, undesirable traits associated with full feeding are reduced, and health and performance of the hen are improved, only by severely restricting feed intake (Yu et al. 1992a; Yu et al. 1992b) which also impacts bird welfare (Renema and Robinson 2004, Decuypere et al. 2006; Decuypere et al. 2010). It has been recognized that while the ovaries of adult broiler breeder hens contain twice the number of yellow follicles as compared to that of layer hens, egg production is comparatively poor, which can't be blamed solely on obesity because even with the marked improvement experienced with severe feed restriction, broiler breeder hens still produce only about half the number of eggs of commercial layers (Yu et al. 1992b; Hocking et al. 1987; Hocking and McCormack 1995; Decuypere et al. 2006). Experiments in this thesis were designed to identify effects of feed level on growth and development of cortical follicles in immature hens by utilizing full- and restricted-fed paradigms. Our hypothesis is that genes involved with follicle growth will have greater expression in

full fed than in restricted fed hens. Because ovarian development before puberty is not dependent on gonadotrophins and gonadotrophin levels in broiler breeder animals do not change with feed restriction (Liu et al. 2004; Onagbesan et al. 2006), the changes in gene expression will be due to intra-ovarian factors.

Chapter 2. Feed Restriction Inhibits Early Follicular Development in Young Broiler-Breeder Hens*.

Running Title: Feed Restriction and Follicular Development

Authors: Francisco J Diaz and Kate Anthony

Center for Reproductive Biology and Health, Department of Animal Science.

The Pennsylvania State University, University Park, PA 16802

Keywords: Ovary, Follicle

*Published in Animal Reproduction (2013) 10(2): 79-87 and reprinted here with permission.

Abstract

Ad libitum feeding causes excessive follicular development and is associated with extensive metabolic changes in broiler-breeder hens. Restricting feed intake reduces excessive follicular development, but the mechanisms mediating this response are unknown. In the present study, the effects of feeding on follicular development in immature broiler breeder hens were examined. There was an increase in the proportion of follicles 100-300, 300-500 and >500 µm in diameter and a decrease in follicles <100 µm in full-fed (FF) compared to restricted fed (RF) hens. Increased follicular development in FF hens was associated with greater expression of steroidogenic transcripts (*STAR, CYP11A1, HSD3B* and *CYP19*) within the ovarian cortex of FF hens. These transcripts represent markers of more advanced follicular development. However, increased follicular development in FF hens was not associated with changes in the expression of other factors previously implicated in follicular development, including those encoding TGF-beta ligands (*AMH, BMP6, BMP15* or *GDF9*) or their signaling proteins (SMAD2/3 or SMAD1/5/9). Changes in histone modifications associated with proliferation, including trimethylated histone H3K4, trimethylated histone H3K27 and acetylated histone H3K9 were also not different between treatment groups. However, feed restriction caused serine phosphorylation to localize strongly to the ovarian stroma of FF hens compared to RF hens. In contrast, phosphorylation of tyrosine residues localized more prominently to the surface of granulosa cells from RF hens. Thus, restricted feeding may enhance the efficiency of reproduction by suppressing early follicular development and this is associated with changes in granulosa cell protein phosphorylation status.

Introduction

Avian follicular development is a continuous process from activation of small cortical follicles (<0.1 mm) to ovulation of hierarchical follicles. The largest 5-6 follicles (F1-F6, approximately 9-45 mm) comprise the preovulatory hierarchy. The largest follicle ovulates on a nearly daily basis. To replace hierarchical follicles as they ovulate, one prehierarchical follicle, 6-8 mm in diameter, is selected to enter the hierarchy each day. Granulosa cells from the smallest of the preovulatory follicles have the highest proliferative activity, and this proliferative capacity decreases dramatically as the follicle progresses through the hierarchy (F5 to F1) (Tilly et al. 1992; Tischkau and Bahr 1996; Yao and Bahr 2001; Wang et al. 2007). The mechanisms responsible for follicle selection are proposed to involve an increase in FSH receptor mRNA expression and a release from the inhibitory effects of MAPK signaling (Woods et al. 2005; 2007). Prior to selection a number of slow growing follicles undergo atresia (Tilly et al. 1991b, Johnson et al. 1996). Prehierarchical follicles between 1-5 mm in diameter have not begun to accumulate large amounts of yolk and therefore appear white in color. The mechanisms controlling the growth of these small (1-6 mm) prehierarchical follicles is not well understood, but is associated with specific changes in gene and protein expression (Diaz et al. 2011). Follicles less than 1 mm represent cortical follicles which are completely embedded within the ovarian cortex. The smallest cortical follicles measuring ~0.05 mm in diameter are presumably recruited at regular intervals into the actively growing population, but the signals initiating follicle activation and early growth in birds are not fully characterized.

Genetic selection for growth and development in poultry lines used for meat production (broilers) has been extremely successful. However, for breeding stock (broiler-breeders) a consequence of increased growth rate is a severe decrease in reproductive efficiency, including fewer eggs produced and lowers fertility (Yu et al. 1992a; Yu et al. 1992b; Hocking and McCormack 1995). Paradoxically, the decrease in egg laying capacity in broiler breeder hens is related to increased follicular development and an increased incidence of more than one follicle selected per day. Full-fed broiler-breeder hens may have up to 12-14 hierarchical follicles and up to 2 follicles ovulating on a given day. Ovulation of two oocytes can lead to one oocyte entering the body cavity which can cause infection or results in two oocytes in a single shell which results in non-viable embryos. Currently, the only effective way to control ovarian hyperactivation in broiler-breeder hens is through dietary calorie restriction (Yu et al. 1992a; Yu et al. 1992b; Hocking and McCormack 1995). Thus, the broiler hen is a useful model to study the effects of level of nutrition on ovarian function. In the present study, we used a full-fed *versus* restricted fed model to establish changes within the ovary in young broiler-breeder hens. The results demonstrate that feed restriction reduces growth of very small follicles and alters the overall level of protein phosphorylation within the ovarian cortex.

Materials and Methods

Animals

Female white Leghorn chicks were purchased from Hy-line International. Animals were raised according to the management protocols established by Hy-line

International (Hy-line 2007). At 17 weeks of age, hens were photostimulated by increasing light duration to 15 hours per day to induce ovarian development. Ovaries from actively laying leghorn hens were collected at 35-45 weeks for determination of follicle number (Table 2.1). Broiler-breeder hens (Cobb 500) were generously donated by a local hatchery (Longeneckers Hatchery, Harrisburg, PA). Day old chicks were raised in floor pens for 2 weeks and were then allocated to separate pens (9 animals per pen). One group was fed ad libitum (full-fed) and another group was restricted fed according to commercial grower's guidelines (Cobb-Vantress 2008). At 16 weeks, animals were weighed and ovaries collected for analysis as described below. Some animals were photostimulated (12:12 hours light dark cycle) and ovaries collected at 22-24 weeks to characterize follicular development at the beginning of laying period (Table 2.1). All procedures described herein were reviewed and approved by the Pennsylvania State University Institutional Animal Care and Use Committees, and were performed in accordance with The Guiding Principles for the Care and Use of Laboratory Animals.

Histology and immunofluorescence

Ovaries were collected from 16 week full-fed (FF) and restricted-fed (RF) broiler breeder hens (n=9/group). Small sections (~1 cm^3) of cortex were fixed in 4% paraformaldehyde in PBS overnight. Paraffin embedded tissues were sectioned (6 µm) and stained with hematoxylin and eosin. Brightfield images were acquired on a Nikon Te200 compound microscope with an attached DP20 Olympus digital color camera and DP software. The diameter of every follicle was measured in three of the largest sections of ovarian cortex from randomly selected FF and RF animals (n=6), and the

proportion of follicles <100, 100-300, 300-500 and >500 µm was calculated. Sections (6 µm) from randomly selected animals (n=3) from each group (FF and RF) and were used for immunostaining as described previously (Diaz et al. 2011) with the following primary antibodies: anti-histone H3K4me3 (1:800, Cell Signaling, #9751), anti-histone H3K27me3 (1:100, Cell Signaling, #9733), anti-histone H3K9Ac (1:200, Cell Signaling #9671), pSMAD1/5/9 (1:200, Cell Signaling, #9511), pSMAD2 (1:200, Cell Signaling, #3101) phosphoserine (1:400, Zymed, #61-8100) and phosphotyrosine (1:50, Cell Signaling, #8954). After washing in phosphate buffered saline with 0.05% tween-20 (PBST), sections were incubated with goat anti-rabbit IgG Alexa Fluor 594 (1:2000, Invitrogen) for 1 hour, followed by washing with PBST and mounting with DAPI anti-fade gold (Invitrogen). Epi-fluorescence images were acquired on an AxioScope 2 Plus (Leica, Bannockburn, IL) and a DP70 Olympus digital color camera and DP software.

Isolation of total mRNA and qPCR

Total RNA was isolated from ovarian cortex using the RNAeasy mini kit (Qiagen, Valencia, CA). Equal amounts of total RNA (1 µg) were reverse transcribed into cDNA as described previously (Diaz et al. 2006) using the QuantiTect Reverse Transcription kit (Invitrogen, Carlsbad, CA). Amplification of specific transcripts was conducted using gene specific primers (Table 2.2). The C_T values for *ACTB* mRNA (actin) were used as the normalizer as described previously (Livak and Schmittgen 2001; Diaz et al. 2011). For each primer pair, only a single product of the predicted size was identified. All amplification products were sequenced to confirm specificity of the reaction. All

transcripts were analyzed in cortex samples of individual animals from FF and RF groups (n=9). Values shown for transcript abundance are the mean ± SEM.

Data and statistical analysis

Abundance of specific mRNAs was analyzed by real-time PCR using the $2^{-\Delta\Delta C}{}_t$ method (Livak and Schmittgen 2001). Statistical differences in mRNA abundance and proportion of follicles were analyzed by student's *t*-test, $P<0.05$. Data in Table 2.1 were analyzed by one way ANOVA followed by Fisher's LSD, $P<0.05$.

Results

Effect of feed restriction on prehierarchical and hierarchical follicles

To demonstrate that the level of feeding employed in this study causes ovarian dysfunction, broiler-breeder hens were raised under full-fed or restricted-fed conditions for 22-24 weeks. The light cycle was changed from 8 to 12 hours at 16 weeks to stimulate development of preovulatory follicles. Ovaries were collected at first lay (22-24 weeks) and the preovulatory (9-45 mm) and prehierarchical (6-8) follicles were counted (Table 2.1). The full-fed and restricted-fed treatments were maintained for the full duration of the experiments (22-24 weeks). As a comparison, follicles were also counted from actively laying white Leghorn hens that are not subject to ovarian hyper activation under *ad libitum* feeding conditions. As shown in Table 2.1, FF broiler hens have an average of 11.6 hierarchical follicles and 11 prehierarchical (6-8 mm) follicles. Feed restriction reduced the number of both groups of follicles by ~50% ($P<0.05$). In

contrast, laying hens have about half as many hierarchical follicles as full-fed broilers (5.4), but a similar number of prehierarchical follicles (10.7) ($P<0.05$).

Effect of feed restriction on ovarian development in young hens

To investigate effects of feed restriction on ovarian development in immature, 16 week old broiler-breeder hens before photostimulation, chicks (Cobb 500) were raised under FF and RF conditions for 16 weeks. Ovaries were then collected for mRNA and protein analysis. Ovarian weight of FF hens was almost three times that of RF birds (Figure 2.1A, $P<0.05$). This is consistent with the larger bodyweight of the FF birds (Figure 2.1B, $P<0.05$). To determine changes in proportion of follicles at different sizes, sections of ovarian cortex from FF and RF hens (n=6) were stained with H&E and the follicles counted. FF birds had a higher proportion of follicles 100-300, 300-500 and >500 µm compared to RF animals, but had fewer follicles <100 µm in diameter than RF hens (Figure 2.2A, $P<0.05$). Greater follicular development in FF hens was associated with increased relative levels (fold change) of steroidogenic transcripts (*STAR*, *CYP11A1*, *HSD3B*, and *CYP19*) (Figure 2.2B, $P<0.05$).

Effect of feed restriction on TGF-beta ligands and pSMAD signaling

AMH, BMP6, BMP15 and GDF9 are members of the TGF-beta family that signal through SMAD1/5/9 or SMAD2/3 pathways. The relative levels of *AMH, BMP6* and *GDF9* mRNA did not differ in the cortex of 16 week old FF and RF hens, but *BMP15* mRNA was moderately decreased in FF compared to RF hens (Figure 2.3A, $P<0.05$). To determine whether signaling through the pSMAD2/3 (GDF9) or pSMAD1/5/9 (AMH,

BMP6, BMP15) pathways is altered by feeding level, we examined levels of phosphorylated (activated) pSMAD2 and pSMAD1/5/9 in the cortex of FF and RF hens. Phosphorylated SMAD1/5/9 was similar in FF and RF hens as determined by immunofluorescence (Figure 2.3B). Interestingly, pSMAD1/5/9 was much more intense in the granulosa cell layer compared to the ovarian stroma. Levels of pSMAD2 were also similar in FF and RF hens, but unlike pSMAD1/5/9, pSMAD2 was more uniformly distributed in the granulosa and the stroma cells (Figure 2.3C).

Changes in follicular growth were not associated with changes in specific histone modifications

Ovarian sections from FF and RF hens (n=3) were immunostained with antibodies recognizing trimethylated histone H3K4, trimethylated histone H3K27 and acetylated H3K9 (Figure 2.4 A-C). Immunostaining for trimethylated H4K4 was uniform throughout the ovarian cortex and was similar between FF and RF hens. Trimethylated H3K27 was much more intense in the granulosa cells compared to the stroma, but as with trimethylated H3K4 was similar in FF and RF hens. Likewise, acetylated H4K9 was also higher in the granulosa compared to the surrounding stroma, but was not different between FF and RF hens.

Changes in global serine and tyrosine phosphorylation

The overall levels of serine and tyrosine phosphorylation were determined as an indication of kinase activity. Sections of ovarian cortex were incubated with anti-phosphoserine or anti-phosphotyrosine antibodies. Several interesting observations

were made. The oocyte showed very high and discrete localization of phosphoserine proteins in the cytoplasm in both FF and RF hens (Figure 2.5A). The phosphoserine immunostaining signal in the oocyte cytoplasm was associated with vesicle-like structures (Figure 2.5B). However, phosphoserine localized more prominently to the ovarian stroma of FF compared to RF hens (Figure 2.5A). The oocyte showed little if any phosphotyrosine staining. However, the granulosa cells in particular showed discrete staining on the cell surface (Figure 2.5C). Moreover, phosphotyrosine localized more prominently to the granulosa cell plasma membrane in RF than FF hens (Figure 2.5C).

Discussion

Dietary factors have profound influences on ovarian function through direct effects on the ovary and indirect effects on the endocrine hypothalamic-pituitary axis. In broiler-breeder hens, free access to feed causes severe ovarian dysfunction. Dietary calorie restriction is the only effective way to normalize ovarian function (Yu et al. 1992a; Yu et al. 1992b; Hocking and McCormack 1995). However, the physiological changes caused by feed restriction that lead to reduced follicular development are not known. Thus, the broiler-breeder hen is an excellent model to study the effect of increased feed intake and obesity on ovarian function. To begin identifying the direct effect of nutritional status on ovarian function, the present study examines the effect of full or restricted feed intake on follicular development before sexual maturity. Ovarian development before photostimulation is not dependent on gonadotrophins and feed restriction does not appear to alter gonadotrophin levels in adult animals (Liu et al.

2004; Onagbesan et al. 2006). Thus, by focusing on the immature rearing period, the direct effects of feed restriction on growth of small follicles can be more easily separated from possible indirect effects on gonadotrophin stimulation. The findings show that feed restriction suppresses growth of small cortical follicles, but these effects are not associated with changes in signaling by the TGF-beta family of proteins or with change in histone modifications in the granulosa cells. However, feed restriction altered the localization of phosphoserine and phosphotyrosine proteins in small follicles. The findings clearly show that feed restriction decreases early follicular development in young broiler-breeder hens. Ovarian weight was 3-4 times larger in full-fed than restricted hens at 16 weeks of age. The increase in ovarian weight parallels a similar increase in body weight, but larger ovaries in FF hens are also the result of more advanced follicular development. FF hens had more actively growing follicles (100-300, 300-500 and >500 µm) than restricted hens. Greater follicular development could be the result of greater follicle activation. Indeed, FF hens had fewer follicles <100 µm in diameter, which includes the quiescent pool of follicles. The depletion on follicles <100 µm in FF hens suggests accelerated activation compared to restricted hens. Consistent with more advanced follicular development, the ovarian cortex of FF hens had higher relative levels of *HSD3B, STAR, CYP11A1* and *CYP19* mRNA which are known to increase during development of small cortical follicles (0.5 to 1 mm) (Diaz et al. 2011). These steroidogenic factors continue to increase throughout the prehierarchical period as follicles produce increasing levels of steroids, such as estradiol (Tilly et al. 1991a; Li and Johnson 1993; Johnson et al. 2002). To establish that our dietary regimen caused ovarian dysfunction, some animals were exposed to increasing photoperiod to induce

development of preovulatory follicles (photostimulation). Changes in the number of hierarchical (>9 mm) and prehierarchical follicles (6-8 mm) in FF and RF broiler hens compared to white leghorn hens (Table 2.1) give some clues as to the cause of ovarian dysfunction. First, both FF broiler and layer hens have ~11 prehierarchical follicles, but FF hens have twice as many hierarchical follicles. This suggests that *ad libitum* feeding results in broiler-breeder hens having a more permissive follicle selection mechanism that allows more than one follicle to enter the hierarchy each day. Secondly, feed restriction causes a 50% decrease in prehierarchical follicles in RF hens which reduces the pool of follicles available to enter the hierarchy. Thus, excessive folliclular development in full-fed broiler hens is likely caused by both permissive follicle selection combined with increased availability of selectable prehierarchical follicles. Our present findings demonstrate that feed restriction decreases the number of prehierarchical follicles available for selection (6-9 mm) and decreases development of small cortical follicles, eventually limiting availability of selectable follicles. Current work is focused on identifying the signaling pathways affected by feed restriction responsible for decreased follicular development.

Greater follicular development in FF hens could be caused by greater follicular activation or increased growth or survival of activated follicles. There was no change in specific histone modifications associated with proliferation such as trimethylated histone H3K4 (Schneider et al. 2004) and acetylated histone H3K9 (Yang and Seto 2007) or a decrease in trimethylated histone H3K27, which is associated with repressed chromatin (Trojer and Reinberg 2007). Thus changes in histone modifications are not part of the mechanism promoting greater follicular development.

In mammals and other vertebrates, early follicular development is driven by members of the TGF-beta superfamily, such as AMH, BMPs, activin and GDF9. The role of these ligands in avian follicular development is not as well understood. Small follicles (~1 mm) express the highest levels of many TGF-beta proteins, including *GDF9* and *BMP15* (Johnson et al. 2005b; Elis et al. 2007; Johnson et al. 2008), suggesting that these ligands are particularly active during early stages of follicular development. Consistent with this idea, GDF9 from small avian follicles stimulates proliferation of granulosa cells (Johnson et al. 2005b) and could be a major pathway stimulating follicular development in FF broiler hens. Avian follicles express all the components of the SMAD signaling pathway (Davis et al. 2001; Lovell et al. 2003; Schmierer et al. 2003; Johnson et al. 2005a; Johnson et al. 2005b; Johnson et al. 2006; Al-Musawi et al. 2007; Elis et al. 2007; Lovell et al. 2007; Johnson et al. 2008; Diaz et al. 2011). Both activin and GDF9 signal through the SMAD2/3, while BMPs and AMH signal through a separate SMAD1/5/9 pathway. However, the current findings do not support a change in activation of pSMAD proteins as the main cause of increased follicular development in immature broiler-breeder hens. This is in contrast to adult broiler-breeder animals where full-feeding causes an increase in *AMH* mRNA and protein compared to restricted-fed hens (Johnson et al. 2009). This difference could be caused by the different complement of follicles present on the ovary in immature versus adult ovaries.

Protein kinase activity is essential for normal cell homeostasis. Phosphorylation of specific serine and tyrosine amino acid residues in target proteins is a hallmark of many signaling pathways. A surprising finding in the present study was the observed changes in the localization of global serine and tyrosine phosphorylation caused by feed

restriction. In full-fed hens, serine phosphorylation was present in both somatic cells and in the oocyte. In RF hens, serine phosphorylation was more apparent in the oocyte than the somatic cells, but confirmation is necessary by more robust quantitative methods. Nevertheless, these observations suggest that feed restriction may regulate overall serine phosphorylation in somatic cells. Whether this has an impact on follicular development and the exact pathways affected awaits further study. Interestingly, we observed robust and discrete phosphoserine immunostaining in the oocyte cytoplasm that was associated with vesicle-like structures. It is tempting to speculate that these vesicles are transferred to the oocyte plasma membrane where the contents affect granulosa cell function, but this idea needs to be rigorously tested. In contrast to phosphoserine immunostaining, phosphotyrosine was localized most strongly to the surface of granulosa cells from restricted hens. This observation suggests that feed restriction increased the association of one or more phosphotyrosine proteins with the plasma membrane. Many cell surface receptors have tyrosine kinase activity, including those that bind epidermal growth factor (EGF), fibroblast growth factor, vascular endothelial growth factor, and hepatic growth factor. One possibility is that feed restriction increases tyrosine phosphorylation of the EGF receptor (EGFR). Activation of EGFR and downstream signaling molecules in the granulosa cells is known to suppress follicular growth and differentiation (Woods et al. 2005; Woods and Johnson 2006). Thus, increased tyrosine phosphorylation could reflect higher activity of the EGFR pathway that would then suppress follicular growth in restricted-fed hens.

The present findings begin to uncover some direct effects of feed restriction on follicular development. Restricted feeding clearly suppresses development of small

follicles possibly by altering the pathways that activate tyrosine phosphorylation in the membrane compartment of the granulosa cells. The signaling pathways causing this response are not specifically known, but do not appear to include changes in TGF-beta signaling (SMAD signaling) or histone modifications associated with proliferation. However, feed restriction does cause a robust change in kinase signaling. Specifically, increases in granulosa cell tyrosine phosphorylation, which could indicate the activation of a RTK (receptor tyrosine kinase) pathway, which may be responsible for suppressing follicular development. Future research will identify the pathways associated with decreased follicular growth and how changes in protein phosphorylation are involved in controlling follicular development in broiler-breeder hens.

Acknowledgements

We thank Ashley Halfhill, Tian Sun and Dr. Dan Poole for technical assistance during sample collection and Dr. Alan Johnson for sharing data in Table 2.1.

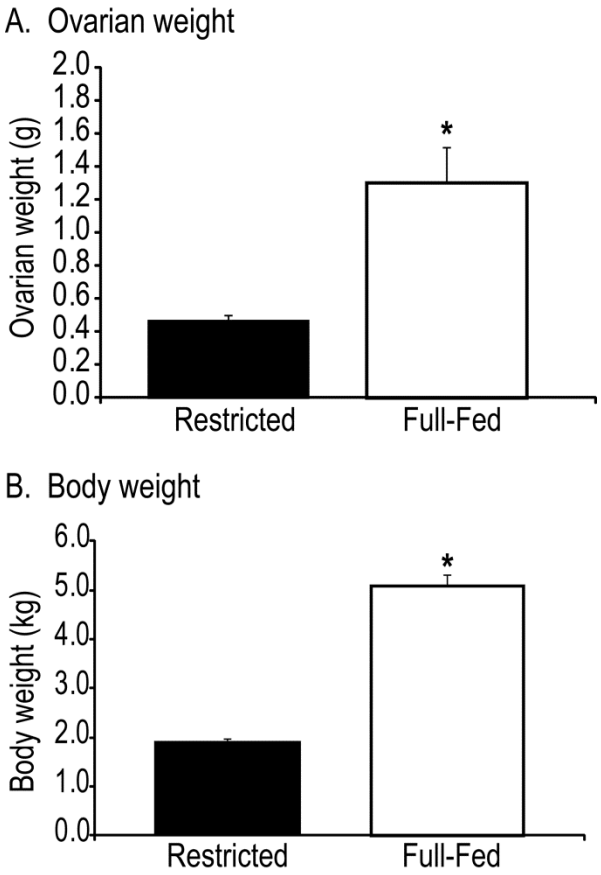

Figure 2.1. **A.** Ovarian weights of FF and RF 16 week old hens. **B.** Body weights of FF and RF hens. *Significant differences by student's *t*-test, P<0.05, n=9. FF = full-fed. RF = restricted-fed.

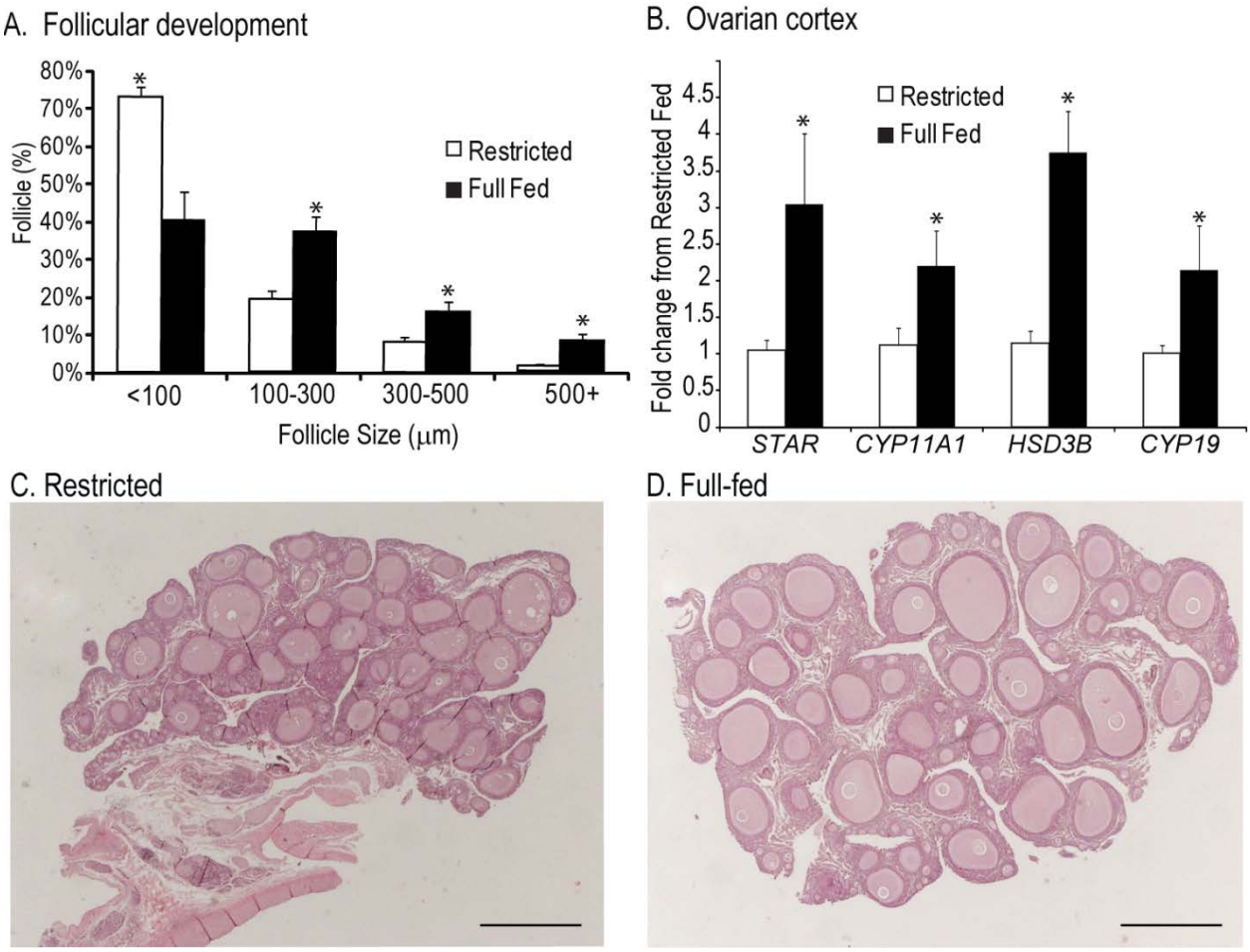

Figure 2.2. **A.** Proportion of follicles <100, 100-300, 300-500 and >500 µm in FF and RF 16 week old broiler-breeder hens. **B.** Fold change of *STAR, CYP11A1, HSD3B* and *CYP19* mRNA in ovarian cortex from FF compared to RF hens (n=9). **C.** Representative H&E section from RF hens. **D.** Representative H&E section from FF hens. *Significant differences by student's *t*-test, P<0.05, n=6-9. Scale bar = 1mm. FF = full-fed. RF = restricted-fed.

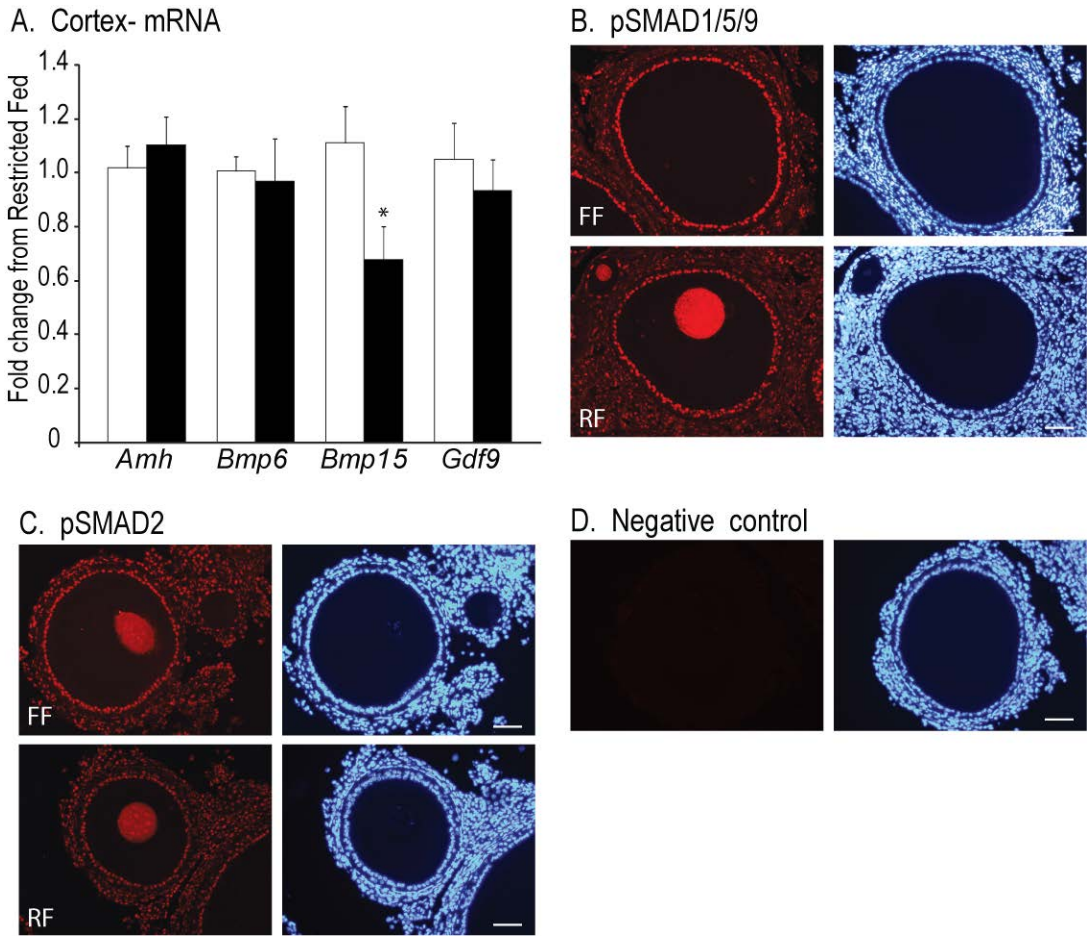

Figure 2.3. **A.** Fold change of *AMH, BMP6, BMP15* and *GDF9* mRNA in ovarian cortex FF compared to RF hens (n=9). **B.** Immunostaining for pSMAD1/5/8 in ovarian cortex from FF and RF hens. **C.** Immunostaining for pSMAD2 in ovarian cortex from FF and RF hens. **D.** Negative control incubated with secondary antibody only. Corresponding DAPI images are also shown. Scale bar = 100 µm. Sections from 3 FF and 3 RF hens were analyzed with similar results. *Indicates significant difference by student's *t*-test, $P<0.05$. FF = full-fed. RF = restricted-fed.

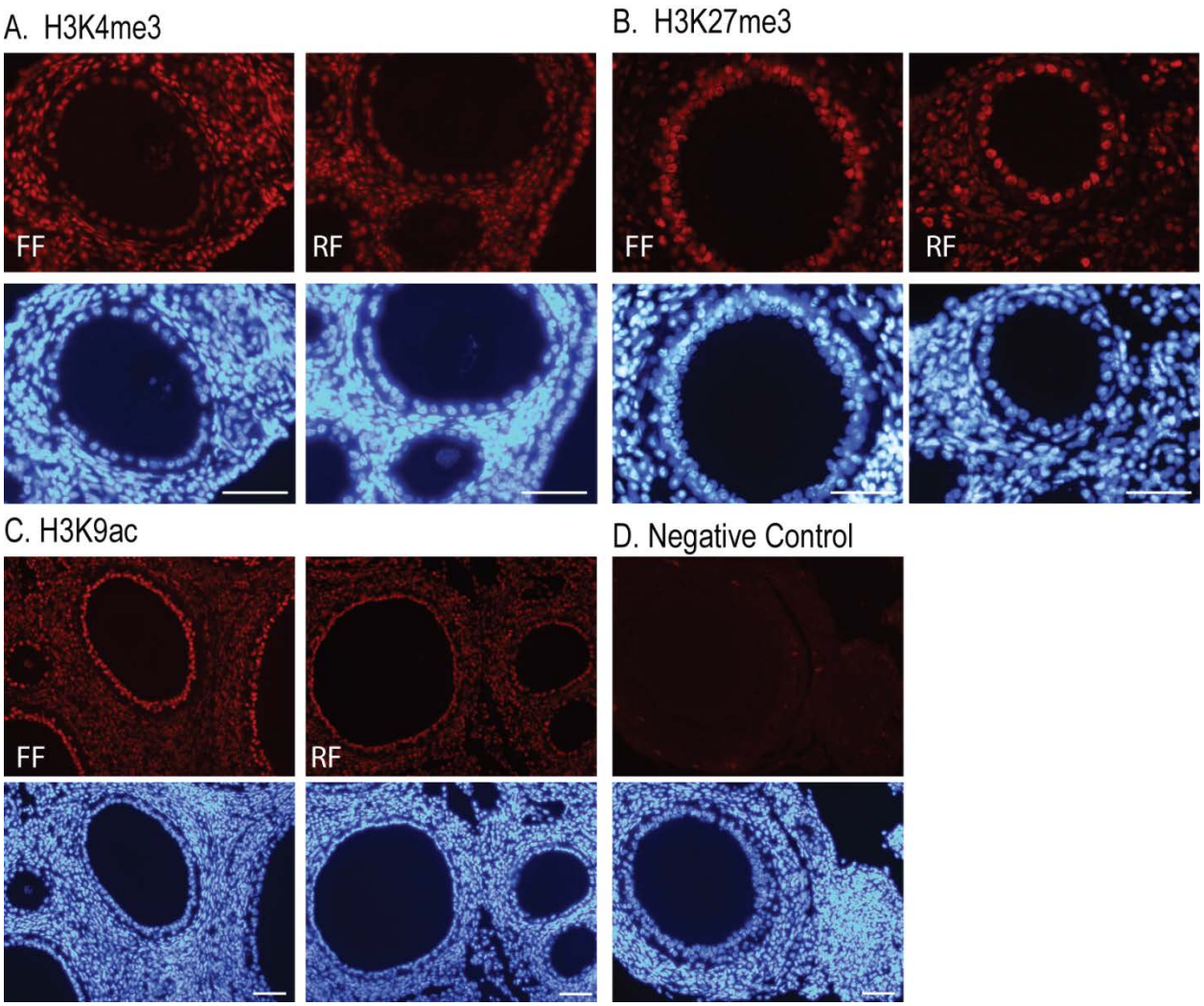

Figure 2.4. Immunostaining for trimethylated histone H3K4 **(A)**, trimethylated histone H3K27 **(B)**, acetylated histone H3K9 **(C),** and negative control **(D)** in ovarian sections from FF and RF hens. Corresponding DAPI images are also shown. Scale bar = 100 µm. Sections from 3 FF and 3 RF hens were analyzed with similar results. FF = full-fed. RF = restricted-fed.

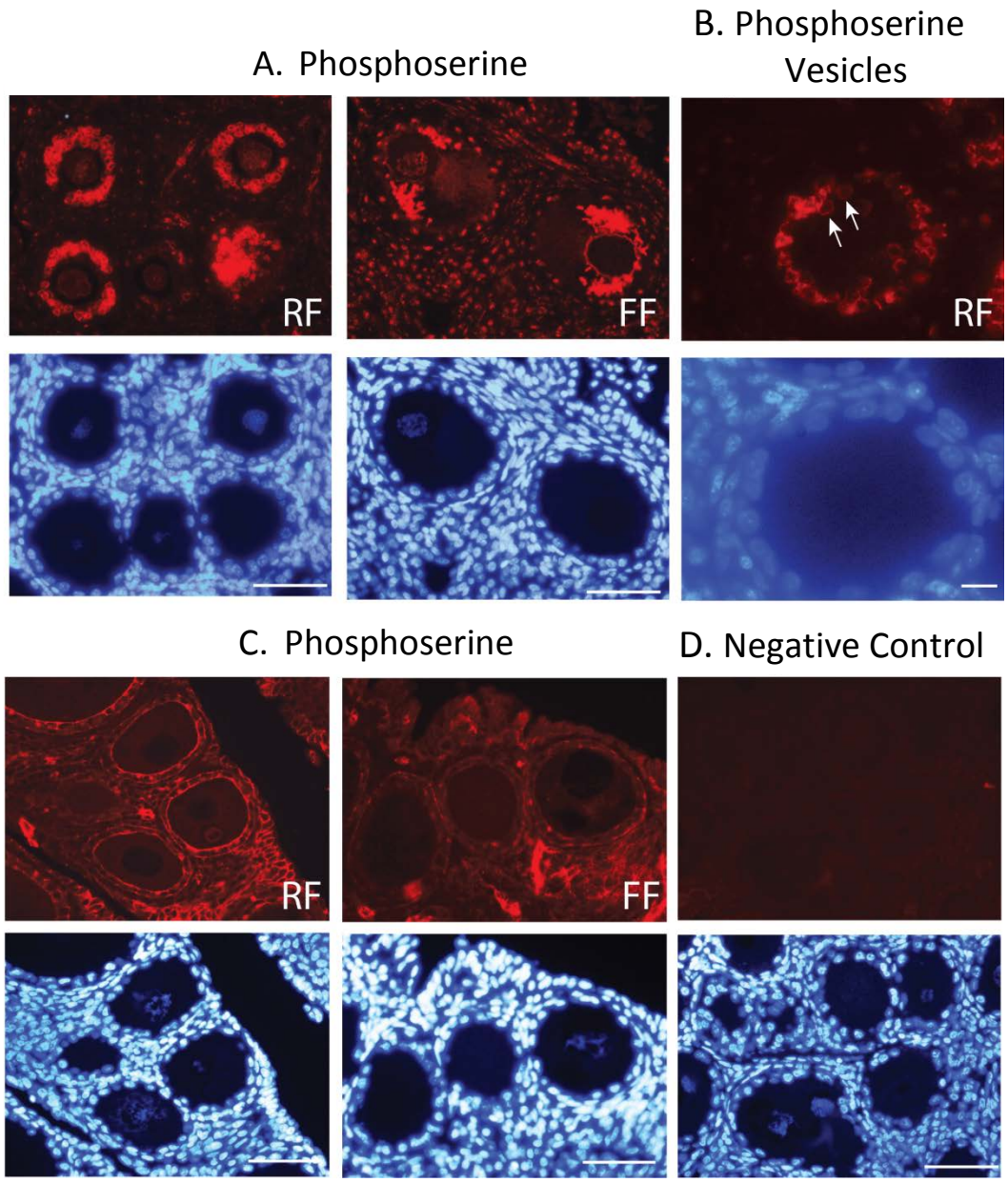

Figure 2.5. **A.** Immunostaining for phosphoserine in ovarian cortex of FF and RF hens. **B.** Higher magnification of phosphoserine positive vesicles (white arrows) in the oocyte. **C.** Immunostaining for phosphotyrosine in ovarian cortex of FF and RF hens. **D.** Negative control section incubated with secondary antibody only. Scale bar = 100 µm, except in panel B, scale bar = 10 µm. FF = full-fed. RF = restricted-fed.

Broiler Breeder (BB)	Preovulatory follicles Mean+/-sem	Prehierarchical cohort Mean+/-sem
Full-fed (n=8)	11.6 +/- 1.0 [b]	11.0 +/- 1.9 [b]
Restricted-fed (n= 8)	6.8 +/- 0.3 [a]	5.0 +/- 0.8 [a]
Laying hen (n= 3)	5.4 +/- 0.12 [a]	10.7 +/- 1.5 [b]

Table 2.1. Number of preovulatory (9-45 mm) and prehierarchical (6-8 mm) follicles
[abc] Significant differences, P<0.05

Gene symbol	Forward	Reverse
ACTB	GCGCAAGTACTCTGTCTGGA	TAGAAGCATTTGCGGTGGA
AMH	GAGCAGCATTTTGGGGACT	CTGAGGAGGTGCTGGAAGA
BMP6	TACCAAGTGCTGCAGGAACA	CTGAGGATTCATCACCCACA
BMP15	TTATCCCCAGCAAACAGCA	GGTGTCGTTGAGGAAGAGGA
CYP11A1	CAAGACATGGCGTGACCA	TGAAGAGGATGCCCGTGT
CYP19	CACATGGGAGATTTCTCTGGA	ACGTGAAATACGCTGGAGGA
GDF9	AATCCCAAAGGCCCATAAGA	GAAGAGCAAATCCACCGAGT
HSD3B	CAGCTGCTCTGGGAAGTCA	GGGTCACCCCTGCAGTTT
STAR	CCAGCGTCAAAGAGGTGAA	GAGCACCGAACACTCACAAA

Table 2.2. Primer sequences used for qPCR
Sequences are 5' to 3'.

Chapter 3. *Ad Libitum* (Full) Feeding of Young Broiler Breeder Hens Causes Increased Follicular Growth at 10 Weeks of Age

Introduction

Modern broiler chicken lines have been genetically selected for fast growth and large muscles, along with increased feed consumption. Unfortunately, this has led to decreased reproductive efficiency in parent lines (broiler breeders). Broiler breeder hens exhibit production of surplus follicles, development of double hierarchies, and inconsistent egg-laying (Yu et al. 1992b; Hocking and McCormack 1995; Chen et al. 2006. Little is known about effects of overfeeding on ovarian function in immature broiler-breeder hens or how early ovarian dysfunction begins in overfed animals. In the previous chapter, we demonstrated that overfeeding causes increased development of small cortical follicles in prepubertal broiler-breeder hens at 16 weeks of age (Chapter 2). Puberty begins at about 20 weeks of age (Cobb 2008) but increased feed consumption may have accelerated puberty onset (Onagbesan et al. 2006). Thus, we examined ovarian morphology at an earlier prepubertal age of 10 weeks. Findings showed that full feeding advanced follicular development in ovaries of broiler breeder hens as early as 10 weeks of age as indicated by heavier ovaries and a greater number of larger-sized follicles in the full-fed (FF) hens compared to restricted-fed (RF). But, the detailed molecular mechanisms explaining this increased in ovarian development remain to be discovered.

Materials and Methods

Animals

Twenty female day-old Cobb 500 chicks were generously donated by Longenecker's Hatchery (Elizabethtown, PA). In accordance to the breeder's guidelines (Cobb-Vantress 2008), from hatching until 2 weeks of age, chicks were fed *ad libitum*, then divided into two experimental groups of 10 birds each. One group continued *ad libitum* (full) feed and the second group was restricted-fed, according to the breeder's guidelines, being closely monitored for weight gain to assure proper growth rate so as to reach correct weight at 10 weeks of age. The same starter, grower, and finisher rations were fed to both groups. Feed was purchased from Wenger Feeds (Rheems, PA). All pullets were started (Day 1) on 24 hours of daylight, slowly decreasing to 8 hours by Day 14 and remained on 8 hours of daylight until the end of the experiment. Hens were weighed and euthanized by cervical dislocation. Ovaries were removed, weighed, and processed according to experiments described below. All procedures described herein were reviewed and approved by the Pennsylvania State University Institutional Animal Care and Use Committee, and were performed in accordance with The Guide for the Care and Use of Agricultural Animals in Research and Teaching (Federation of Animal Science Societies 2010).

DAB immunostaining

Ovaries were collected from full-fed (FF) and restricted-fed (RF) broiler breeder hens (n = 10/group). Small sections (<0.5 cm^3) of cortex were fixed in 4% paraformaldehyde in phosphate buffered saline (PBS) overnight and embedded in

paraffin. Embedded tissues were sectioned (5 μm) on a rotary microtome HM 355 (MICROM International GmbH, Walldorf, Germany); sections were mounted on positively charged microslides and allowed to dry overnight. Three randomly selected animals from each group (FF and RF) were chosen for immunostaining. Sections were dewaxed in Histoclear (Electron Microscopy Sciences, Hatfield, PA), and incubated in antigen retrieval solution (Dako, Glostrup, Denmark) as described previously (Sun et al. 2015). After rinses in ddH_20, sections were incubated in 3% hydrogen peroxide for 10 minutes to eliminate endogenous peroxidase activity, rinsed in ddH_20, rinsed in TBST (tris-buffered saline, 0.1% Tween-20), then incubated in goat blocking buffer (TBST, 5% goat serum) at room temperature for sixty minutes to suppress nonspecific binding. Sections were then incubated overnight at 4^0C with the following primary antibodies: anti-Phosphoserine (1:400, Zymed, #61-8100) and anti-Phospho-FoxO3a (1:400, Cell Signaling, #9465). The next day, tissue sections were stained with DAB immunostaining using Cell Signaling kits according to manufacturer's recommendations (Cell Signaling, Danvers, MA). Sections were rinsed in TBST, followed by a 30-minute incubation with SignalStain Boost IHC Detection Reagent (an amplification reagent with anti-host immunoglobulins-HRP). DAB chromogen was mixed with hydrogen peroxide buffer and applied to the sections. Oxidation of DAB quickly results in formation of a dark brown precipitate at enzymatically active sites of proteins-of-interest. Color intensity increases quickly so must be monitored to avoid over-staining. Sections were submerged in water to stop the reaction.

Histology for follicle counting

A single transverse section (<1 cm^3) was excised from the center (widest part) of each ovary and fixed in 4% paraformaldehyde for 48 hours. Embedding and sectioning is described above. Sections were stained with hematoxylin and eosin using standard methods. Brightfield images were acquired on a Nikon Te200 compound microscope (Melville, NY) with an attached DP20 Olympus digital color camera and DP software (Center Valley, PA). The diameter of every follicle was measured in sections of ovarian cortex from randomly selected FF and RF hens (n = 3 each) and proportions of follicles <100, 100-300, 300-500, and >500 μm in diameter were calculated. Proportions were arcsine-transformed for statistical analysis.

Results

Effect of feed on ovary and body weights at 10 weeks

To determine effects of feed on ovarian development before puberty, female broiler breeders (Cobb 500) were raised in full- (FF) and restricted-fed (RF) conditions until 10 weeks of age. Ovaries were removed for morphological, protein and mRNA analysis. Development of the ovarian cortical surface was similar between FF and RF at 10 weeks (Figure 3.1C), as opposed to increased development observed at 16 weeks in FF as compared to RF ovary (Figure 3.1D). Ovary and body weights of FF hens were about three times those of RF at both 10 (Figure 3.1A, B) and 16 weeks of age (Chapter 2, Figure 2.1A, B). At 10 weeks, FF ovary weights were 0.79 ± 0.04 g (n=9) vs 0.29 ± 0.02 g (n=6) for RF (Figure 3.1A), and FF body weights were 4.00 ± 0.10 kg vs 1.25 ± 0.01 kg (n=10 each) for RF (Figure 3.1B). Ovary-to-body weight ratios were similar

between FF and RF at 10 weeks, FF and RF at 16 weeks, and RF at 10 and 16 weeks, but was significantly (P=0.005) smaller in FF at 10 than at 16 weeks (Figure 3.2). The ratios of ovary to body weight at 10 weeks were, 0.201 in FF and 0.217 in RF with an SEM of 0.01 for both. At 16 weeks, ratios were 0.254 in FF and 0.258 in RF, with SEMs of 0.012 and 0.024, respectively (Figure 3.2).

Effect of feed on cortical follicle growth at 10 weeks

To determine proportions of follicles of different sizes in ovarian cortex of FF and RF hens, sections from the center (widest point) of the ovary (n=3 each of FF and RF) were stained with hematoxylin and eosin and follicles counted. Ovaries of FF hens contained a greater proportion of follicles between 100-300 µm, coincident with moderately smaller proportions of follicles <100 µm in diameter, as compared with RF (Figure 3.3A).

No differences in immunolocalization of phosphoserine or phospho-FOXO3

The overall levels of serine phosphorylation are one measure of kinase activity. To assess whether increased feed affects this measure, sections (n=3) of FF and RF ovarian cortex were incubated with anti-phosphoserine. Immunolocalization of phosphoserine was similar in both FF and RF at 10 weeks. In the oocyte, staining localized to cytoplasm and was stronger around edges and in the nucleus. Unlike at 16 weeks (Figure 2.5), no vesicle-like structures were observed. Phosphoserine staining was also apparent in granulosa cells and in discrete cells within stroma.

FOXO3 is a transcription factor involved in folliculogenesis. To see if the phosphorylated (active) state of FOXO3 is affected by differences in feed consumption, phospho-FOXO3 was measured in FF and RF ovarian cortex sections in 10-week-old hens. Staining was seen throughout cortical structures, including stroma, oocyte cytoplasm, and granulosa and theca cell surfaces. Theca and granulosa cells showed greater staining than surrounding structures. Only the oocyte nucleus showed no staining (Figure 2.8C). No localization differences were observed between the FF and RF.

Discussion

There is an association with overfeeding and compromised ovarian function in adults of many species (Correa and Jacoby 1978) but mechanisms are still being studied. To measure effects of feed consumption on follicle growth before puberty, broiler breeder hens were raised on full (FF) or restricted feed (RF) from hatching until 10 weeks of age. Initial gross observations of ovaries at 16 weeks (Chapter 2) revealed profoundly more ovarian development in FF hens, seen first by more-developed sulci (folds), a sign of cortex distortion that occurs with increasing follicle growth (Waddington and Walker 1988) and second, by emergence of follicles from the cortex. Full feeding may have pushed the 16-week-old hens closer to puberty (Yu et al. 1992a, 1992b; Pishnamazi et al. 2014). Therefore an earlier age of 10 weeks was chosen for a second group of hens. Findings indicated advanced follicle development as early as 10 weeks of age, seen in increased ovarian weight and follicle growth with full feeding (FF). A shift toward larger-sized follicles (100-300 μm) accompanied by a decrease in the

proportion of the smallest follicles (<100 um) suggested greater activation from the primordial follicle pool. Ovary-to-body weight ratios were similar between FF and RF at 10 weeks and 16 weeks. Ratios were also similar between RF of 10- and 16-week-old hens, but not between FF at 10 and 16 weeks, indicating that feed has a greater effect than age on the ratio, and a greater effect on body weight than ovary weight at the younger age. These data are in agreement with others indicating non-uniformity of broiler-breeder pullet carcass traits measured during the rearing period (4-18 weeks) due to feeding level (Yu et al. 1992a, 1992b) or feeding patterns (Pishnamazi et al. 2008; Zuidhof et al. 2015).

Kinases are enzymes that add phosphate groups to serine/threonine and/or tyrosine residues of proteins, thereby changing protein behavior (Krebs 1983). An important group of serine/threonine-specific kinases are mitogen-activated protein kinases (MAPK) which regulate many cellular processes including proliferation, differentiation, gene regulation, and survival (reviewed in Pearson et al. 2001; Gerits et al. 2008). Immunostaining for phosphoserine at 10 weeks of age indicated no differences in localization between FF and RF.

FOXO3 is a transcription factor expressed in the nucleus of both oocyte (John et al. 2008) and granulosa cell (Pisarska et al. 2009). The non-phosphorylated state of FOXO3 is contained within the nucleus and is actively involved in suppressing primordial follicle activation (Castrillon et al. 2003; John et al. 2008). In its phosphorylated state, FOXO3 is sequestered in the cytoplasm (John et al. 2008). Foxo3 null female mice undergo complete depletion of ovarian follicles, and are sterile by 15 weeks of age (Castrillon et al. 2003), while mice fed a high fat diet before puberty

experience impeded ovarian follicle development by 15 weeks of age as a result of increased activity of Foxo3 (Wu et al. 2016). Also, in the hen, as follicles increase in size from 0.5 to 2.0 mm in diameter, *FOXO3* mRNA increases in abundance (Diaz et al. 2011). This current work showed no differential staining pattern between FF and RF for phospho-FOXO3 in cortex of 10-week-old hens. No measures of total protein were done in this present study, but because of the greater proportions of follicles <100 µm observed in ovaries of RF compared to FF hens, it is reasonable to hypothesize that a greater amount of non-phosphorylated FOXO3 would be observed in follicles of RF hens.

Summary

The present findings indicate that over-feeding during the growth (rearing) phase causes increased cortical follicle growth as early as 10 weeks of age in boiler breeder hens. Localization of immunostaining for both phosphoserine and phospho-FOXO3 were similar for both FF and RF. But continued research is necessary to tease out the mechanisms underlying effects of feed on follicle growth.

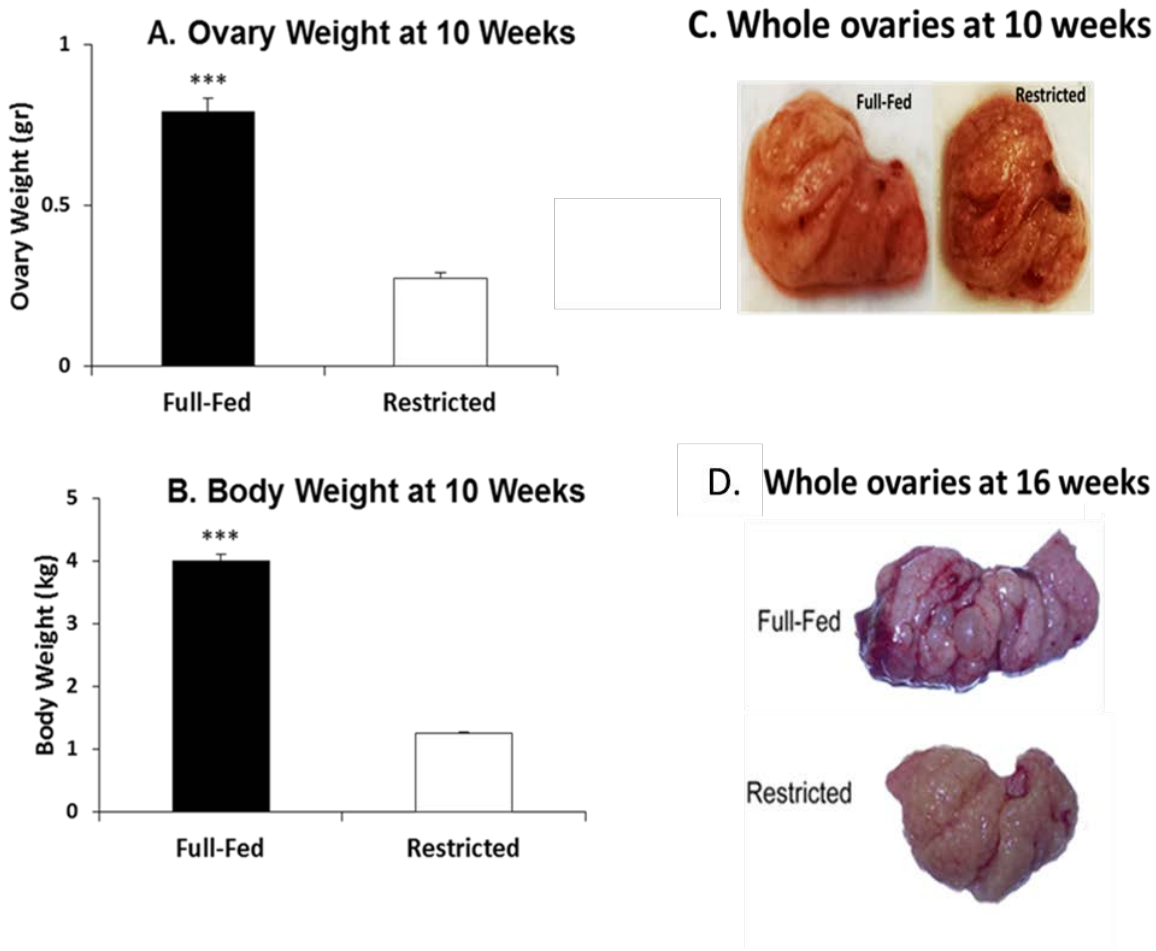

Figure 3.1. **A.** Ovary weights at 10 weeks, n=6 RF and 9 FF. **B.** Body weights in FF and RF at 10 weeks, n=10. **C.** Images of whole ovaries from FF and RF at 10 weeks. **D.** Images of whole ovaries at 16 weeks. ***Significant differences by Student's *t*-test, P< 0.001. FF = full-fed. RF = restricted-fed.

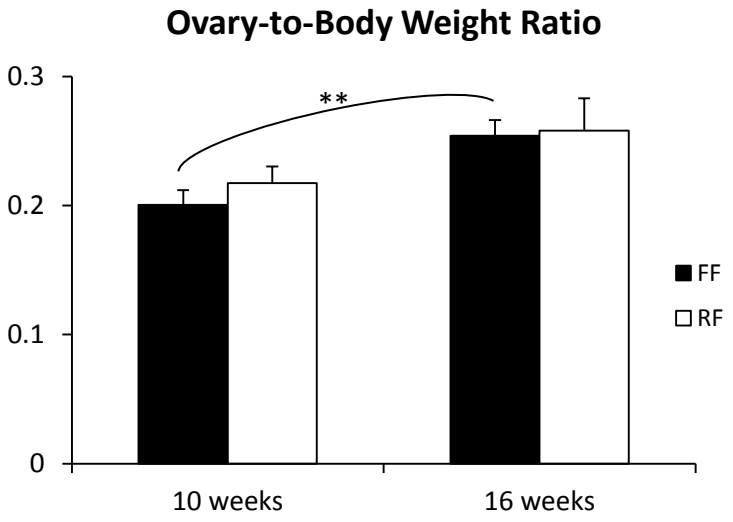

Figure 3.2. Ovary-to-body weight ratios in FF and RF broiler-breeder hens at 10 and 16 weeks of age. **Significant difference by Student's *t*-test, P= 0.005. FF = full-fed. RF = restricted-fed.

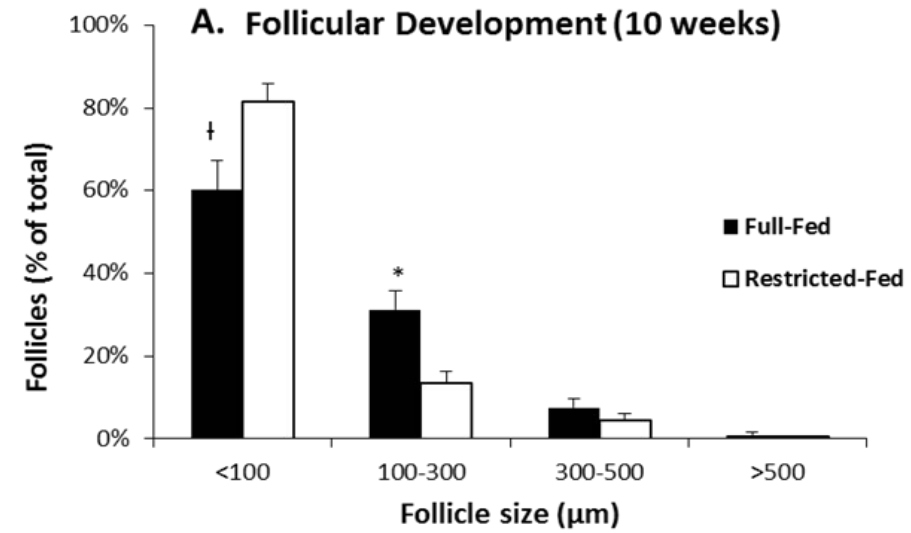

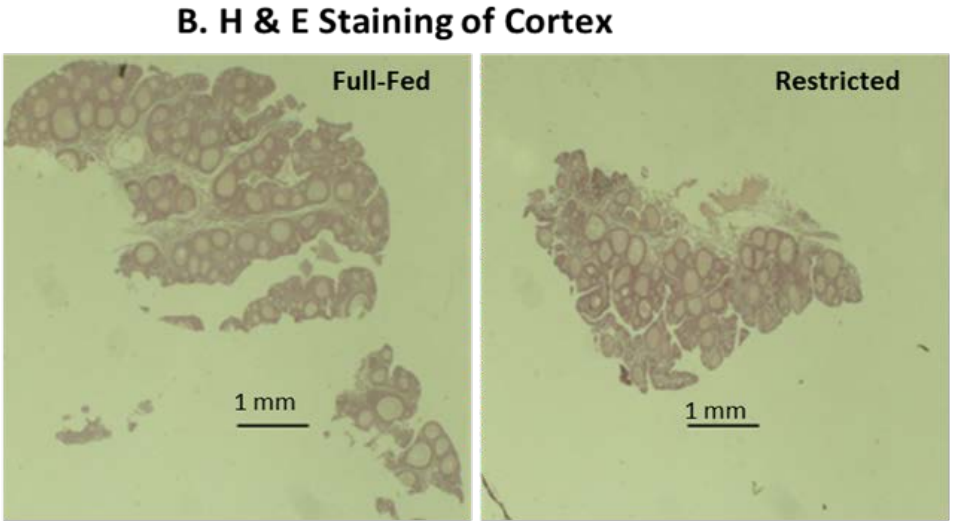

Figure 3.3. 10 weeks. **A.** Proportions of different sized follicles (<100, 100-300, 300-500, and >500 µm) in FF and RF broiler-breeder hens, n=3. **B.** Hematoxylin and Eosin staining of cortex. Student's *t*-test *P<0.05; ŧP<0.10. FF = full-fed. RF = restricted-fed.

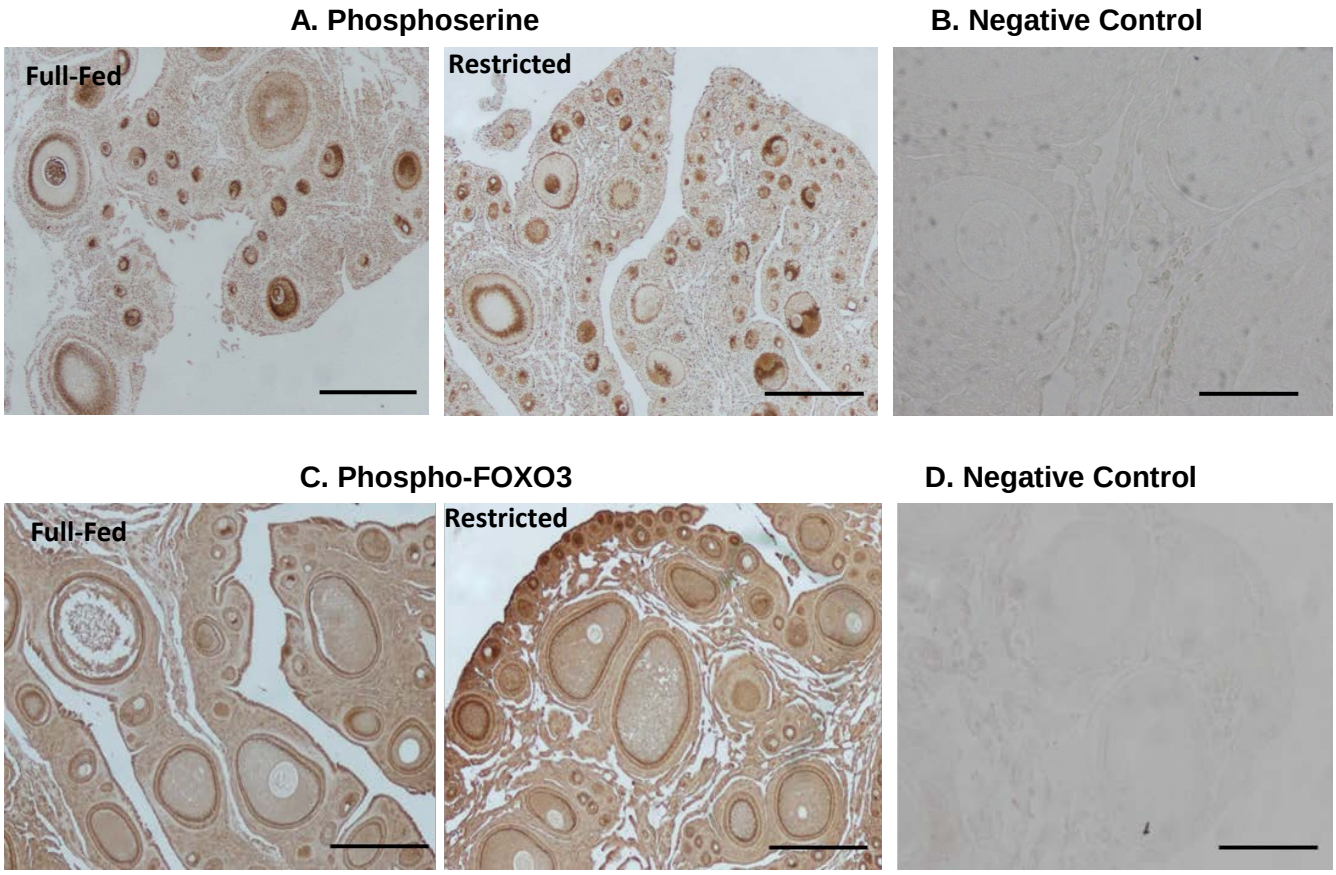

Figure 3.4. 10 weeks. DAB immunostaining in ovarian cortex of FF and RF broiler-breeder hens for (**A**) phosphoserine and (**C**) phospho-FOXO3. Negative control sections **(B** and **D)** incubated with secondary antibody only. n=3 each. Scale bar = 200 µm. FF = full-fed. RF = restricted-fed.

Chapter 4. Gene Expression Patterns in Ovaries of Prepubescent Broiler Breeder Hens Fed Ad Libitum from Hatching

Introduction

The genetic selection for fast growth and increased feed consumption of the broiler chicken has proven problematic for the parent stock. Consequences for the broiler breeders are an inability to control feed intake to match what is needed for proper growth and development, and an accompanying increase in fertility problems (Yu et al. 1992b; Hocking and McCormack 1995; Chen et al. 2006). Previously, we have shown that development of cortical follicles is associated with changes in transcript abundance (Diaz et al. 2011) and that overfeeding causes increased development of small cortical follicles in broiler-breeder hens (Chapters 2 and 3). Thus, we sought to further identify changes in transcript abundance in cortical tissue of prepubertal broiler breeder hens. Microarray analysis was performed on ovarian cortex transcriptome of full- and restricted-fed 16-week-old hens. Following validation of microarray results by qPCR, findings revealed differentially expressed genes (DEG) involved in extracellular matrix structure and remodeling, cell adhesion, cholesterol and steroid biosynthesis, and neuroactive ligand-receptor interaction. These genes can be used as markers of cortical follicle development in the chicken and open up new avenues of inquiry into regulation of cortical follicle growth in birds.

Materials and Methods

Animals

Day-old Cobb 500 chicks were generously donated by Longenecker's Hatchery (Harrisburg, PA) for these experiments. Twenty chicks were raised to 10 weeks of age; eighteen were raised to 16 weeks of age in accordance to the breeder's guidelines (Cobb-Vantress 2008). From hatching until 2 weeks of age, chicks were given full access to feed, after which each age group was divided in half. One treatment group continued on full-feeding (FF) and the second was restricted-fed (RF) according to the breeder's guidelines, being closely monitored to assure recommended growth rate at 10 or 16 weeks. The same starter, grower, and finisher rations were fed to both groups. Feed was purchased from Wenger Feeds (Rheems, PA). All birds remained on 8 hours of daylight until the end of the experiment. Hens were weighed and euthanized by cervical dislocation; ovaries were removed, weighed, and processed according to the experiments described below. All procedures described herein were reviewed and approved by the Pennsylvania State University Institutional Animal Care and Use Committee, and were performed in accordance with The Guide for the Care and Use of Agricultural Animals in Research and Teaching (Federation of Animal Science Societies 2010).

RNA processing

Small sections (<1 cm^3) of cortex from each ovary were placed in RNAlater (Thermo Fisher Scientific, Waltham, MA). Total RNA was isolated from ovarian cortex using the RNAeasy mini kit (Qiagen, Valencia, CA) according to the manufacturer's

instructions and quantified using a NanoDrop 2000 spectrophotometer (Thermo Fisher Scientific, Waltham, MA). For Affymetrix array hybridization, RNA was extracted from the 16-week-old ovarian cortex samples and delivered to the Genomics Core Facility at the Huck Institutes of the Life Sciences at Penn State University for subsequent processing. Sample quality was evaluated on an Agilent Bioanalyzer 2100 (Agilent Technologies, Santa Clara, CA) and only samples with an RNA integrity number (RIN) above 9 were used. All samples (n=9 each) of FF and RF cortical RNA were of high quality (RIN>9). Three samples each were chosen randomly for microarray analysis. RNA processing and chip hybridization were conducted using 3' IVT Express Kit (Thermo Fisher Scientific, Waltham, MA) following manufacturer's recommendations. For qPCR validation, independent samples from both 10- and 16-week-old ovarian cortex were analyzed. RNA quality and quantity were assessed on the Experion Automated Electrophoresis System using the Experion RNA StdSens analysis kit (Bio-Rad, Hercules CA). The Experion features an RNA quality indicator (RQI) for assessment of RNA integrity. This number is between 1 (completely degraded) and 10 (intact RNA). For all of the samples (10-week-old and independent 16-week-old) RQI numbers were between 8.5 and 9.7. A number greater than 7 was considered acceptable. Cortex samples from 4 randomly selected FF and RF hens at both 10 and 16 weeks were analyzed for validation. Equal amounts of total RNA (1 µg) were reverse transcribed into cDNA using the QuantiTect Reverse Transcription kit (Invitrogen, Carlsbad, CA) according to manufacturer's instructions, diluted 1:5 with nuclease-free water and stored at -20^{0}C. Gene specific primers (Tables 4.11and 4.12) were designed with the software Primer3, version 0.4.0 (University of Tartu, Tartu,

Estonia). Amplification reactions were prepared in duplicate, in 10 µl volumes containing 10 ng cDNA, 200 nM of each primer, and 5 µl 2X PerfeCTa SYBR Green FastMix Low Rox (Quanta Biosciences, Inc., Gaithersburg, MD), then run on a 7500 Fast Real-Time PCR System (Applied Biosystems, Foster City, CA) using default fast conditions: initial hold at 95^0C for 20s, followed by 40 cycles each at 95^0C for 3s and 60^0C for 30s. Melting curves were generated to assure only one product was amplified. The C_T value for each reaction was determined using 7500 software (v.2.0.4). Quantification was done using the $2^{-\Delta\Delta}{}_{CT}$ method (Livak and Schmittgen 2001) with *RPL19* mRNA as the normalizer. *RPL19* has been used as a normalizer in chicken granulosa cells (Johnson and Lee 2016). All amplification products were sequenced for gene verification. Values shown for transcript abundance are the mean ± SEM.

Analysis of microarray data

Six Affymetrix GeneChip Chicken Genome Arrays were purchased from Affymetrix (Santa Clara, CA). Each array contains 33,457 chicken and viral transcripts, which allows for analysis of over 28,000 chicken genes. Information for sequences are publicly available from GenBank®, UniGene (Build 18; 15 May 2004), and Ensembl (version 1, released May 2004). Probe sets on the array were designed with 11 oligonucleotide pairs to detect each transcript. RNA from ovarian cortical tissue of one 16-week-old animal was hybridized to one array, totaling three FF and three RF arrays.

Software for analysis

Two programs were employed in analysis of the microarray data. Probe intensities for each array were converted to a tabular format and stored in a .DAT file (GeneChip Expression Analysis Technical Manual P/N 702232 Rev. 3). The .DAT files were then imported into the first program, Array Star 11.0.0 (DNASTAR, Inc., Madison, WI). The data were normalized using Robust Multi-array Average (RMA) which is most commonly used with Affymetrix chips (Irizarry et al. 2003). Expression levels were averaged for the three RF and the three FF. FF was compared to RF (control), fold changes were generated and the 33,457 transcripts were ranked from the most abundant to the least abundant in FF. To determine significant ($P<0.05$) differences in transcript abundance, Student's *t*- test was applied to each gene.

Two gene lists were generated with an arbitrary cut off value of 2-fold change; one list contained transcripts with greater and one with lesser abundance in FF (relative to RF) and imported into the second program, a computational database called DAVID v6.7 (Database for Annotation, Visualization and Integrated Discovery) at https://david.ncifcrf.gov/home.jsp. DAVID is a compilation of multiple databases and analytical tools that are used in combination to help identify particular pathways and biological functions from large data sets (Huang et al. 2009a; Huang et al. 2009b). Outputs from DAVID are described in the Results section.

Results

Data analysis with DAVID software

ArrayStar generated a list of the >33,000 transcripts from the microarray, ranked from the most abundant to the least abundant in FF, relative to RF. The top most and least abundant transcripts with at least a 2-fold change were used for subsequent analysis. Duplicate and unannotated genes were removed resulting in151 DEG with greater abundance (Table 4.1 in Appendix) and 237 with lesser abundance (Table 4.2 in Appendix) in FF compared to RF samples. The two lists were then imported into DAVID to help organize the genes into groups of biological relevance. DAVID placed the DEG into three categories; 1) genes of similar biological function, 2) Gene Ontology (GO) Terms, and 3) Kyoto Encyclopedia of Genes and Genomes (KEGG) pathways.

To enrich for genes of similar biological function, DAVID uses the software EASE (Expression Analysis Systematic Explorer) (Hosack et al. 2003), a variation of the Fisher's Exact Test. Drawing on information from published databases and experiments, the software assigns individual genes to sets based on biological relevance. Gene grouping allows the researcher a quick view of areas of interest (Huang et al. 2007). An enrichment score is calculated for the set based on the representation of the set to the list, which is compared to all known genes of that function in the genome. If the genes in the set have a greater representation in the list than can be explained by chance, it is considered significant. A score of 1.3 is equivalent to a p-value of 0.05, but the group enrichment scores are relative rather than absolute values. A higher score for a set indicates that those genes are over-represented in the set. Importantly, all gene sets are potentially interesting. Sets of

enriched genes with greater abundance in FF are listed in Table 4.3. Sets with lesser abundance in the FF are in Table 4.4.

The Gene Oncology Consortium (http://geneontology.org) was formed in 1998 to develop a consistent naming convention for genes, gene functions and products. The consortium developed three ontologies: biological processes, cellular component, and molecular functions (Ashburner et al. 2000). Its strength lies in its ability to match lists of genes to GO terms for biological relevance (Boyle et al. 2004). In this microarray experiment, the top 11 GO terms for transcripts with greater abundance in FF are listed in Table 4.5, and for lesser abundance in FF in Table 4.6.

The DEG were also sorted according the KEGG database (http://www.genome.jp/kegg). KEGG pathways are compiled from known and published biological interactions, gene and protein databases, and molecular networks for linking genomes to life at a cellular level (Kanehisa et al. 2003). Pathways identified in this experiment are in Tables 4.7 and 4.8 for gene transcripts of greater and lesser abundance, respectively, in 16-week-old FF hens.

Finally, DAVID compiles the data from these three categories to identify fundamental themes of biological relevance. There are six themes revealed in this microarray analysis: 1) extracellular matrix structure and remodeling, 2) cellular and biological adhesion, 3) cholesterol and steroid biosynthesis, 4) neuroactive ligand-receptor interaction, 5) transcription regulation, and 6) defense response to bacterium.

Category 1: Gene Enrichment Groups

Gene enrichment groups with greater abundance in 16-week-old FF hens

The list of 151 DEG with greater abundance in FF was imported into DAVID for analysis, but only relatively few genes were selected for any category. For gene enrichment, 23 genes were assigned to five sets; the first three sets showed significant enrichment scores (≥2.8) and contained genes found in extracellular matrix (ECM). The fourth set included RAS and SAR1 small GTPases, and the fifth consisted of genes involved in early development (Table 4.3).

Gene enrichment groups with lesser abundance in 16-week-old FF hens

The list of DEG with lesser abundance in FF contained 237 genes. After import into DAVID, less than 30% of them were assigned into gene enrichment groups. Sixty three genes were filtered into nine enrichment sets (Table 4.4). Four sets had significant scores (≥1.8), and included transcription factors and homeobox genes, as well as gene transcripts involved in defense response to bacterium and neuron-related transcription regulation. Set 5 contained ion channels; Set 6, calcium binding; Set 7, metal binding; Set 8, neurotransmitter receptors; Set 9, kinases.

Category 2: Gene Ontology (GO) terms

Terms associated with DEG of greater abundance in FF

The next category used by DAVID was GO terms. In the three ontologies of GO terms; Biological Process, Cellular Component, and Molecular Function, 39, 27, and 33 genes, respectively, were identified with greater abundance in the FF, from the list of

151 genes (Table 4.1 Appendix). The top 11 GO terms represented by these genes are listed in Table 4.5, falling into three main themes: ECM, Adhesion, and Steroidogenesis. ECM again was the main focus, having 31 genes associated with 4 - 6 ECM GO terms. The second theme, Adhesion, claimed 13 genes, but eight had multiple functions and overlapped with the ECM terms, leaving five clearly in Adhesions. Steroidogenesis was comprised of 6 unique genes. The individual genes within each GO term are listed in Table 4.6.

Terms associated with DEG of lesser abundance in FF

From the list of 237 genes (Table 4.2 Appendix), 44-58 genes were assigned to only two ontologies (molecular function, and biological processes). The top 11 GO terms with associated genes are listed in Table 4.7. Twenty-seven genes associated with Transcription theme. Eighteen genes were assigned terms for tissue and embryonic organ growth and morphogenesis, which did not fall into any of the six major themes. Individual genes within each GO term are listed in Table 4.8.

Category 3: KEGG pathways

Pathways from DEG with greater abundance in FF

The third category, KEGG pathways (Table 4.9), revealed four pathways from the list of 151 genes (Table 4.1 Appendix), but again with much gene overlap. The first two pathways, ECM-Receptor Interaction and Focal Adhesion shared eight out of 11 genes: *COL1A2, COL3A1, COL4A2, COL6A1, COL6A2, COL6A3, FN1,* and *LAMA2*. But ECM-Receptor Interaction also included *CD36*, while Focal Adhesion also included *PTEN* and

MYLK. The remaining two pathways were Steroid Hormone Biosynthesis and Androgen and Estrogen Metabolism which shared three out of four genes: *CYP19A1, HSD3B1, HSD17B1*, with *CYP11A1* being included in Steroid Hormone Biosynthesis.

Pathways from DEG with lesser abundance in FF

Three KEGG pathways (Table 4.10) were identified from the list of 237 genes (Table 4.2 Appendix): Cell Adhesion Molecules (6 genes: *CD80, CLDN11, CLDN18, NRXN3, NLGN1*, and *NEGR1*), Neuroactive Ligand-Receptor Interaction (9 genes: *CHRM5, GABRA5, GABBR2, GRID1, GRM1, MC2R*, *OXTR, DRD4*, and *GABRA5*), and Map Signaling Pathway (8 genes: *CACNA1C, CACNA2D3, MECOM, FGF13, MAPK12, NGFB/ NGF, RPS6KA2* and *TGFBR2*). The genes listed in the three pathways were specific to those pathways, with no overlapping functions.

Selection of differentially expressed genes for qPCR validation

To help choose a focus for this thesis, and to increase confidence in the microarray results, representative genes were selected for validation by qPCR on an independent group of cortical samples (n=4 each of 10- and 16-week-old RF and FF). The selected genes had to fit two criteria: 1) they fell into at least one of the three DAVID categories and; 2) they were cleanly differentially expressed between the 3 FF and 3 RF birds, with no overlap of values in the microarray data set. For example, *Col6a1* was listed for ECM involvement in Gene Enrichment, GO terms, and KEGG pathway. And its expression values were 11.4, 11.2, 11.3 in FF and 10.3, 9.6, 9.4 in RF. So it was selected for validation. Groups of representative DEG that spanned the

categories generated by DAVID were chosen from the lists of both greater and lesser abundance in FF. Primers were designed and tested by qPCR to verify a single product by melting curve analysis and sequencing. However, as the comparisons progressed, and the literature indicated, more genes were selected from the two DEG lists to help complete an interpretation of the data. For example, a major gene transcript in our analysis, *VIPR2*, (Vasoactive Intestinal Polypeptide Receptor 2), was not included in any of the DAVID categories. But it was the most differentially expressed gene in the entire array, and the literature indicated strong connections between Vasoactive Intestinal Polypeptide (VIP) and steroidogenesis. It was selected along with *VIP* and *VIPR1* to include in the analysis. Ultimately, 43 DEG were used in the comparison of FF and RF on independent ovarian cortex samples, consisting of 26 with higher abundance (Table 4.11) and 17 with lower abundance (Table 4.12) in FF. The normalizer gene, *RPL19*, is in Table 4.12.

qPCR validation results from both 10- and 16-week-old hens

The 43 genes chosen for validation spanned several areas of biological significance based on the six fundamental themes provided by DAVID outputs: 1) Transcription Regulation; 2) Defense Response to Bacterium; 3) Extracellular Matrix Structure and Remodeling; 4) Cell Adhesion; 5) Cholesterol and Steroid Biosynthesis; and 6) Neuroactive Ligand-Receptor Interaction. Many genes have more than one function and DAVID placed them in several categories. Understandably, the themes are intimately connected by shared genes and pathways, but for this current work, each gene was placed in only one theme based on the best interpretation of the data, to help

understand their relevance and contribution to the observations of increased follicle growth in the full-fed hens.

Themes 1 and 2. Transcription Regulation and Defense Response to Bacterium

Results of qPCR analysis were not in agreement with those of the microarray for these first two themes. None of the gene transcripts selected could be validated on independent samples of ovarian cortical tissue from either 10- or 16-week-old hens (Figure 4.1).

Theme 3. Extracellular Matrix Structure and Remodeling

At 16 weeks, laminin (*LAMA2*), a component of basal lamina, and the collagen (COL) transcripts all showed greater abundance in FF compared to RF, while at 10 weeks there was no difference. Matrix metallopeptidases (MMP), which degrade ECM, had large sample variability in FF for *MMP9* (gelatinase) at 16 weeks and *MMP10* (stromelysin) at 10 weeks obscuring any possibility of significance. But, at 16 weeks, *MMP10* is clearly greater in FF. Four and a half LIM domains 2 (*FHL2)*, involved in assembly of extracellular membranes, approached significance in FF at both ages. Fibronectin and versican, which bind a variety of ECM components affecting local organization and molecular interactions, had significantly ($P \leq 0.02$) greater abundance in FF than in RF at 16 weeks, while approaching significance ($P \leq 0.08$) in FF at 10 weeks. Annexin A2 (*ANXA2*), which regulates many cellular functions, was the only transcript in this theme to show a significantly ($P \leq 0.02$) greater abundance in FF at both ages (Figure 4.2).

Theme 4. Cell Adhesion

Half of the genes had a greater differential expression at 10, than at 16 weeks of age: *CD36* (a scavenger protein); *MYH11* (a smooth muscle myosin which is a contractile protein that utilizes ATP hydrolysis and actin binding to lend elasticity); periostin (*POSTN*, a cell-adhesion protein that influences ECM restructuring); and phosphatase and tensin homolog (*PTEN*, a phosphatase) were all more abundant in FF than in RF. Claudin (*CLDN18)*, a component of tight junctions, monoglyceride lipase (*MGLL*), and cadherin (*CDH13),* a calcium-dependent cell-adhesion protein, all had greater abundance in FF at 16 weeks than at 10 weeks of age. *CCDC80,* which promotes cell adhesion and matrix assembly, was significantly (P≤0.04) more abundant in FF at both ages (Figure 4.3).

Theme 5. Cholesterol and Steroid Biosynthesis

The cholesterol transporter genes, *STAR* and *STARD4*, had greater abundance in FF than in RF at both ages. At 16 weeks the steroid biosynthesis enzymes, *CYP11A1, CYP19A1, HSD17B1* and *HSD3B2*, showed significantly (P<0.02) greater abundance in FF, but at 10 weeks, *CYP11A1* and *CYP19A1* only approached significance in FF and there was no difference in either *HSD17B1* or *HSD3B2*. Both of the cholesterol biosynthesis gene transcripts *DHCR24* and *HMGCR* are reductases and had greater abundance in FF at 16 weeks, but at 10 weeks, *DHCR24* showed a tendency towards significance while there was no difference in the rate-limiting *HMGCR* (Figure 4.4).

Theme 6. Neuroactive Ligand-Receptor Interaction

G protein-coupled receptors *CHRM5* (cholinergic receptor muscarinic 5) and *DRD4* (dopamine D4 receptor) are both adenylyl cyclase inhibitors. At 16 weeks both had less abundance in FF but at 10 weeks, only *DRD4* was significantly (P=0.01) less in FF. Of the ionotropic GABA A receptors, *GABRA3* was less abundant in FF at 10 weeks, while *GABRA5* was less abundant at 16 weeks. No differential expression was seen for either *VIP*, G protein-coupled receptors *GABBR2* and *VIPR1*, or ionotropic glutamate receptor (*GRID1*) for either treatment or age. But both *VIPR2* and *NELL2* (neural EGF-like 2) were significantly greater (P<0.02 and <0.05, respectively) in FF at both ages (Figure 4.5).

Discussion

Bioinformatics analysis

Microarray technology has been in existence for many years since its inception in the early 1990's (Fodor et al. 1991; Schena et al. 1995). A microarray is a form of gene expression profiling that allows observation of the activity of tens of thousands of genes at the same point in time, and is a powerful tool to detect relative differences in expression of groups of genes in two or more conditions. A finite number of DNA sequences (probes) of known genes amounts to several thousand and represents genome-wide coverage. Fluorescently labeled targets (sample RNA) hybridize to the DNA probes. The more target that hybridizes to the probe, the greater the intensity of the fluorescence, which determines the relative abundance of nucleic acid sequences in the target. Microarrays have been used extensively in the scientific community, but have

been under scrutiny for several years, particularly if the arrays are used for diagnostics, such as in cancer studies. Probe design and integrity, as well as choice of platform, method of normalization and, especially, the reliability of the measurements to detect fold changes of genes that are expressed at low levels, have all been discussed (reviewed in Draghici et al. 2006). Making sense of the large amount of information resulting from a microarray analysis can be daunting. How to identify differences between treatments and trust that these differences are real is a great challenge. Databases such as DAVID have become popular because they utilize several tools in combination to provide researchers with a large picture of how groups of genes are working together in their biological system.

From the large list of >33,000 gene transcripts that comprise the microarray, two small lists of DEG were produced for analysis in this project. Using a cut-off value of 2.0-fold difference, one list consisted of 151 genes with greater abundance and one consisted of 237 genes with less abundance in FF as compared with RF. After importing these lists into DAVID, six "themes" were identified: transcription regulation, defense response to bacterium, ECM structure and remodeling, cell adhesion, cholesterol and steroid biosynthesis, and neuroactive ligand-receptor interaction.

Transcription Activity and Defense Response Gene Transcripts

None of the genes in these two themes could be verified by qPCR (Figure 4.1). To clarify however, the samples of 16-week-old ovarian cortex used to validate all genes for this thesis had been stored at -80^{0}C for 5 years. An initial qPCR analysis performed within a year of collecting the samples did validate these genes (data not

shown). But, since tissue samples processed five years later were used in all other theme validations, it is unlikely that only genes involved in transcription and defense were selectively degraded. The ovarian cortical tissue at 16 weeks of age is a heterogeneous cell mixture, so individual pieces from the same ovary are most likely comprised of different cellular compositions.

Extracellular Matrix and Cell Adhesion Genes

In the present study, the largest sets of differentially expressed genes pertained to structural and proteinaceous ECM proteins. ECM proteins are found in all tissues of the ovary. They assemble many matrices to accommodate the particular needs of the cells. These include structural stroma, endothelium, basal lamina, and the membranes of granulosa and theca (reviewed in Rodgers et al. 1999). ECM proteins regulate morphology, communication, proliferation and steroidogenesis within the ovary (reviewed in Berkholtz et al. 2006). Many cell adhesion transcripts also identify with the extracellular matrix. Indeed, the contributions of cell adhesion molecules to the integrity of extracellular matrix and health of developing follicles are essential. In mouse primary follicles cultured in the absence of ascorbic acid, changes in the ECM and cell adhesion environment cause oocytes to become separated from the granulosa and theca layers due to breakdown of the follicular basement membrane (Tagler et al. 2014). Many of the differentially expressed transcripts discussed in the ECM/cell adhesion themes are also involved in regulating steroidogenesis. Progesterone production was greater from porcine granulosa cells grown on collagen (type I or type IV), laminin, or fibronectin than if plated on tissue culture plastic (Sites et al. 1996). Type IV collagen and laminin form

the backbone of basal lamina, which is located between the granulosa and theca cells (Rodgers et al. 1999). Production of steroid begins with cholesterol and transportation of low density lipids into the steroidogenic cells. Annexin 2 (ANXA2) may play a part in that process. ANXA2, which was greater in FF at both ages (Figure 4.2) inhibits proprotein convertase subtilisin/kexin type 9 (PCSK9) from binding to the low density lipoprotein receptor (LDLR) and causing its degradation (Ly et al. 2014), therefore allowing more lipid to enter the cell for cholesterol production. The microarray results showed greater abundance in FF for *LDLR* (Table 4.1), but primers were not designed for that gene, so could not be verified by qPCR.

Cholesterol and Steroid Biosynthesis Genes

Steroid hormones (progesterone, testosterone, and estradiol) are produced locally in the ovary, from the steroidogenic somatic cells within the cortex (Boucek and Savard 1969; Nitta et al. 1991; Gonzalez et al. 1994). Essential for ovarian development (reviewed in Bruggeman et al. 2002), steroids are derived from cholesterol that is either brought into the cell from the circulation via endocytosis or synthesized de novo from acetate, (reviewed in Azhar et al. 2003). In the present project, validation was done on gene transcripts involved in cholesterol biosynthesis and transport, as well as steroid biosynthesis (Figure 4.4). Cholesterol biosynthesis, which occurs in the endoplasmic reticulum, involves many enzymes. Two are depicted in the present study: 3-hydroxy-3-methylglutaryl coenzyme A reductase (*HMGCR*) and 24-dehydrocholesterol reductase (*DHCR24*) (reviewed in Sharpe et al. 2015). For processing into steroids, cholesterol must be transported into steroid-synthesizing

organelles. The first step is the binding of cholesterol to transporters for trafficking. One transporter, STARD4, is soluble and able to traffic cholesterol and sterols between the plasma membrane, smooth endoplasmic reticulum (ER) and mitochondria for processing (Soccio and Breslow 2003; Garbarino et al. 2012). The other is STAR, which is bound to the outer mitochondrial membrane and is critical for bringing cholesterol into position for its transfer to the inner mitochondrial membrane where it will come in contact with CYP11A1, the P450 side chain cleavage enzyme that catalyzes the first step in steroidogenesis, cleavage of the cholesterol side chain, producing pregnenolone (reviewed in Miller 2007). Subsequent processing of pregnenolone by the remaining three enzymes in the present analysis occurs in the ER. (Hydroxysteroid (17-Beta) Dehydrogenase 1 (HSD17B1), converts estrone to estradiol and androstenedione to testosterone; 3 beta-hydroxysteroid dehydrogenase (HSD3B2), converts prenenolone to progesterone and androstenediol to testosterone; and aromatase (CYP19A1) catalyzes the formation of aromatic estrogens (estrone and estradiol) from androgens (androstenedione and testosterone) respectively. In the present qPCR analysis, all transcripts of cholesterol and steroid biosynthesis genes had greater abundance in FF than in RF at 16 weeks. At 10 weeks of age, the shift toward increased abundance in the transcripts for steroidogenesis can already be seen particularly in the early rate-limiting steps (Figure 4.4). These data support the microarray results as well as other research showing that steroidogenesis is a sign of advanced follicle growth (Diaz et al. 2011).

Neuroactive Ligand-Receptor Interaction Genes

Neuronal contribution to ovarian development and steroid production has been studied for many years (Dominguez et al. 2011). The neurotransmitter vasoactive intestinal polypeptide (VIP) has become the molecule-of-interest in this thesis. Initial interest was due to results of this neural theme and later as the literature identified the role of VIP in steroidogenesis in rats (Rosas et al. 2015), mice (Kowalewski et al. 2010) and chickens (Johnson et al. 1994). Many of the gene transcripts in this theme are known to associate with VIP. Both *VIP* and vasoactive intestinal polypeptide receptor 1 (*VIPR*1) showed no difference in relative abundance with either treatment or age, but *VIPR2* had more than three-fold greater abundance in FF at both ages (Figure 4.5). VIPR1 and VIPR2 are G protein-coupled receptors that signal via cAMP. Abundance of cAMP in a cell is dependent on the amount of adenylyl cyclase present. Dopamine receptor D4 (*DRD4*) is an adenylyl cyclase inhibitor that, in the current project, was less abundant in FF at both ages. Experiments with cultured GH4C1 cells (somatomammotroph from pituitary) demonstrated that activation of DRD4 reduced VIP-stimulated cAMP levels by 50% (Sanyal and Van Tol 1997).

Two receptors for neurotransmitter gamma-aminobutyric acid (GABA), *GABRA3* and *GABRA5*, were also less abundant in ovaries of FF hens. GABA is a major inhibitory neurotransmitter in the brain, able to conduct neurotransmission through its ionotropic $GABA_A$ receptors (Pritchett et al. 1989). In studies with cat cerebral cortex, introduction of GABA antagonists significantly elevated the resting release of VIP (Wang et al. 1986). GABA binding sites had been identified decades ago in ovaries of human, associated with ovarian membranes (Erdo and Laszlo 1984), and rat, associated with

granulosa cells (Schaeffer and Hsueh 1982). But not until recently did research reveal a role for $GABA_A$ receptors in folliculogenesis in mammals. Although the mechanisms are unknown, $GABA_A$ subunit levels change in the cumulus cells (CC) of maturing oocytes in mouse (Dai et al 2016). Immature oocytes expressing a germinal vesicle (GV), or nuclear membrane, are fully grown but immature in that they contain the full complement of homologous chromosomes and are in meiotic arrest. With breakdown of the GV, meiosis resumes in metaphase I (MI) and the oocyte undergoes asymmetric division where one copy of the homologous chromosomes remains in the cytoplasm and the other is in the extruded polar body (reviewed in Holt et al. 2013). The MII oocyte is considered mature and able to be fertilized (reviewed in Trounson et al. 2001). In CC collected from GV and MII oocytes in mice, *GABRA3* mRNA abundance of MII decreased to ~one tenth that at the GV stage while *GABRA5* increased 2-fold from GV to MII. Protein abundance of GABRA5 in CC of GV oocytes was also approximately twice that of MII (Dai et al. 2016). The role of $GABA_A$ receptors in chicken folliculogenesis is largely unknown, but in the present study, abundance of *GABRA3* and *GABRA5* transcripts were significantly less ($P \leq 0.03$) in the ovarian cortex of FF at 10 weeks and 16 weeks, respectively, as compared to RF, and may reflect changes that occur with follicle development.

NELL2 (neural EGF-like 2) is a neural tissue-specific thrombospondin-like-1 protein which binds to protein kinase C (PKC) through its epidermal growth factor (EGF)-like domains (Kudura et al. 1999). It is expressed in glutamatergic neurons (Ha et al. 2008) and glutamate stimulates release of VIP in cerebral cortex of the cat (Wang et al. 1986). No literature was found on NELL2 functioning in the ovary, but in rat brain

NELL2 mRNA increases as the female approaches puberty, ultimately affecting GnRH secretion (Ha et al. 2008; Zhou and Li 2014). The pattern seen in brain is reflected in ovarian cortex of the present study where *NELL2* transcript abundance is about four-fold greater in FF than in RF at both prepubertal ages and hens given full feed attain puberty at an earlier age than hens on restricted feed (Onagbesan et al. 2006).

Summary

The microarray analysis and qPCR validation revealed four distinct gene expression themes present in the ovaries of full fed hens. These included genes involved in extracellular matrix organization and cell adhesion; steroidogenesis and neuroactive ligand-receptor interaction. These themes were not unexpected, especially in the context of the environment of developing follicles. Extracellular matrix remodeling, a dynamic process involving restructuring of varied components and an intimate relationship with signaling and adhesion molecules, must occur to accommodate growing follicles. A hallmark of advanced follicle growth is the ability to synthesize steroids. This was apparent in the cortex of the FF hens, which showed a greater abundance of transcripts for cholesterol transporters and the enzymes that support estrogen formation. A large part of steroid production is dependent on neuronal signaling. In association with vasoactive intestinal polypeptide, several neuroactive receptor gene transcripts in the present data highlight steroidogenic activity. The DEG within these themes offer insight into the complex developmental changes observed in ovaries of hens given full access to feed before puberty. In the present study, more transcripts were differentially expressed at 16 than 10 weeks, coincident with the

greater size and development of the ovary at that advanced age. Taken together, these data encourage investigation into possible mechanisms responsible for increased cortical follicle growth resulting from excess feed intake.

Table 4.3. Gene enrichment sets with greater abundance in FF at 16 weeks

Gene Set 1	Enrichment Score: 4.94
Gga.2073.1.S1_at	alpha-1 collagen (I)
Gga.4257.1.S1_at	collagen, type VI, alpha 2
Gga.2558.1.S1_a_at	similar to collagen, type XIV, alpha 1 (undulin)
Gga.3587.1.S1_at	matrilin 3
Gga.888.1.S1_at	collagen, type VI, alpha 3
GgaAffx.25534.1.S1_s_at	collagen, type III, alpha 1
GgaAffx.21771.1.S1_at	collagen, type VI, alpha 1
GgaAffx.22999.1.S1_s_at	collagen, type I, alpha 2
Gene Set 2	Enrichment Score: 3.14
Gga.3108.1.S1_at	four and a half LIM domains 2
Gga.8880.1.S1_at	membrane metallo-endopeptidase
Gga.3075.1.S1_at	ADAMTS-like 3
Gga.12800.1.S1_at	matrix metallopeptidase 3 (stromelysin 1, progelatinase)
Gene Set 3	Enrichment Score: 2.8
Gga.595.1.S1_at	NEL-like 2 (chicken)
Gga.9630.1.S1_s_at	low density lipoprotein receptor
Gga.3587.1.S1_at	matrilin 3
Gga.4974.1.S2_at	Versican
Gene Set 4	Enrichment Score: 0.33
GgaAffx.11519.1.S1_at	ras homolog gene family, member G (rho G)
GgaAffx.8303.1.S1_at	RAS-like, estrogen-regulated, growth inhibitor
Gga.6296.1.S1_at	SAR1 homolog B (S. cerevisiae)
Gga.9972.1.S1_at	RAS, dexamethasone-induced 1
Gene Set 5	Enrichment Score: 0.1
Gga.3316.1.S1_s_at	hematopoietically expressed homeobox
Gga.90.1.S1_at	mesenchyme homeobox 2
GgaAffx.21361.1.S1_at	homeobox C10
Gga.260.2.S1_a_at	doublesex and mab-3 related transcription factor 1

Table 4.4. Gene enrichment sets with lesser abundance in FF at 16 weeks	
Gene Set 1	Enrichment Score: 3.38
Gga.9289.1.S1_at	transcription factor AP-2 beta (activating enhancer binding protein 2 beta)
Gga.10531.1.S1_at	TEA domain family member 1 (SV40 transcriptional enhancer factor)
Gga.190.1.S1_at	gastrulation brain homeobox 1
GgaAffx.6552.2.S1_s_at	estrogen-related receptor beta
GgaAffx.5095.1.S1_at	SATB homeobox 2
Gene Set 2	Enrichment Score: 3.28
Gga.738.1.S1_at	goosecoid homeobox
GgaAffx.20085.1.S1_s_at	SRY (sex determining region Y)-box 5
Gga.10.1.S1_at	orthodenticle homeobox 2
Gga.190.1.S1_at	gastrulation brain homeobox 1
Gga.4046.1.S1_at	Meis homeobox 2
Gga.919.1.S1_at	distal-less homeobox 5
Gga.758.1.S1_at	LIM homeobox transcription factor 1, beta
Gga.695.1.S1_at	homeobox D12
Gga.276.1.S1_at	early B-cell factor 1
Gga.1546.1.S1_at	paired related homeobox 1
Gga.957.1.S1_at	homeobox A11
GgaAffx.20140.1.S1_at	distal-less homeobox 6
Gene Set 3	Enrichment Score: 2.12
Gga.495.1.S1_at	gallinacin 2
GgaAffx.21842.2.S1_s_at	Gal 6
GgaAffx.21842.1.S1_s_at	Gal 7
GgaAffx.21849.1.S1_s_at	cathelicidin antimicrobial peptide
Gga.729.1.S1_at	mature avidin; similar to Avidin-related protein 3
Gene Set 4	Enrichment Score: 1.8
Gga.11325.1.S1_at	glial cells missing homolog 1 (Drosophila)
Gga.276.1.S1_at	early B-cell factor 1
GgaAffx.1950.1.S1_at	core-binding factor, runt domain, alpha subunit 2; translocated to, 2
GgaAffx.6552.2.S1_s_at	estrogen-related receptor beta
Gene Set 5	Enrichment Score: 1
GgaAffx.8254.1.S1_at	calcium channel, voltage-dependent, L type, alpha 1C subunit
GgaAffx.1237.1.S1_at	glutamate receptor, ionotropic, delta 1
GgaAffx.9020.1.S1_at	potassium channel tetramerisation domain containing 8
GgaAffx.4551.1.S1_at	gamma-aminobutyric acid (GABA) A receptor, alpha 3
GgaAffx.3918.5.S1_s_at	transient receptor potential cation channel, subfamily C, member 7

Table 4.4 (con't) Gene enrichment groups with lesser abundance in FF at 16 weeks

GgaAffx.2955.1.S1_at	potassium voltage-gated channel, Shab-related subfamily, member 1
GgaAffx.23423.2.S1_s_at	potassium inwardly-rectifying channel, subfamily J, member 5
Gene Set 6	Enrichment Score: 0.77
GgaAffx.9996.1.S1_s_at	sushi domain containing 1
Gga.10988.1.S1_a_at	EF-hand calcium binding domain 1
Gga.15599.1.S1_s_at	similar to sparc/osteonectin, cwcv and kazal-like domains proteoglycan (testican) 1
Gga.2869.1.S1_at	similar to Kv channel-interacting protein; Kv channel interacting protein 4
GgaAffx.8988.1.S1_s_at	signal peptide, CUB domain, EGF-like 1
GgaAffx.22908.2.S1_s_at	calpain 8
Gene Set 7	Enrichment Score: 0.51
GgaAffx.8356.1.S1_s_at	molybdenum cofactor sulfurase
GgaAffx.6820.1.S1_at	transmembrane protein 195
Gga.3667.1.S1_at	similar to reversion-induced LIM protein; PDZ and LIM domain 4
GgaAffx.7323.1.S1_at	Parkinson disease (autosomal recessive, juvenile) 2, parkin
GgaAffx.7583.1.S1_at	myosin VIIA and Rab interacting protein
Gga.10828.1.S1_at	SET and MYND domain containing 3
GgaAffx.8709.1.S1_at	zinc finger protein 407
Gga.153.1.S2_at	Zic family member 1 (odd-paired homolog, Drosophila)
GgaAffx.23310.1.S1_at	GLIS family zinc finger 1
Gene Set 8	Enrichment Score: 0.5
GgaAffx.8821.1.S1_at	melanocortin 2 receptor (adrenocorticotropic hormone)
GgaAffx.3186.1.S1_at	dopamine receptor D4
GgaAffx.8403.1.S1_at	gamma-aminobutyric acid (GABA) B receptor, 2
Gga.14911.1.S1_at	oxytocin receptor
GgaAffx.7793.4.S1_s_at	glutamate receptor, metabotropic 1
Gga.10566.1.S1_at	cholinergic receptor, muscarinic 5
Gene Set 9	Enrichment Score: 0.19
GgaAffx.4776.1.S1_s_at	myosin IIIA
Gga.23.1.S1_s_at	Eph receptor A6
GgaAffx.7275.2.S1_s_at	ribosomal protein S6 kinase, 90kDa, polypeptide 2
Gga.3047.2.S1_at	EPH receptor A5
GgaAffx.1062.1.S1_at	calcium/calmodulin-dependent protein kinase kinase 1, alpha
GgaAffx.5596.4.S1_s_at	ATP-binding cassette, sub-family B (MDR/TAP), member 1
Gga.19162.1.S1_at	ret proto-oncogene
GgaAffx.22016.1.S1_at	BR serine/threonine kinase 2
Gga.10214.1.S1_s_at	mitogen-activated protein kinase 12

Table 4.5. Top 11 Gene Ontology terms from 151 DEG with greater abundance in 16-week-old full-fed hens imported into DAVID

Term No.	Category	Term	Description	Involved Genes [No. (%)]	P-Value
1	GOTERM_CC_FAT	GO:0005578	proteinaceous extracellular matrix	18 (11.9)	2.90E-12
2	GOTERM_CC_FAT	GO:0031012	extracellular matrix	18 (11.9)	7.10E-12
3	GOTERM_CC_FAT	GO:0044421	extracellular region part	20 (13.2)	5.20E-10
4	GOTERM_CC_FAT	GO:0005576	extracellular region	25 (16.6)	4.50E-09
5	GOTERM_CC_FAT	GO:0044420	extracellular matrix part	8 (5.3)	1.70E-06
6	GOTERM_BP_FAT	GO:0030198	extracellular matrix organization	6 (3.9)	2.10E-04
7	GOTERM_BP_FAT	GO:0022610	biological adhesion	13 (8.6)	2.30E-04
8	GOTERM_BP_FAT	GO:0007155	cell adhesion	13 (8.6)	2.30E-04
9	GOTERM_BP_FAT	GO:0030155	regulation of cell adhesion	6 (3.9)	2.70E-04
10	GOTERM_BP_FAT	GO:0006694	steroid biosynthetic process	6 (3.9)	1.00E-05
11	GOTERM_BP_FAT	GO:0008202	steroid metabolic process	6 (3.9)	8.00E-04

Table 4.6. Involved genes comprising GO terms listed in Table 4.5.

A. Gene Symbol	GO term 1 / 2	GO term 3	GO term 4	GO term 5	GO term 6
ADAMTSL3	X	X	X		
ALB		X	X		
ANXA2	X	X	X	X	X
CCDC80	X	X	X	X	X
CDH13		X	X		
COL14A1	X	X	X		
COL1A1	X	X	X	X	
COL1A2	X	X	X	X	X
COL3A1	X	X	X	X	
COL4A2	X	X	X	X	
COL6A1	X	X	X		
COL6A2	X	X	X		
COL6A3	X	X	X		
DEFB1			X		
FN1	X	X	X	X	
GDF9			X		
GRP			X		
LAMA2	X	X	X	X	
MATN3	X	X	X		
MMP3	X	X	X		
MMP9	X	X	X		X
MYH10, MYH11					X
POSTN	X	X	X		X
VCAN	X	X	X		
VIP			X		
WFDC1			X		

B. Gene Symbol	GO term 7 / 8	GO term 9
CCDC80		X
CD36	X	X
CDH13	X	X
COL6A1	X	
COL6A2	X	
COL6A3	X	
COL14A1	X	
COL20A1	X	
FAT4	X	
FN1	X	
LAMA2		X
LYVE1	X	
NELL2	X	
POSTN	X	
PRLR		X
PTEN		X
VCAN	X	

C. Gene Symbol	GO term 10/11
CYP11A1	X
DHCR24	X
HMGCR	X
HSD17B1	X
HSD3B1	X
STAR	X

Table 4.6. Involved genes comprising GO terms from Table 4.5.

A. ECM-related.
B. Cell Adhesion-related.
C. Steroid-related.

Table 4.7. Top 11 Gene Ontology terms from 237 DEG with lesser abundance in 16-week-old full-fed hens imported into DAVID

Term No.	Category	Term	Description	Involved Genes [No. (%)]	P-Value
1	GOTERM_MF_FAT	GO:0030528	transcription regulator activity	27 (11.9)	5.10E-06
2	GOTERM_MF_FAT	GO:0003700	transcription factor activity	21 (8.9)	2.20E-05
3	GOTERM_BP_FAT	GO:0048562	embryonic organ morphogenesis	9 (3.8)	4.10E-05
4	GOTERM_BP_FAT	GO:0048568	embryonic organ development	10 (4.2)	4.40E-05
5	GOTERM_BP_FAT	GO:0048598	embryonic morphogenesis	12 (5.1)	5.80E-05
6	GOTERM_BP_FAT	GO:0007423	sensory organ development	10 (4.2)	8.40E-05
7	GOTERM_BP_FAT	GO:0043583	ear development	7 (3.0)	2.00E-04
8	GOTERM_BP_FAT	GO:0001501	skeletal system development	10 (4.2)	3.10E-04
9	GOTERM_BP_FAT	GO:0042472	inner ear morphogenesis	6 (2.5)	4.30E-04
10	GOTERM_BP_FAT	GO:0042471	ear morphogenesis	6 (2.5)	4.90E-04
11	GOTERM_BP_FAT	GO:0051252	regulation of RNA metabolic process	24(10.1)	8.40E-04

Table 4.8. Involved genes comprising GO terms listed in Table 4.7.

A. Gene Symbol	GO term 1	GO term 2	GO term 11
PRRX1	X	X	X
GSC	X	X	X
DLX5	X	X	X
DLX6	X	X	X
OTX2	X	X	X
EPAS1	X	X	X
HOXA11	X	X	X
HOXD12	X	X	X
LMX1B	X	X	X
MEIS2	X	X	X
SOX5	X	X	X
NKX2-1	X	X	X
SATB2	X	X	X
TEAD1	X	X	X
CDX2	X	X	X
GCM1	X	X	X
TFAP2B	X	X	X
CBFA2T2	X	X	X
EBF1	X	X	X
ESRRB	X	X	X
GBX1	X	X	X
HDAC9	X		X
ANKRD1	X		X
SUPT3H	X		
CNOT2	X		
ASCL1	X		
NHLH2	X		
TNFRSF1B			X

B. Gene Symbol	GO term 3	GO term 4	GO term 5	GO term 6	GO term 7	GO term 8	GO term 9 / 10
PRRX1	X	X	X	X	X	X	X
GSC	X	X	X	X	X	X	
DLX5	X	X	X	X	X		X
DLX6	X	X	X	X	X		X
OTX2	X	X	X	X	X		X
EPAS1		X					
HOXA11			X			X	
HOXD12			X			X	
LMX1B				X			
MEIS2				X			
SOX5						X	
COL2A1	X	X	X	X	X	X	X
ZIC1	X	X	X	X	X		X
RBP4	X	X	X	X		X	
TGFBR2	X	X	X			X	
RET			X				
WWOX						X	
MGP						X	

Table 4.8. Involved genes comprising GO terms from Table 4.7.
A. Transcription and regulation.
B. Embryonic organ development

Table 4.9. KEGG_PATHWAYs from 151 DEG with greater abundance FF at 16 weeks.

Term	No. Genes	% Involved	P-Value
ECM-receptor interaction	9	5.9	1.50E-06
Focal adhesion	10	6.6	2.80E-04
Steroid hormone biosynthesis	4	2.6	4.10E-03
Androgen and estrogen metabolism	3	2.0	2.10E-02

Table 4.10. KEGG_PATHWAYs from 237 DEG with lesser abundance in FF at 16 weeks.

Term	No. Genes	% Involved	P-Value
Cell adhesion molecules (CAMs)	6	2.5	1.90E-02
Neuroactive ligand-receptor interaction	9	3.8	3.10E-02
MAPK signaling pathway	8	3.4	5.40E-02

Table 4.11. Gene transcripts and primers with greater abundance in FF

Gene	forward primer	reverse primer
CCDC80	GGCCAACCTCCTGGACTATT	CTTGTTGCCATCTTGCAGAA
CD36	GGCCATCTTTGGAGGAGTTC	AACAGAGCTTCCTGGCACAA
CDH13	TTACTCTGTCCTTTCTGCTGTCC	CAGGTTCAGAATTGGCTGGT
COL1A2	TGCTCAGCTTTGTGGATACG	GTGGCCCTTTGTCTCCTCTA
COL4A2	CGCGTGTTTCTGTTTGTCAG	CCTCCACTGCAGTCTCTTCC
COL6A1	GCTGCACGACTCCTTCTTG	TGTCCAGCACAAAGAACAGG
CYP11a1	CAAGACATGGCGTGACCA	TGAAGAGGATGCCCGTGT
CYP19A1	CACATGGGAGATTTCTCTGGA	ACGTGAAATACGCTGGAGGA
DHCR24	CTCCATCCTCTTCGACGTGT	ATCTCCTGCCACCTTCCTC
FHL2	AGGGAGGACAGCCCCTACT	GAAGCAGGTTTCATGCCAGT
FN1	GGGGAACACGTTGGTCTGTA	GCGCTCATAAGTCTCCCCTA
HMGCR	TGGAACTATGAGTGCCCAAA	CCGAGTTGCCTTAGGTTCTG
HSD17B1	GAGAAGACCACGGTGCTGAT	GGCCAGGTCACGCATAGT
HSD3B2	CAGCTGCTCTGGGAAGTCA	GGGTCACCCCTGCAGTTT
LAMA2	AAGTTTGCCGTTCCTCCTG	GCATTGGTTGTGATGAGAGC
MGLL	AAAGCGGAGTCCTCAAAACA	CCATGAGCGATAAACACGAG
MMP10/MMP3	GGCTCCAGAAACTGCAAATG	TCAGCCATGTGGTTGAGATT
MMP9	GACCACATGGACCTCACGTA	GTGAAGGTGAGGGGAGTGAC
MYH11	CTCCAAAGTGGAGGACATGG	TGGGTTTATCACAACGCAGA
NELL2	TGACCTTAAAACAAGCCCATTT	TGCCTGTACGGTAATGCAAC
POSTN	TCCACGTTTTTCTTGTCTGCT	TGGTTCCCATAACTTGCTGA
PRLR	TGTTCCTTCCTCTGACCACA	CATCTGAACCAGGCTTCCAC
PTEN	CCTCAACCTTTGCCGGTAT	TGTCTGAATTTTCATCCAGTCCT
STAR	CCAGCGTCAAAGAGGTGAA	GAGCACCGAACACTCACAAA
STARD4	GCTACCAGGCTGCAGAACA	TCCACTGAATTCTTCTGATGGTT
VCAN	CATCATATGGATGTGCTCTACGTT	TATGGTGGGTGTGGTTGAAA
VIP	CGACTGGGAAACAGACTGC	TCAATAATTCTGGACAGATCGAAA
VIPR2	AGGAAGCAAAGTGCATGGAA	TTGGACAAGGGACAGTGACA

Table 4.12. Gene transcripts and primers with lesser abundance in FF

Gene	forward primer	reverse primer
CATHL3	GCTGTGGACTCCTACAACCAA	CCATGATGGTGAAGTTGAGGT
CHRM5	CCTGTGGCTAGCACTGGATT	TCATGATGCCAGCTCTTTTG
CLDN18	CGGCCATATTTCACCATTCT	CGGATGCACTTCATAGCAAA
DLX5	AGCCCCTACCACCAGTACG	ATAAATAGTCCGCGGTTTGC
DRD4	GCTCAAGACCACCACCAACT	CAGTGCTGAGGGACCACAC
GABBR2	TGGTGGTGTATGTGCAACTG	GGCACTGTCCGGAAGAAATA
GABRA3	TGGCATCTCTCTCTCTTGCTG	AGGATGCGTGTGAAAATGGT
GABRA5	CTGGAATGGACAATGGAACA	TCCTCTTTTCCTGGTGCTGT
GAL7	GGATCCTTTACCTGCTGCTG	TTCGACAGATCCCTGGAAAG
GRID1	GGTGGCAGAAATTCATCGTC	TGGCAAAGACTCTGCTGATG
LECT2	CAGCGGGAATCCTTTCAATA	TGATCCATCAGTGCAGATGAC
NEGR1	ACTCCCAGAACAATGCAGGT	AGATGGAGGGCTCTGGTTTC
RBP4	CGTGTGAGCAGCTTCAAAGT	AGTGAACTGGGCAACCACAT
**RPL19*	CCCAACGAGACCAACGAG	CCAAGGTGTTCTTCCTGCAT
SATB2	CGTGGGAGGTTTGATGATTC	ACCAGCTGGCTAAAGAGCAC
SUPT3H	GGATGGGCAAATCAACAAGT	CAGCTGAGTGTGGACGATGT
TEAD1	GTGTGGGAGGAGGAAAATCA	TGGCAAGAACCTGAATGTGA
VIPR1	CCTGGCAGAGATCACTGAGG	AAGTACTTTGGGCATGGCTTC

*Normalizer

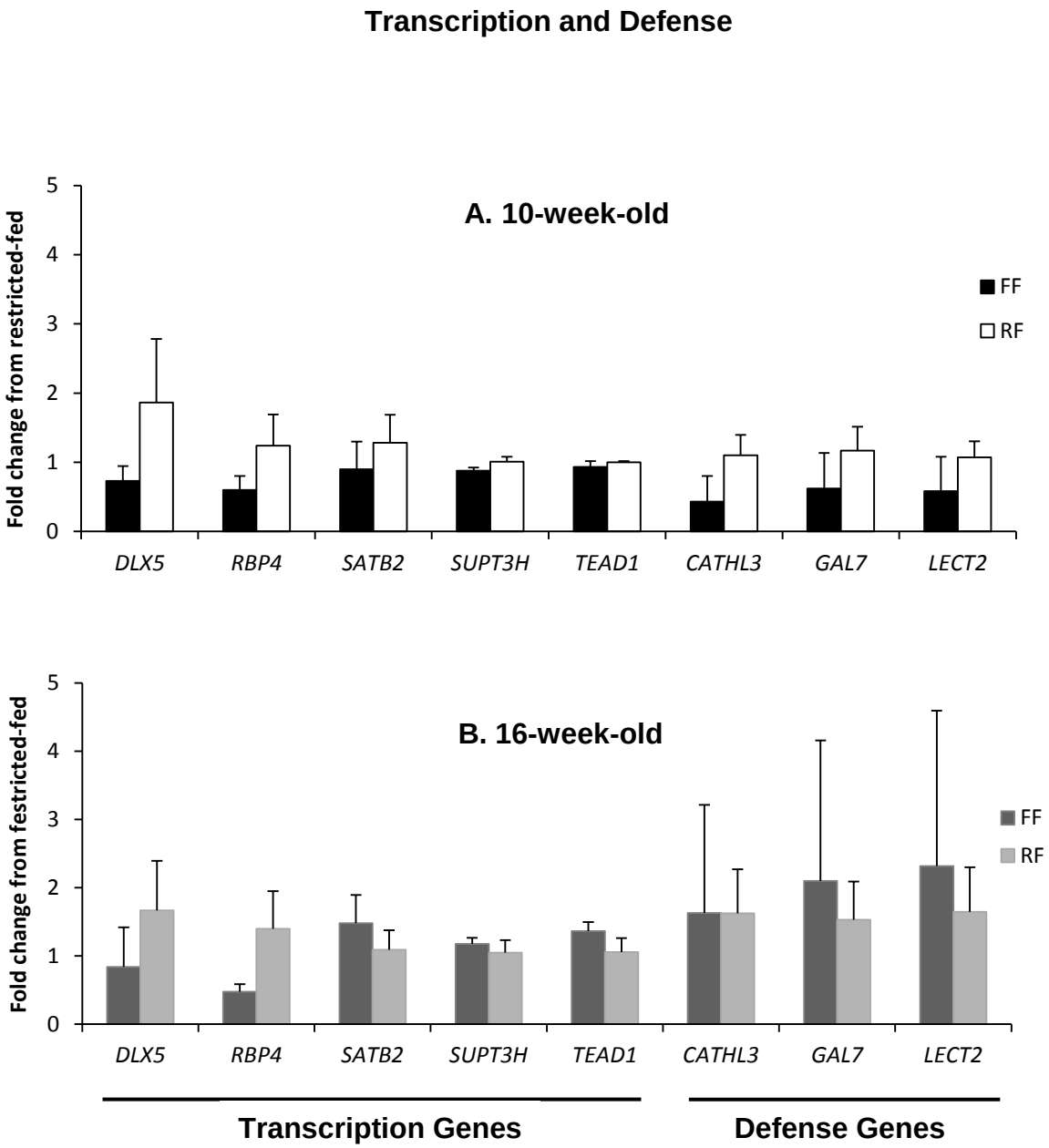

Figure 4.1. Relative differential expression by qPCR of transcription regulation and defense response gene transcripts between full- (FF) and restricted-fed (RF) broiler breeder hens. **A**. 10-week-old; n=4. **B.** 16-week-old; n=4.

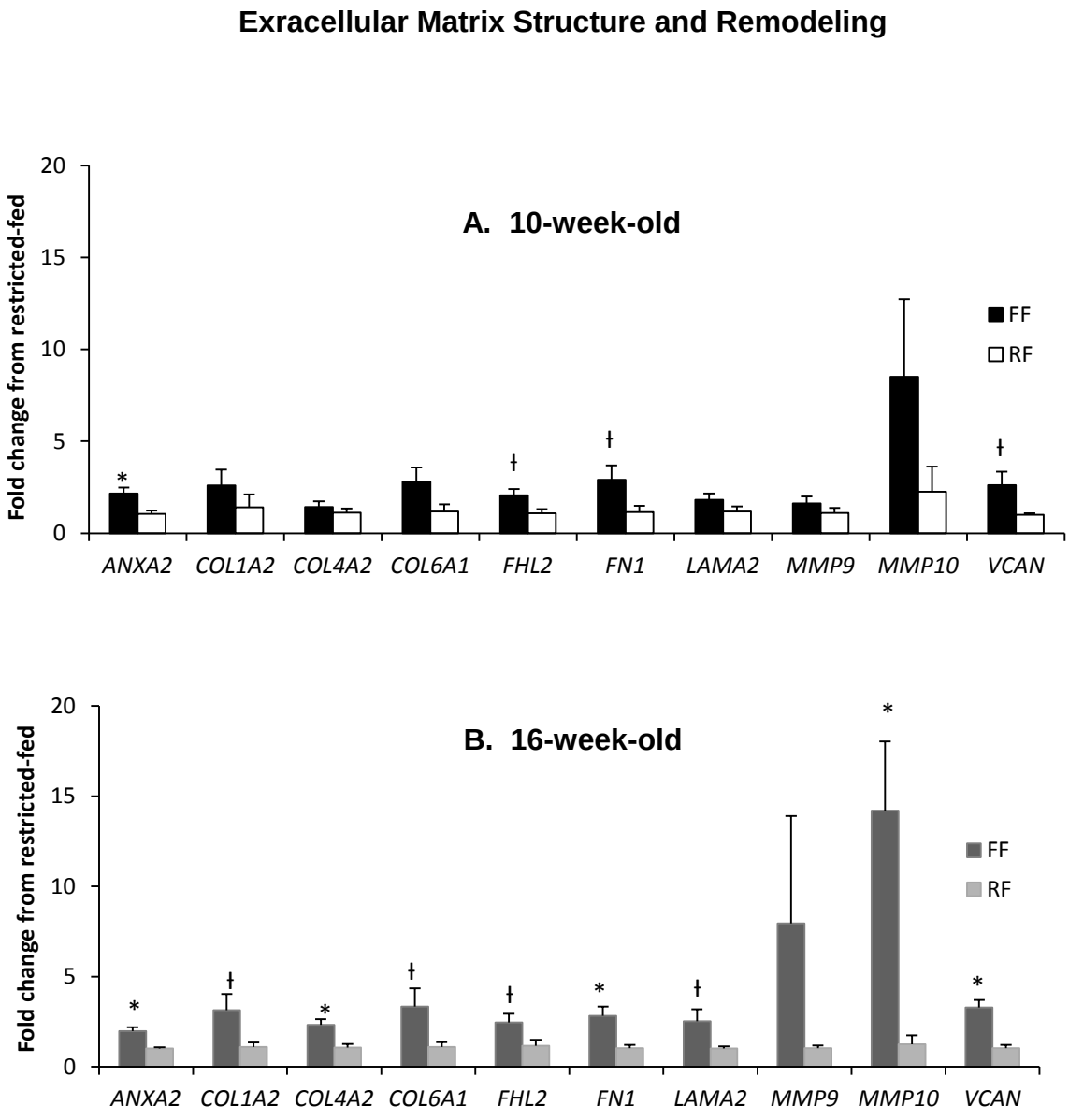

Figure 4.2. Relative differential expression by qPCR of extracellular matrix transcripts between full- (FF) fed and restricted-fed (RF) broiler breeder hens.
A. 10-week-old; n=4. **B**. 16-week-old; n=4. Student's *t*-test, *P<0.05, ł P≤0.10.

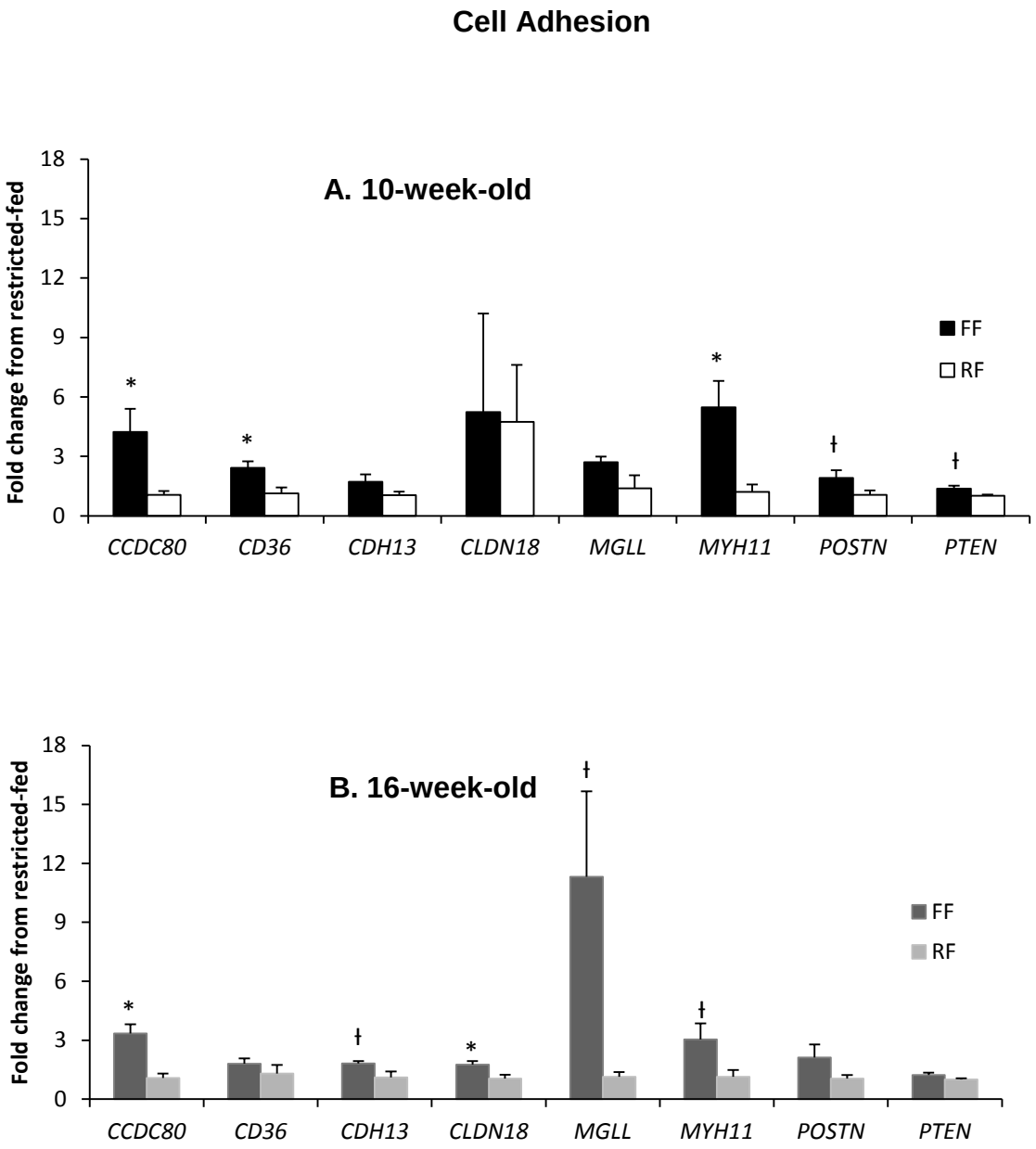

Figure 4.3. Relative differential expression by qPCR of cell adhesion gene transcripts between full- (FF) fed and restricted-fed (RF) broiler breeder hens.
A. 10-week-old; n=4. **B**. 16-week-old; n=4. Student's *t*-test, *P<0.05, ł P≤0.10.

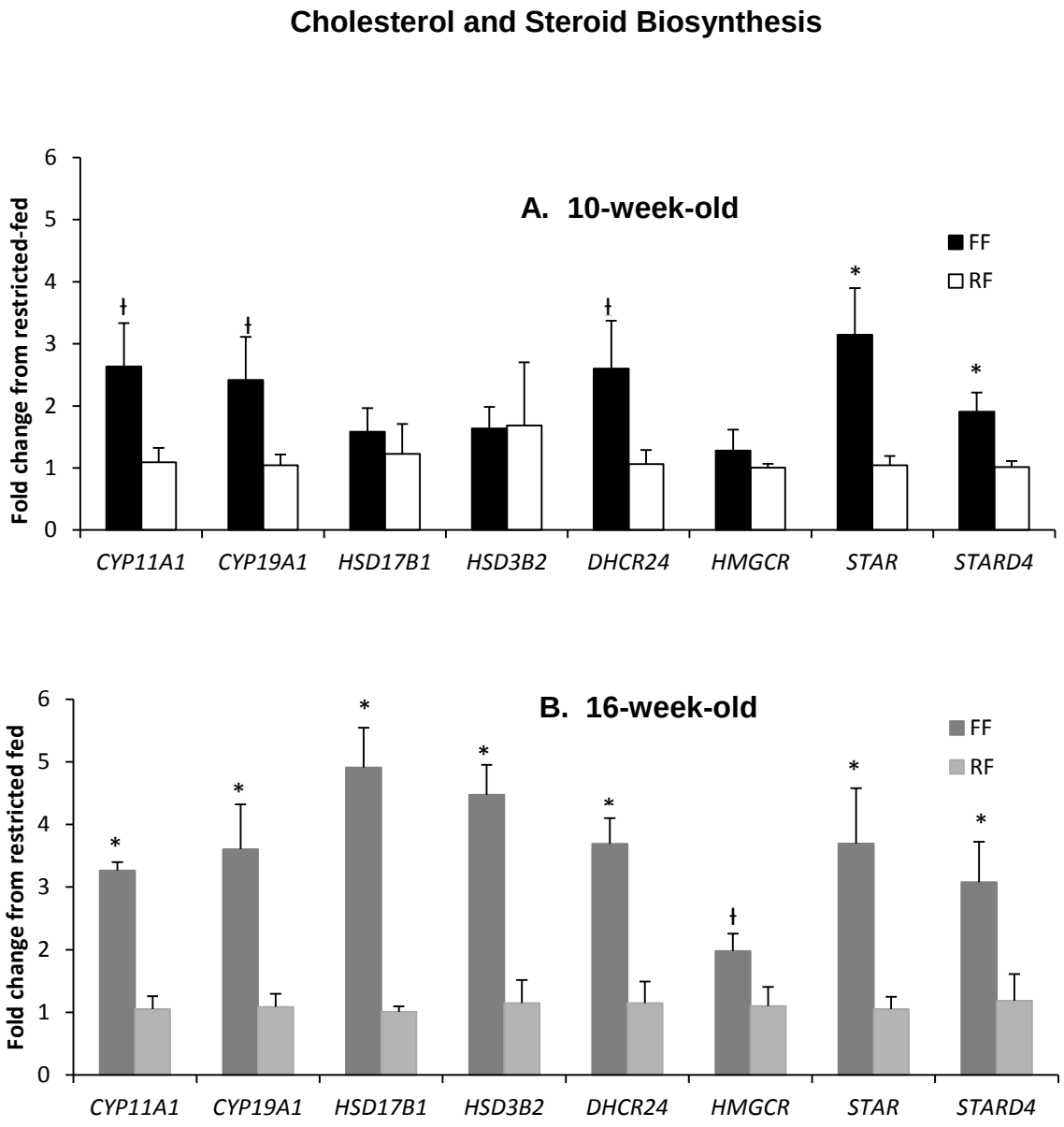

Figure 4.4. Relative differential expression by qPCR of cholesterol and steroid biosynthesis gene transcripts between full-(FF) fed and restricted-fed (RF) broiler breeder hens. **A.** 10-week-old; n=4. **B**. 16-week-old; n=4.
Student's *t*-test, *P<0.05, ł P≤0.10

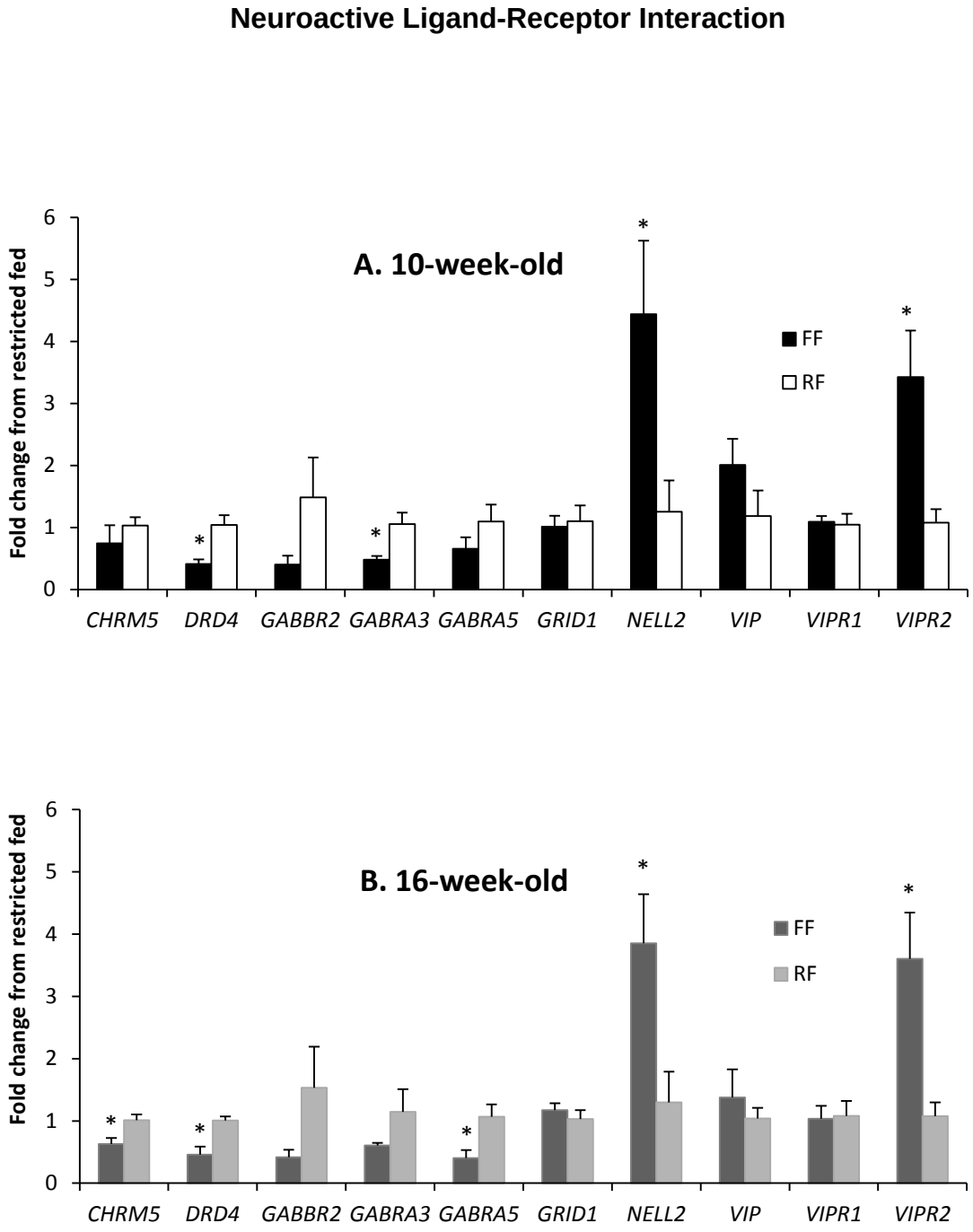

Figure 4.5. Relative differential expression by qPCR of neuroactive ligand-receptor gene transcripts between full- (FF) fed and restricted-fed (RF) broiler breeder hens. **A.** 10-week-old; n=4. **B**. 16-week-old; n=4. Student's *t*-test, *P<0.05.

Chapter 5. Vasoactive Intestinal Polypeptide Promotes Steroidogenesis in Cortical Follicles

Introduction

VIP initiates steroidogenesis in cultured granulosa cells of the rat (Davoren and Hsueh 1985) and hen (Johnson and Tilly 1988) and so far seems to be the only neuropeptide able to promote steroidogenesis in the ovary (Advis et al. 1989). Acting through the cAMP-dependent pathway, VIP exerts its effects through G protein-coupled receptors, VIPR1 and VIPR2, causing increases in adenylyl cyclase (reviewed in Laburthe et al. 2002). Much has been learned about the function of VIP in the adult chicken ovary through *in vitro* culture of granulosa cells of pre-hierarchical and hierarchical follicles (Johnson and Tilly 1988; Johnson et al. 1994; Kim 2013; Kim and Johnson 2016) but little is known of the effects of VIP in follicles still contained within the cortex. Differentially expressed genes identified in Chapter 3 pointed to steroid biosynthesis, including increased abundance of *VIPR2* mRNA occurring in the full fed hens, which led to the hypothesis that VIP can affect steroidogenesis in the immature ovary. Experiments to test this hypothesis were performed on cortical follicles excised from ovaries of actively laying broiler breeder hens and cultured overnight with and without VIP. *STAR* transcript abundance was measured from all cultures as an indicator of steroidogenic activity. The results corroborate our hypothesis, that VIP does maintain *STAR* transcript abundance in cultured cortical follicles. Moreover, *VIPR2* abundance decreased, while *VIPR1* was induced in the VIP-treated follicles suggesting that responsiveness to VIP may change in cortical follicles upon VIP stimulation.

Materials and Methods

Animals

Day-old Cobb 500 female chicks were purchased from Longeneckers Hatchery (Harrisburg, PA). In accordance to the breeder's guidelines (Cobb-Vantress 2008), at Day 1, birds were started on 24 hours of day light, slowly decreasing to 8 hours by Day 14 and maintained on 8 hours until week 20, when hens were moved to individual cages. Light was incrementally increased to maintenance of 16 hours daily until the end of the experiment. All hens in the experiments were fed the same rations. For the first four weeks of life, pullets were fed a standard starter ration, switched to a grower ration until nine weeks of age, then to a developer/finisher ration until the end of the experiment. All pullets were fed ad libitum for the first week, after which they were divided into two groups: one group continued on full feed, the second group was restricted fed according to breeder's guidelines (Cobb-Vantress 2008), being closely monitored for weight gain to assure a proper rate of growth through the growing, finishing, and production stages until the end of the experiment, at ~55 weeks. Hens were weighed and euthanized by cervical dislocation. Ovaries were removed and placed in sterile, ice cold phosphate buffered saline. Cortical tissue sections were excised for the two experiments described below. All procedures described herein were reviewed and approved by the Pennsylvania State University Institutional Animal Care and Use Committee, and were performed in accordance with The Guide for the Care and Use of Agricultural Animals in Research and Teaching (Federation of Animal Science Societies 2010).

Follicle excision and culture

For the first two experiments, strips of cortex containing small follicles were cut from the ovary and placed in Complete DMEM (Dulbecco's Modified Eagle Medium (DMEM; HyClone, Thermo Scientific) containing 2.5% fetal bovine serum, 100 I.U./ml penicillin, 100 ug/ml streptomycin and 0.1mM non-essential amino acids). Follicles 0.4 mm in diameter were excised from the strips by carefully teasing away the cortical connective tissue with fine forceps and hypodermic needles. Five follicles were used for each sample replicate. The first five follicles teased out were labeled Fresh (Time 0) and flash frozen in liquid nitrogen before excising the remainder. The remaining follicles were divided into media with or without either, 1 µM Vasoactive Intestinal Octacosapeptide (Chicken) (Phoenix Pharmaceuticals, Inc. Burlingame, CA), or 10 ng/ml rhFSH (National Hormone and Pituitary Program, Torrance, CA). FSH (a known activator of steroidogenesis) was used as a control treatment. In chickens, a three-hour challenge with [10 ng/ml] FSH is adequate to induce *STAR* expression in granulosa cells of the 9-12 mm follicle (Johnson and Lee 2016). When all the follicles to be cultured were placed in the appropriate culture media, each follicle was punctured with a 30G hypodermic needle to remove oocyte contents and allow better perfusion of the follicle with treatment media. For each replicate, 200 µl of the media containing the follicles was transferred to a free standing 2 ml micro-centrifuge tube and allowed to equilibrate at 40^0C with 5% CO_2 for 30 minutes. Lids were screwed on tightly and the tubes were placed in a gently-shaking 40^0C water bath overnight (17 hours). Transcript abundance for *STAR*, *CYP11A1*, *VIPR1* and *VIPR2* in VIP-treated samples, or *STAR* and *FSHR* in FSH-treated samples, were measured by qPCR and gene-specific

primers. Statistical analyses were performed by one way ANOVA with tukey's post hoc test.

Results

The 0.4 mm follicular size was chosen because it fell within the cut-off for large cortical follicles (Chapter 2). Because these follicles contain both theca and granulosa layers (Figure 4.1) the hypothesis for these experiments was that the 0.4 mm follicles would be responsive to the steroidogenic activator VIP and thus be able to synthesize *STAR*.

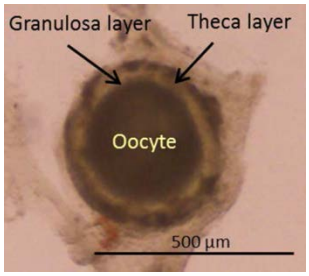

Figure 5.1. Image of 0.4 mm cortical follicle.

Effect of VIP on *STAR*, *CYP11A1*, *VIPR1* and *VIPR2* transcript abundance in cortical follicles cultured 17 hours

VIP is a large protein composed of 28 amino acid residues (Said and Mutt 1972), with a very short half-life of ~1 minute (Domschke et al. 1978). The efficacy of piercing each follicle to assure contact of the somatic cells with the treatment media was tested in a 14 hour culture with and without 1 µM VIP (Figure 4.2). VIP [1 µM] reliably induces progesterone production in granulosa cells from large preovulatory chicken follicles (Johnson et al. 1994) and mouse follicles (Kowalewski et al. 2010). Piercing follicles allowed greater contact with VIP as indicated by a two-fold increase in *STAR*

abundance as compared to whole, unpierced follicles (Figure 4.2). Fourteen hours was ample time to allow a three-fold increase in *STAR* as compared to no-VIP control (Figure 4.2). To determine whether an acute challenge could also induce *STAR* transcript abundance, a four hour challenge was conducted with pierced follicles, but abundance of *STAR* transcript just reached significance (P=0.49) after four hours (Figure 4.3), thus subsequent cultures were extended to 17 hours, using pierced follicles. After 17 hours, follicles cultured with no steroidogenic activator lost their ability to maintain *STAR* abundance, but in the presence of VIP could maintain *STAR* equal to that of fresh samples (Figure 4.4A). VIP was not able to maintain transcript abundance of either *CYP11A1* (Figure 4.4B) or *VIPR2* (Figure 4.4D). *VIPR1*, however, was induced five-fold over fresh and did not decrease in the control samples (Figure 4.4C).

Effect of FSH on *STAR* and *FSHR* transcript abundance in cortical follicles cultured 17 hours

FSH is a known steroidogenic activator in adult ovaries, but was not able to maintain *STAR* in 0.4 mm follicles cultured for 17 hours (Figure 4.3A) although the follicles do express the FSH receptor, *FSHR* (Figure 4.3B). FSH was bioactive, as verified by the large increase in *STAR* transcript abundance in granulosa cells from the 9-12 mm (most recently selected) follicle from a laying turkey hen cultured four hours (Figure 4.4).

Discussion

In the adult chicken ovary, cycling LH and FSH affect the expression of *STAR* and subsequent synthesis of steroids, particularly progesterone in the prehierarchical follicles (Johnson et al. 2002). But in the immature ovary, all follicles are contained within the cortex and do not rely on gonadotropins for development. Nalbandov and Card (1946) demonstrated that exogenous injections of FSH and LH administered every 30 days could not cause follicles to grow beyond 1 mm until after puberty (at 150 days of age). Before puberty, other activators of *STAR* and steroid synthesis, such as VIP, need to be considered. In the present study, VIP, but not FSH, was able to maintain *STAR* transcript abundance in cultured cortical follicles, denoting its ability to initiate steroid biosynthesis. But expression of *STAR* transcript was greater in follicles cultured for 17 than for 4 hours, which suggests actions of an inhibitor of *STAR* transcription whose effectiveness decreases with time in culture. This inhibition has been seen in undifferentiated granulosa cells of preselected (6-8 mm) follicles challenged with FSH. While a 3-hour challenge produced negligible amounts of *STAR* transcript, an 18-hour culture followed by 3-hour FSH challenge produced >10-fold increase in *STAR* (Lee and Johnson 2016). One inhibitory pathway, via β-arrestin-mediated desensitization, has been implicated in desensitization (inhibition) of both FSHR and VIP receptors in granulosa cells of preselected follicles by preventing signaling through cAMP (Kim 2014). Present data show that VIP was not able to maintain mRNA abundance of P450 side chain cleavage enzyme, (*CYP11A1)*. This is possibly due to insufficient culture time. In cultured granulosa cells of 6-8 mm follicles, a significant increase in *CYP11A1* mRNA occurs between 8-16 hours following FSH treatment (Li and Johnson 1993) but,

with VIP treatment, increases are seen after 24 hours (Johnson et al. 1994). VIP was also not able to maintain *VIPR2* mRNA expression after 17 hours, but *VIPR1* abundance was increased 5-fold over fresh (Time 0) samples. These findings were unexpected because the ratio of *VIPR1:VIPR2* abundance was not consistent with that encountered in cortical tissue of full-fed hens (Chapter 3). No information was found in the literature that identified changes in VIP receptor abundance or signaling that regulated ovarian cortical follicle growth and development. However, in cultures of developing cells from other tissues, changes in VIP receptors transcript abundance have been detected. One study showed that the ratio of mRNA abundances of *VIPR1* and *VIPR2* change through the five stages of neuronal differentiation of cultured mouse embryonic stem (ES) cells. Stage 1 is undifferentiated ES cells, stage 2 is aggregation of ES cells, stages 3 and 4 are the use of defined medium to enrich for CNS stem cells of interest, and stage 5 is final differentiation of the stem cells into neurons (Lee et al. 2000). Transcripts for both VIP receptors are present throughout the 5 stages of ES cell differentiation, and they are both moderately expressed at stage 1. At stage 2 (formation of embryoid bodies) *VIPR1* predominates. But when the cells begin to differentiate through stages 3, 4 and 5 *VIPR2* becomes most abundant (Hirose et al**. 2005**). Another study measured development of mouse thymocytes and T cell commitment. T cell development, specification and ultimate commitment, are based on purification of staged precursor cells. The precursor cells are CD4 and CD8 double negative (DN) initially divided into stages DN1, DN2, DN3, and DN4. DN1 cells are the earliest and contain the pluripotent early thymic precursor cells. DN2 are beginning to differentiate. DN3 are pre- and post-β selection cells. DN4 cells are just prior to the

CD4, CD8 double positive cells that precede total commitment (Laurent et al. 2004; Yui et al. 2010). Vomhof-DeKrey et al. (2011) demonstrated, using a thymocyte cell line and receptor knock-out studies in mice, that *VIPR1* expression was at least 18-fold greater than that of *VIPR2* in the first and last stages of commitment, DN1 (completely uncommitted) and DN4 (fully committed), respectively, while the ratio was reversed (*VIPR2* mRNA expression was at least 4 times that of *VIPR1*) as the cells differentiated through β chain selection cell stages DN2 and DN3.

The two G protein coupled receptors have the capacity to activate many pathways. Besides the ability of both receptors to couple to adenylyl cyclase, phospholipase C or the calcium/InsP3 pathways, VIPR1 and VIPR2 possess protein sequence differences that offer them responsiveness to different activating molecules (reviewed in Laburthe et al. 2007; Langer and Robberecht 2007). Taken together, these data indicate that the two VIP receptors have different responsibilities in developing cells. More specifically, *VIPR1* transcript abundance predominates in cells whose emphasis is maintenance or proliferation; *VIPR2* abundance is greater in cells that are differentiating. Functions for receptors in developing cells in the above examples can be extended to cells within the ovarian cortex. *VIPR2* mRNA was greater than that of *VIPR1* in cortical tissue, most likely resulting from differentiation of any of the myriad of cells that make up the cortex. But in culture of 0.4 mm cortical follicles, no differentiation was occurring; *VIPR2* was not induced and *VIPR1* predominated.

Summary

In cultured cortical follicles, 1 µM VIP was able to maintain *STAR* abundance after 17 hours. By comparison, in 10 ng/ml FSH-treated follicles, *STAR* abundance was reduced to one-tenth that of Fresh samples. This indicates that in the immature ovary, steroidogenic activity can be initiated by a neurotransmitter, namely VIP. There was also a change in the balance of the two receptors with VIP treatment. *VIPR1* abundance was five-fold greater in the VIP-treated sample compared to the Fresh sample, but *VIPR2* abundance was not maintained in the VIP-treated follicles. Although these data seem divergent from those observed in microarray analysis of ovarian cortex (Chapter 3), results cannot be compared because experiments are not the same. However, they do suggest uncommon roles for the two receptors. A characterization of relationships and activities of VIP and its receptors in the ovarian cortex, particularly in developing follicles, will add to our understanding of growth and development of the smallest follicles.

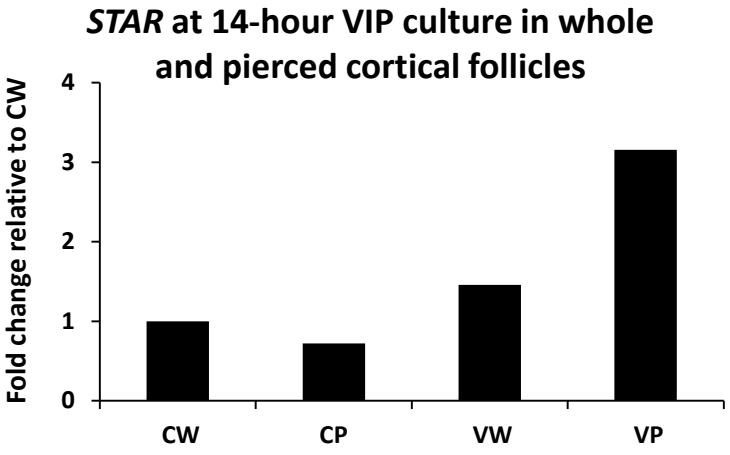

Figure 5.2. 0.4 mm follicles from white leghorn cortex cultured with or without 1 µM VIP for 14 hours to test ability of VIP to induce *STAR* expression in intact whole (w) or pierced (p) follicles. CW = control whole, CP = control pierced, VW = VIP-treated whole, VP = VIP-treated pierced. Relative *STAR* abundance was measured, n=1.

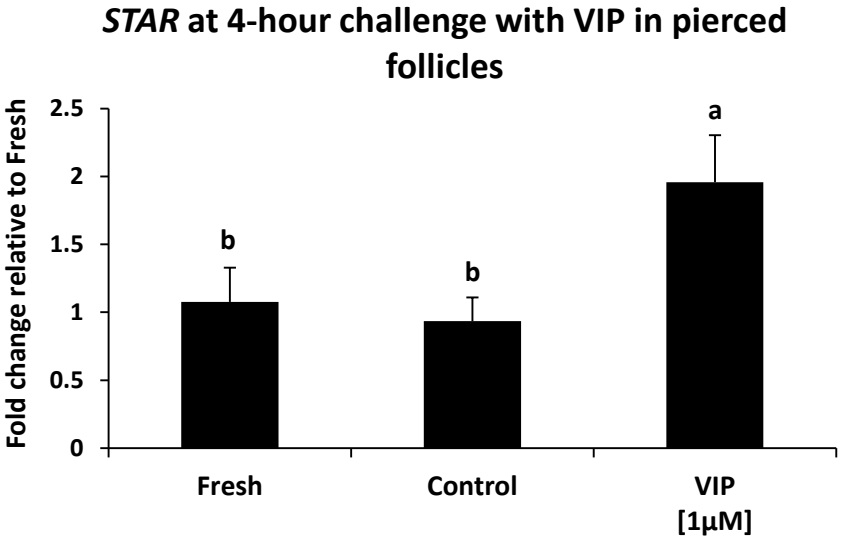

Figure 5.3. 0.4 mm follicles from broiler breeder cortex were cultured with or without 1 µM VIP for 4 hours to determine time necessary to observe relative differences in *STAR* abundance. n=4. $P \leq 0.05$.

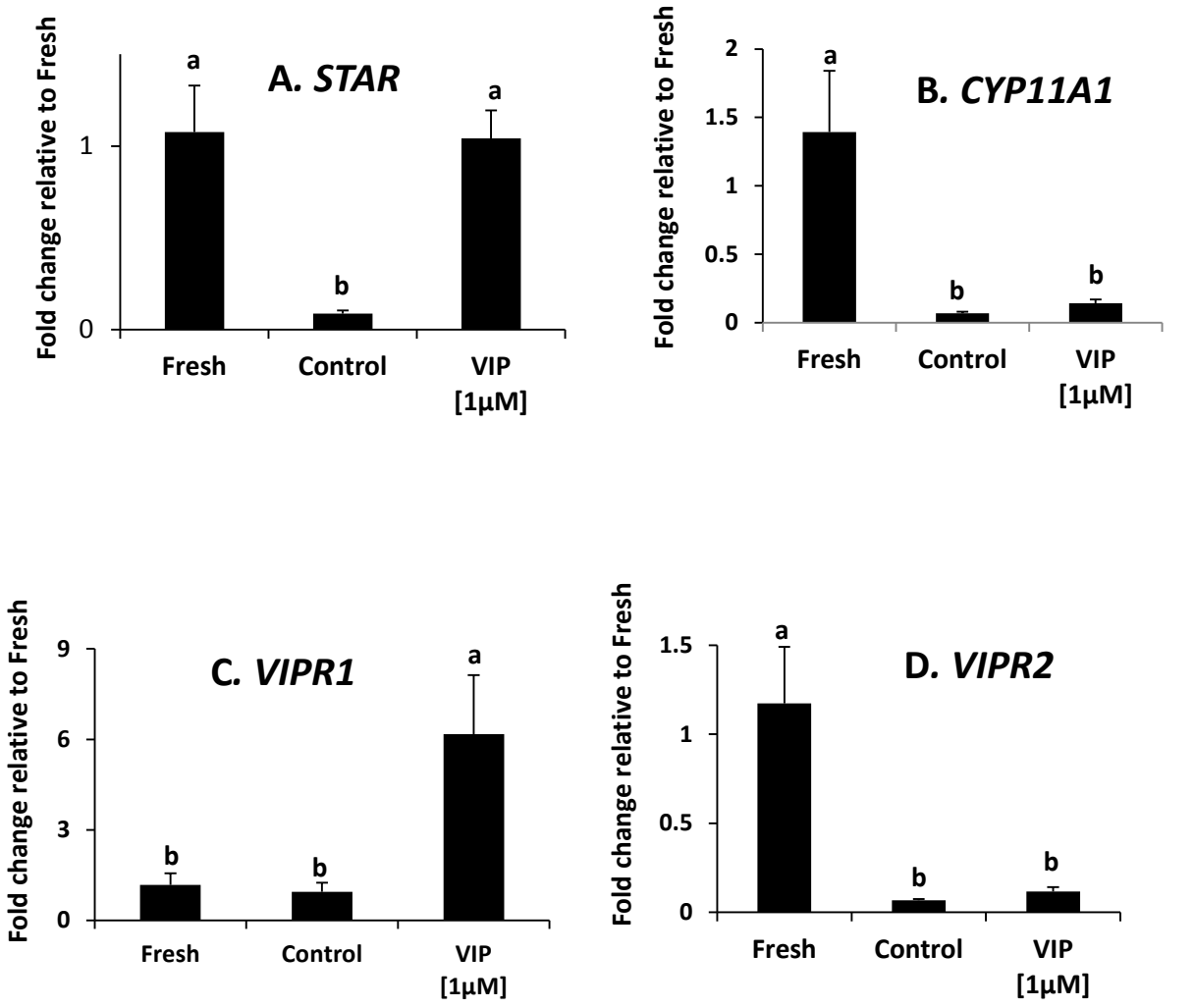

Figure 5.4. 0.4 mm follicles from broiler breeder cortex were cultured with 1 µM VIP for 17 hours. Relative abundance was measured for *STAR* (**A**), *CYP11A1* (**B**), *VIPR1* (**C**), and *VIPR2* (**D**). n=4. $P < 0.05$.

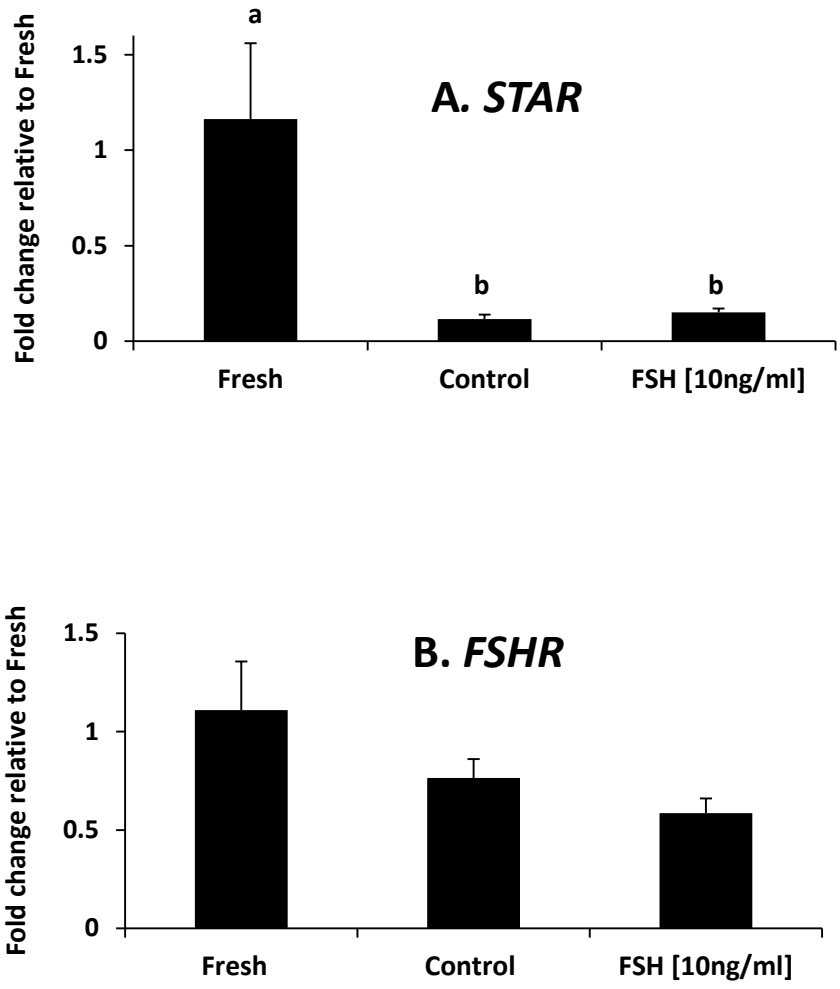

Figure 5.5. 0.4 mm follicles from broiler breeder cortex cultured with 10 ng/ml FSH for 17 hours, n=4. **A.** Relative *STAR* abundance. **B.** Relative *FSHR* abundance. $P < 0.05$.

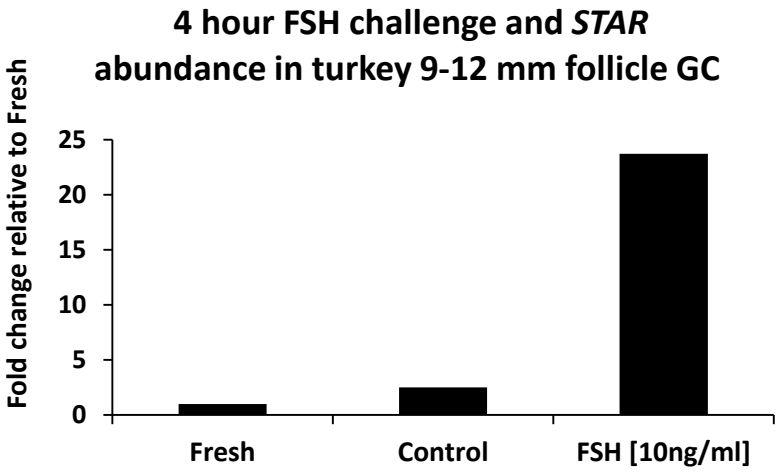

Figure 5.6. Bioactivity of FSH was ensured with a four-hour challenge in granulosa cells from turkey 9-12 mm follicle, n=1.

PROJECT SUMMARY

The purpose of experiments in this project was to identify factors influenced by feed intake in ovaries of immature hens, which could help explain excessive follicle growth and development and reduced fertility observed in adult hens. At both prepubertal ages tested, 10 and 16 weeks, ovaries of hens given full access to feed were larger and heavier than those on restricted feeding, containing greater proportions of larger-sized follicles as well as concomitant decreases in the smallest follicles. The shift to larger-sized follicles was greater at 16 than at 10 weeks of age. Phosphoserine and phosphotyrosine immunohistochemical staining of cortical sections showed differences between FF and RF at 16 weeks. Phosphoserine staining highlighted vesicle-like structures in oocyte cytoplasm of restricted-fed hens. Further research is necessary, but these vesicles could play a role in intra-follicular communication as has been studied in mammals. Phosphotyrosine staining was more intense near the plasma membrane of granulosa cells from restricted-fed hens. Follicle growth is reduced with restricted-, relative to full-feeding, and the increased staining could indicate activity of an inhibitory pathway.

To identify changes in transcript abundance we utilized microarray analysis of ovarian cortex transcriptome of full- (FF) and restricted-fed (RF) 16-week-old hens and computational software, Database for Annotation, Visualization and Integrated Discovery (DAVID). Differentially expressed genes (DEG) disclosed four themes: extracellular matrix (ECM) structure and remodeling, cell adhesion, cholesterol and steroid biosynthesis, and neuroactive ligand-receptor interaction. Most DEG in these themes had greater abundance in FF than RF, and greater difference at 16 than 10

weeks, reflecting the larger size and advanced development of FF ovaries, particularly at 16 weeks.

Developing follicles require an accommodating environment. Genes involved in ECM restructuring and cell adhesion, such as annexin, fibronectin, versican, myosin, and coiled-coil domain containing 80, had greater transcript abundance in FF than RF at both ages, while cadherin, claudin, matrix metalloproteinase, and collagens were also greater in FF than RF at 16 weeks. An important function of ovarian follicles is production of steroids, which increases with advanced follicle growth. At both 10 and 16 weeks, in FF as compared to RF ovaries, there was greater abundance of transcripts for cholesterol synthesis (*DHCR24*) and transporters (*STAR* and *STARD4*), as well as enzymes that support estrogen formation (*CYP11A1* and *CYP19A1*). *HMGCR, HSD3B2* and *HSD17B1* were also greater at 16 weeks in FF as compared to RF.

Transcripts in the neuroactive ligand-receptor interaction theme have unrelated functions such as *NELL2* (increased in FF at both ages) and $GABA_A$ receptors (*GABRA3* has lesser abundance in FF at 10 weeks and *GABRA5* has lesser abundance in FF at 16 weeks, compared to RF). However several transcripts highlight steroidogenic activity. Two have lesser abundance in FF as compared to RF are adenylyl cyclase inhibitors; *DRD4* at both ages and *CHRM5* at 16 weeks. But G protein-coupled receptor vasoactive intestinal polypeptide receptor 2 (*VIPR2*) has greater abundance in FF at both ages.

Greater transcript abundance of *VIPR2* in FF as compared to RF, coupled with increased transcripts involved in steroidogenesis, and support in the literature for VIP actions in the ovary, led to the hypothesis that VIP could initiate *STAR* mRNA

production in cortical follicles. Cortical follicles cultured with VIP for 17 hours maintained *STAR* abundance to equal that of fresh follicles. But without a steroidogenic activator, follicles lost *STAR* abundance to 1/10 that of fresh. Unexpectedly, the proportion of transcript abundance of the two VIP receptors in the cultured cortical follicles was different than that of the cortical tissue samples in the microarray analysis. *VIPR2* transcript abundance was greater than that of *VIPR1* in cortical tissue, but in cultured 0.4 mm follicles, *VIPR1* transcript abundance was dominant. This change in the balance of receptor expression could mean that the two receptors have different responsibilities within the ovary. A study of the literature revealed a role for VIPR1 in cell maintenance and proliferation, while VIPR2 expression predominated during differentiation.

Reproductive dysfunction is severe in the broiler breeder hens. Problems associated with increased growth rate and body size include excessive follicle development and multiple ovulations, but reduced egg production and fertility. These problems are exacerbated with full feeding. Data in this project highlight genetic markers and biological pathways distinguished in ovaries of immature full fed hens and show that ovarian dysfunction in broiler hens begins with the smallest cortical follicles in prepubertal animals.

REFERENCES

Abir R, Nitke S, Ben-Haroush A, and Fisch B. In vitro maturation of human primordial ovarian follicles: clinical significance, progress in mammals, and methods for growth evaluation. Histology and Histopathology 2006; 21:887–898. Review.

Adair LS and Gordon-Larsen P. Maturational timing and overweight prevalence in US adolescent girls. American Journal of Public Health 2001; 91(4): 642-4.

Advis JP, Ahmed CE, and Ojeda SR. Direct Hypothalamic Control of Vasoactive Intestinal Peptide (VIP) Levels in the Developing Rat Ovary. Brain Research Bulletin 1989; 22: 605-610.

Ahmed CE, Dees WL, and Ojeda SR. The immature rat ovary is innervated by vasoactive intestinal peptide (VIP)-containing fibers and responds to VIP with steroid secretion. Endocrinology 1986; 118: 1682-1689.

Al-Musawi SL, Gladwell RT, and Knight PG. Bone morphogenetic protein-6 enhances gonadotrophin-dependent progesterone and inhibin secretion and expression of mRNA transcripts encoding gonadotrophin receptors and inhibin/activin subunits in chicken granulosa cells. Reproduction 2007; 134; 293-306.

Armstrong DG. Ovarian aromatase activity in the domestic fowl (Gallus domesticus). Endocrinology 1984; 100: 81-86.

Ashburner M, Ball CA, Blake JA, Botstein D, Butler H, Cherry JM, Davis AP, Dolinski K, Dwight SS, Eppig JT, Harris MA, Hill DP, Issel-Tarver L, Kasarskis A, Lewis S, Matese JC, Richardson JE, Ringwald M, Rubin GM, and Sherlock G. Gene Ontology: tool for the unification of biology. Nature Genetics 2000; 25: 25-29.

Azhar S, Leers-Sucheta S, and Reaven E. Cholesterol uptake in adrenal and gonadal tissues: the SR-BI and 'selective' pathway connection. Frontiers in Bioscience 2003; 8: s998-1029. Review.

Bahr JM. The Chicken Ovary as a Model of Follicular Development. Seminars in Reproductive Endocrinology 1991; 9(4): 352-359.

Bahr JM, Wang S-C, Huang MY, and Calvo FO. Steroid Concentrations in Isolated Theca and Granulosa Layers of Preovulatory Follicles during the Ovulatory Cycle of the Domestic Hen. Biology of Reproduction 1983; 29: 326-334.

Barberi M, Muciaccia B, Morelli MB, Stefanini M, Cecconi S, and Canipari R. Expression localisation and functional activity of pituitary adenylate cyclase-activating polypeptide, vasoactive intestinal polypeptide and their receptors in mouse ovary. Reproduction 2007; 134(2): 281-92.

Bédécarrats GY, McFarlane H, Maddineni SR, and Ramachandran R. Gonadotropin-inhibitory hormone receptor signaling and its impact on reproduction in chickens. General and Comparitive Endocrinology 2009; 163(1-2): 7-11.

Bédécarrats GY, Baxter M, and Sparling B. An updated model to describe the neuroendocrine control of reproduction in chickens. General and Comparitive Endocrinology 2016; 227:58-63.

Berkholtz BA, Extracellular Matrix Functions in Follicle Maturation. Seminars in Reproductive Medicine 2006; 24(4): 262–269.

Boucek RJ, and Savard K. Steroid formation by the avian ovary in vitro (Gallus domesticus). General and Comparative Endocrinology 1970; 15(1): 6-11.

Boyle EI, Weng S, Gollub J, Jin H, Botstein D, Cherry JM, and Sherlock G. GO::TermFinder--open source software for accessing Gene Ontology information and finding significantly enriched Gene Ontology terms associated with a list of genes. Bioinformatics 2004; 20(18): 3710-5.

Broekmans FJ, Scheffer GJ, Bancsi LF, Dorland M, Blankenstein MA, and te Velde ER. Ovarian reserve tests in infertility practice and normal fertile women. Maturitas 1998; 30(2): 205-14.

Bruggeman V, Van As P, and Decuypere E. Developmental endocrinology of the reproductive axis in the chicken embryo. Comparative Biochemistry and Physiology Part A: Molecular & Integrative Physiology 2002; 131(4): 839-46.

Castrillon DH, Miao L, Kollipara R, Horner JW, and DePinho RA. Suppression of Ovarian Follicle Activation in Mice by the Transcription Factor Foxo3a. Science 2003; 301: 215-218.

Cecconi S, Rossi G, Barberi M, Scaldaferri L, and Canipari R. Effect of pituitary adenylate cyclase-activating polypeptide and vasoactive intestinalpolypeptide on mouse preantral follicle development in vitro. Endocrinology 2004;145: 2071–79.

Chen SE, McMurtry JP,and Walzem RL. Overfeeding-Induced Ovarian Dysfunction in Broiler Breeder Hens is Associated with Lipotoxicity. Poultry Science 2006; 85: 70-81.

Chen N, Li Y, Wang W, Ma Y, Yang D, and Zhang Q. Vasoactive intestinal peptide can promote the development of neonatal rat primordial follicles during in vitro culture. Biology of Reproduction 2013; 88(1): 12, 1-8.

Chun S-Y, Billig H, Tilly JL, Furuta I, Tsafriri A, and Hsueh JW. Gonadotropin suppression of apoptosis in cultured preovulatory follicles: mediatory role of endogenous insulin-like growth factor I. Endocrinology 1994; 135: 1845-1853.

Clauer P. (2016) Modern Meat Chicken Industry. University Park, PA: The Pennsylvania State University, College of Agricultural Sciences.

Cobb-Vantress. Cobb Breeder Management Guide. Siloam Springs 2008, AR: Cobb-Vantress.

Correa H and Jacoby J. Nutrition and fertility: some iconoclastic results. The American Journal of Clinical Nutrition 1978; 31: 1431-1436.

da Silveira JC, Rao Veeramachaneni DN, Winger QA, Carnevale EM, and Bouma GJ. Cell-Secreted Vesicles in Equine Ovarian Follicular Fluid Contain miRNAs and Proteins: A Possible New Form of Cell Communication within the Ovarian Follicle. Biology of Reproduction 2012; 86(3): 71, 1-10.

Davis AJ, Brooks CF and Johnson PA. Activin A and gonadotropin regulation of follicle-stimulating hormone and luteinizing hormone receptor messenger RNA in avian granulosa cells. Biology of Reproduction 2001; 65: 1352-1358.

Davoren JB and Hsueh AJW. Vasoactive intestinal peptide: a novel stimulator of steroidogenesis by cultured rat granulosa cells. Biology of Reproduction 1985; 33: 37-52.

Decuypere E, Hocking PM, Tona K, Onagbesan O, Bruggeman V, Jones EKM, Cassy S, Rideau N, Metayer S, Yego Y, Putterflam J, Tesseraud S, Collin A, Duclos M, Trevidy JJ, and Williams J. Broiler breeder paradox: a project report. World's Poultry Science Journal 2006; 62: 443-453.

Decuypere E, Bruggeman V, Everaert N, Yue Li, Boonen R, De Tavernier J, Janssens S, and Buys N. The Broiler Breeder Paradox: ethical, genetic and physiological perspectives, and suggestions for solutions. British Poultry Science 2010, 51: 5, 569-579.

Dees WL, Ahmed CE, and Ojeda SR. Substance P- and vasoactive intestinal peptide-containing fibers reach the ovary by independent routes. Endocrinology 1986; 119(2): 638-41.

de Melo Bernardo A, Sprenkels K, Rodrigues G, Noce T, and Chuva De Sousa Lopes SM. Chicken primordial germ cells use the anterior vitelline veins to enter the embryonic circulation. Biology Open 2012; 1:1146-1152.

de Melo Bernardo A, Heeren AM, van Iperen L, Fernandes MG, He N, Anjie S, Noce T, Ramos ES, and de Sousa Lopes SM. Meiotic wave adds extra asymmetry to the development of female chicken gonads. Molecular Reproduction and Development 2015; 82(10): 774-86.

Diaz FJ and Anthony K. Feed restriction inhibits early follicular development in young broiler-breeder hens. Animal Reproduction 2013; 10 (2): 79-87.

Diaz FJ, Anthony K, and Halfhill AN. Early avian follicular development is characterized by changes in transcripts involved in steroidogenesis, paracrine signaling and transcription. Molecular Reproduction and Development 2011; 78: 212-223.

Diaz FJ, O'Brien MJ, Wigglesworth K, and Eppig JJ. The preantral granulosa cell to cumulus cell transition in the mouse ovary: Development of competence to undergo expansion. Devopmental Biology 2006;299: 91-104.

Dissen GA, Romero C, Hirshfield AN, and Ojeda SR. Nerve growth factor is required for early follicular development in the mammalian ovary. Endocrinology 2001; 142(5): 2078-86.

Dominguez R, Flores A, and Cruz-Morales SE. Hormonal and neural mechanisms regulating hormone steroids secretion. Edited by: Hassan A. 2011, Publisher In Tech, 3-32. ISBN 978-953-307-866-3,Chap.1.

Domschke S, Domschke W, Bloom SR, Mitznegg P, Mitchell SJ, Lux G, and Strunz U. Vasoactive intestinal peptide in man: pharmacokinetics, metabolic and circulatory effects. Gut 1978; 19(11): 1049-53.

Dong J, Albertini DF, Nishimori K, Rajendra Kumar T, Lu N, and Matzuk MM. Growth differentiation factor-9 is required during early ovarian folliculogenesis. Nature 1996; 383: 531-535.

Draghici S, Khatri P, Eklund AC, Szallasi Z. Reliability and reproducibility issues in DNA microarray measurements. Trends in Genetics 2006; 22(2): 101-9. Review.

Edney ATB, and Smith PM. Study of obesity in dogs visiting veterinary practices in the United Kingdom.Veterinary Record 1986; 118: 391-396.

Elis S, Dupont J, Couty I, Persani L, Govoroun M, Blesbois E, Batellier F, and Monget P. Expression and biological effects of bone morphogenetic protein-15 in the hen ovary. Endocrinology 2007;194: 485-497.

Etches RJ, Petitte JN, and Anderson-Langmuir CE. Interrelationships between the hypothalamus, pituitary gland, ovary, adrenal gland, and the open period for LH release in the hen (Gallus domesticus). Journal of Experimental Zoology 1984; 232(3): 501-11. Review.
Fahrenkrug J and Emson PC. Vasoactive Intestinal Polypeptide: Functional Aspects. British Medical Bulletin 1982; 38(3): 265-270.

Federation of Animal Science Societies 2010. Guide for the care and use of agricultural animals in research and teaching. Champaign (IL): Federation of Animal Science Societies.

Flaws JA, DeSanti A, Tilly KI, Javid RO, Kugu K, Johnson AL, Hirshfield AN, and Tilly JL. Vasoactive Intestinal Peptide-Mediated Suppression of Apoptosis in the Ovary: Potential Mechanisms of Action and Evidence of a Conserved Antiatretogenic Role through Evolution. Endocrinology 1995; 136(10): 4351-4359.

Fodor SP, Read JL, Pirrung MC, Stryer L, Lu AT, and Solas D. Light-directed, spatially addressable parallel chemical synthesis. Science 1991; 251(4995): 767-73.

Gabbay-Benziv R, Ao A, Fisch B, Zhang L, Oron G, Kessler-Icekson G, Ben-Haroush A, Krissi H, and Abir R. Vasoactive Intestinal Peptide and Its Receptors in Human Ovarian Cortical Follicles. PLoS ONE 2012; 7(5): e37015.

Garbarino J, Pan M, Chin HF, Lund FW, Maxfield FR, and Breslow JL. STARD4 knockdown in HepG2 cells disrupts cholesterol trafficking associated with the plasma membrane, ER, and ERC. Lipid Research 2012; 53(12): 2716-25.

George FW and Ojeda SR. Vasoactive intestinal peptide enhances aromatase activity in the neonatal rat ovary before development of primary follicles or responsiveness to follicle-stimulating hormone. Proceedings of the National Academy of Sciences USA 1987; 84: 5803-5807.

Gerits N, Kostenko S, Shiryaev A, Johannessen M, and Moens U. Relations between the mitogen-activated protein kinase and the cAMP-dependent protein kinase pathways: Comradeship and hostility. Cellular Signaling 2008; 20: 1592-1607.

German AJ. The Growing Problem of Obesity in Dogs and Cats. Journal of Nutrition 2006; 136(7 Suppl): 1940S-1946S.

Gilbert AB. The Ovary. In Bell DJ and Freeman BM (Eds.), Physiology and Biochemistry of the Domestic Fowl. 1971 (pp.1163-1208). New York: Academic Press.

Gilbert AB, Perry MM, Waddington D, and Hardie MA. Role of atresia in establishing the follicular hierarchy in the ovary of the domestic hen (Gallus domesticus). Journal of Reproduction and Fertility 1983; 69(1): 221-7.

Ginsburg M. Primordial germ cell formation in birds. Ciba Foundation Symposium 1994; 182: 52-67.

Gonzalez CB, Cantore ML, and Passeron S. Steroidogenesis in immature chicken ovary. Hormonal stimulation of adenylyl cyclase system by luteinizing hormone and beta-adrenergic agonists. Cell Biology International 1994; 18(2): 103-10.

Griffin HD and Goddard C. Rapidly growing broiler (meat-type) chickens: their origin and use for comparative studies of the regulation of growth. International Journal of Biochemistry 1994; 26(1):19-28.

Ha CM, Choi J, Choi EJ, Costa ME, Lee BJ, and Ojeda SR. NELL2, a neuron-specific EGF-like protein, is selectively expressed in glutamatergic neurons and contributes to the glutamatergic control of GnRH neurons at puberty. Neuroendocrinology 2008; 88(3): 199-211.

Harmar AJ, Fahrenkrug J, Gozes I, Laburthe M, May V, Pisegna JR et al. Pharmacology and functions of receptors for vasoactive intestinal peptide and pituitary adenylate cyclase-activating polypeptide: IUPHAR Review 1. Br J Pharmacol 2012; 166: 4–17.

Heck A, Onagbesan O, Tona K, Metayer S, Putterflam J, Jego Y, Trevidy JJ, Decuypere E, Williams J, Picard M, and Bruggeman V.Effects of ad libitum feeding on performance of different strains of broiler breeders. British Poultry Science 2004; 45(5): 695-703.

Heindel JJ, Sneeden J, Powell CJ, Davis B, and Culler MD. A novel hypothalamic peptide, pituitary adenylate cyclase-activating peptide, regulates the function of rat granulosa cells in vitro. Biology of Reproduction 1996; 54: 523–530.

Hirose M, Hashimoto H, Shintani N, Nakanishi M, Arakawa N, Iga J, Niwa H, Miyazaki J,and Baba A. Differential expression of mRNAs for PACAP and its receptors during neural differentiation of embryonic stem cells. Regulatory Peptides 2005; 126(1-2): 109-13.

Hocking PM, Gilbert AB, Walker M and Waddington D. Ovarian follicular structure of White Leghorns fed ad libitum and dwarf and normal broiler breeders fed ad libitum or restricted until point of lay. British Poultry Science 1987; 28(3): 493-506.

Hocking PM and McCormack HA. Differential sensitivity of ovarian follicles to gonadotrophin stimulation in broiler and layer lines of domestic fowl. Reproduction and Fertility 1995; 105: 49-55.

Hosack DA, Dennis G Jr, Sherman BT, Lane HC, Lempicki RA. Identifying biological themes within lists of genes with EASE. Genome Biology 2003; 4(10): R70.

Huang DW, Sherman BT, Tan Q, Collins JR, Alvord WG, Roayaei J, Stephens R, Baseler MW, Lane HC, and Lempicki RA. The DAVID Gene Functional Classification Tool: a novel biological

module-centric algorithm to functionally analyze large gene lists. Genome Biology 2007; 8: R183.

Huang DW, Sherman BT, and Lempicki RA. Bioinformatics enrichment tools: paths toward the comprehensive functional analysis of large gene lists. Nucleic Acids Research 2009a; 37 (1): 1-13.

Huang DW, Sherman BT, and Lempicki RA. Systematic and integrative analysis of large gene lists using DAVID bioinformatics resources. Nature Protocols 2009b; 4 (1): 44-57.

Huang EJ, Manova K, Packer AI, Sanchez S, Bachvarova RF and Besmer P. The murine steel panda mutation affects kit ligand expression and growth of early ovarian follicles. Developmental Biology 1993; 157: 100-109.

Hummel S, Osanger A, Bajari TM, Balasubramani M, Halfter W, Nimpf J, and Schneider WJ. Extracellular matrices of the avian ovarian follicle. Molecular characterization of chicken perlecan. Journal of Biological Chemistry 2004; 279(22): 23486-94.

Hy-line I 2007 Hy-line variety w-36 commercial management guide. Hy-line International, des Moines, IA.

Irizarry RA, Hobbs B, Collin F, Beazer-Barclay YD, Antonellis KJ, Scherf U, and Speed TP. Exploration, normalization, and summaries of high density oligonucleotide array probe level data. Biostatistics 2003; 4 (2): 249-264.

Ishimaru Y, Komatsu T, Kasahara M, Katoh-Fukui Y, Ogawa H, Toyama Y, Maekawa M, Toshimori K, Chandraratna RAS, Morohashi K-i, and Yoshioka H. Mechanism of asymmetric ovarian development in chick embryos. Development 2008; 135: 677-685.

Jackowska M, Kempisty B, Woźna M, Piotrowska H, Antosik P, Zawierucha P, Bukowska D, Nowicki M, Jaśkowski JM, and Brüssow KP. Differential expression of GDF9, TGFB1, TGFB2 and TGFB3 in porcine oocytes isolated from follicles of different size before and after culture in vitro. Acta Veterinaria Hungarica 2013; 61(1): 99-115.

John GB, Gallardo TD, Shirley LJ, and Castrillo DH. Foxo3 is a PI3K-dependent molecular switch controlling the initiation of oocyte growth. Developmental Biology 2008; 321: 197-204.

Johnson AL and Tilly JL. Effects of vasoactive intestinal peptide on steroid secretion and plasminogen activator activity in granulosa cells of the hen. Biology of Reproduction 1988; 38: 296-303.

Johnson AL. Steroidogenesis and actions of steroids in the hen ovary. Critical Reviews in Poultry Biology 1990; 2: 319-346.

Johnson AL, Li Z, Gibney JA, and Malamed S. Vasoactive intestinal peptide-induced expression of Cytochrome P450 cholesterol side-chain cleavage and 17a-Hydroxylase enzyme activity in hen granulosa cells. Biology of Reproduction 1994; 51:327-333.

Johnson AL, Bridgham JT, Witty JP, and Tilly JL. Susceptibility of avian granulosa cells to apoptosis is dependent upon stage of follicle development and is related to endogenous levels of bcl-xlong gene expression. Endocrinology 1996; 137: 2059–2066.

Johnson AL. Ovarian Cycles and Follicle Development in Birds. Reproduction 1999; 3: 564-574. Review.

Johnson AL, Bridgham JT, and Jensen T. Bcl-X (LONG) protein expression and phosphorylation in granulosa cells. Endocrinology 1999; 140: 4521–4529.

Johnson AL and Bridgham JT. Regulation of Steroidogenic Acute Regulatory Protein and Luteinizing Hormone Receptor Messenger Ribonucleic Acid in Hen Granulosa Cells. Endocrinology 2001; 142(7): 3116-3124.

Johnson AL, Bridgham JT, and Swenson JA. Activation of the Akt/Protein Kinase B Signaling Pathway Is Associated with Granulosa Cell Survival. Biology of Reproduction 2001; 64: 1566-1574.

Johnson AL, Solovieva EV, and Bridgham JT. Relationship between Steroidogenic Acute Regulatory Protein Expression and Progesterone Production in Hen Granulosa Cells During Follicle Development. Biology of Reproduction 2002; 67: 1313-1320.

Johnson PA, Woodcock JR, and Kent TR. Effect of activin A and inhibin A on expression of the inhibin/activin beta-B-subunit and gonadotropin receptors in granulosa cells of the hen. General Comparative Endocrinology 2006; 147: 102-107.

Johnson AL and Woods DC. Ovarian dynamics and follicle development. In: Jamieson, B.G.M. (Ed). Reproductive Biology and Phylogeny of Aves. Science Publishers, Inc. 2007; Chapter 6: 243-277.

Johnson AL. Ovarian follicle selection and granulosa cell differentiation. Poultry Science 2015; 94(4): 781-5. Review.

Johnson PA, Brooks CF, and Davis AJ. Pattern of secretion of immunoreactive inhibin/activin subunits by avian granulosa cells. General and Comparitive Endocrinology 2005a; 141: 233-239.

Johnson PA, Dickens MJ, Kent TR, and Giles JR. Expression and Function of Growth Differentiation Factor-9 in an Oviparous Species, Gallus domesticus. Biology of Reproduction 2005b; 72: 1095-1100.

Johnson PA, Kent TR, Urick ME, and Giles JR. Expression and regulation of anti-mullerian hormone in an oviparous species, the hen. Biology of Reproduction 2008; 78: 13-19.

Johnson PA, Kent TR, Urick ME, Trevino LS, and Giles JR. Expression of anti-Mullerian hormone in hens selected for different ovulation rates. Reproduction 2009; 137: 857-863.

Johnson PA. Follicle selection in the avian ovary. Reproduction in Domestic Animals 2012; 47 Suppl 4: 283-7.

Johnson AL and Lee J. Granulosa cell responsiveness to follicle stimulating hormone during early growth of hen ovarian follicles. Poultry Science 2016; 95(1): 108-14.

Kanehisa M, Goto S, Kawashima S, Okuno Y, and Hattori M. The KEGG resource for deciphering the genome. The KEGG resource for deciphering the genome. Nucleic Acids Research 2004; 32 (Database issue):D277-80.

Kasson BG, Meidan R, Davoren JB, and Hsueh AJ. Identification of subpopulations of rat granulosa cells: sedimentation properties and hormonal responsiveness. Endocrinology 1985; 117(3): 1027-34.

Kezele P, Nilsson E, and Skinner MK. Cell-cell interactions in primordial follicle assembly and development. Frontiers in Bioscience 2002; 7: d1990-6. Review.

Kezele P and Skinner MK. Regulation of ovarian primordial follicle assembly and development by estrogen and progesterone: endocrine model of follicle assembly. Endocrinology 2003; 144(8):3329-37.

Kim D, Oco´n-Grove O, and Johnson AL. Bone Morphogenetic Protein 4 Supports the Initial Differentiation of Hen (Gallus gallus) Granulosa Cells. Biology of Reproduction 2013; 88(6): 161, 1-7.

Kim D. Regulatory Mechanisms of G Protein-Coupled Receptor (GPCR) Signaling at Follicle Selection in the Hen Ovary (Doctoral dissertation). The Pennsylvania State University, ProQuest Dissertations Publishing, 2014. (Accession No. 10170363)

Kim D and Johnson AL. Vasoactive intestinal peptide promotes differentiation and clock gene expression in granulosa cells from prehierarchal follicles. Molecular Reproduction and Development 2016; 83(5):455-63.

King D (2013). Ovary. Retrieved October 12, 2016, from SIUC / School of Medicine / Anatomy / David King http://www.siumed.edu/~dking2/erg/ovary.htm

King SR and LaVoie HA. Gonadal transactivation of STARD1, CYP11A1 and HSD3B. Frontiers in Bioscience (Landmark Edition) 2012; 17: 824-46.

Kinney TB Jr and Shoffner RN. Heritability Estimates and Genetic Correlations among Several Traits in a Meat-Type Poultry Population. Poultry Science 1965; 44: 1020-32.

Kopelman RG. Obesity as a medical problem. Nature 2000; 404(6): 635-643.

Kowalewski MP, Dyson MT, Boos A, and Stocco DM. Vasoactive intestinal peptide (VIP)-mediated expression and function of steroidogenic acute regulatory protein (StAR) in granulosa cells. Molecular and Cellular Endocrinology 2010; 328: 93-103.

Krebs EG. Historical perspectives on protein phosphorylation and a classification system for protein kinases. Philosophical Transactions of the Royal Society of London. Series B. 1983; 302(1108): 3-11.

Kuroda S, Oyasu M, Kawakami M, Kanayama N, Tanizawa K, Saito N, Abe T, Matsuhashi S, and Ting K. Biochemical characterization and expression analysis of neural thrombospondin-1-like proteins NELL1 and NELL2. Biochemical and Biophysical Research Communications 1999; 265(1): 79-86.

Laburthe M, Couvineau A, and Marie J-C. VPAC receptors for VIP and PACAP. Receptors and Channels 2002; 8: 137-153. Review.

Laburthe M, Couvineau A, and Tan V. Class II G protein-coupled receptors for VIP and PACAP: Structure, models of activation and pharmacology. Peptides 2007; 28(9): 1631-9. Review.

Langer I and Robberecht P. Molecular mechanisms involved in vasoactive intestinal peptide receptor activation and regulation: current knowledge, similarities to and differences from the A family of G-protein-coupled receptors. Biochemical Society Transactions 2007; 35(Pt 4): 724-8.

Laurent J, Bosco N, Marche PN, and Ceredig R. New insights into the proliferation and differentiation of early mouse thymocytes. International Immunology 2004; 16(8): 1069-80.

LaVoie HA. Epigenetic control of ovarian function: The emerging role of histone modifications. Molecular and Cellular Endocrinology 2005; 243: 12–18. Review.

Lawrence IE Jr and Burden HW. The origin of the extrinsic adrenergic innervation to the rat ovary. Anatomical Record 1980; 196(1): 51-9.

Lebbe M and Woodruff TK. Involvement of androgens in ovarian health and disease. Molecular Human Reproduction 2013; 19(12): 828-37. Review .

Lee SH, Lumelsky N, Studer L, Auerbach JM, and McKay RD. Efficient generation of midbrain and hindbrain neurons from mouse embryonic stem cells. Nature Biotechnology 2000; 18(6): 675-9.

Leghari IH, Zhao D2 Mi Y, and Zhang C. Isolation and culture of chicken primordial follicles. Poultry Science 2015; 94(10): 2576-80.

Lennartsson A and Ekwall K. Histone modification patterns and epigenetic codes. Biochimica et Biophysica Acta 2009; 1790: 863-868.

Leung PC and Armstrong DT. Interactions of steroids and gonadotropins in the control of steroidogenesis in the ovarian follicle. Annual Review of Physiology 1980; 42: 71-82.

Li Z and Johnson AL. Regulation of P450 Cholesterol Side-Chain Cleavage Messenger Ribonucleic Acid Expression and Progesterone Production in Hen Granulosa Cells. Biology of Reproduction 1993; 49: 463-469.

Liu HK, Lilburn MS, Koyyeri B, Anderson JW, and Bacon WL. Preovulatory surge patterns of luteinizing hormone, progesterone, and estradiol-17 beta in broiler breeder hens fed ad libitum or restricted fed. Poultry Science 2004; 83: 823-829.

Liu K, Rajareddy S, Liu L, Jagarlamudi K, Boman K, Selstam G, and Reddy P. Control of mammalian oocyte growth and early follicular development by the oocyte PI3 kinase pathway: new roles for an old timer. Developmental Biology 2006; 299(1): 1-11.

Livak KJ and Schmittgen TD. Analysis of relative gene expression data using real-time quantitative PCR and the 2-[Delta][Delta]CT method. Methods 2001; 25: 402-408.

Lovell TM, Al-Musawi SL, Gladwell RT, and Knight PG. Gonadotrophins modulate hormone secretion and steady-state mRNA levels for activin receptors (type I, IIA, IIB) and inhibin co-receptor (betaglycan) in granulosa and theca cells from chicken prehierarchical and preovulatory follicles. Reproduction 2007; 133: 1159-1168.

Lovell TM, Gladwell RT, Groome NP, and Knight PG. Ovarian follicle development in the laying hen is accompanied by divergent changes in inhibin A, inhibin B, activin A and follistatin production in granulosa and theca layers. Endocrinology 2003; 177: 45-55.

Ly K, Saavedra YG, Canuel M, Routhier S, Desjardins R, Hamelin J, Mayne J, Lazure C, Seidah NG, and Day R. Annexin A2 reduces PCSK9 protein levels via a translational mechanism and interacts with the M1 and M2 domains of PCSK9. The Journal of Biological Chemistry 2014; 289(25): 17732-46.

Magoffin DA and Magarelli PC. Preantral follicles stimulate luteinizing hormone independent differentiation of ovarian theca-interstitial cells by an intrafollicular paracrine mechanism. Endocrine 1995 ;3(2): 107-12.

Mayerhofer A, Dissen G, Costa M, and Ojeda SR. A role for neurotransmitters in early follicular development: induction of functional follicle-stimulating hormone receptors in newly formed follicles of the rat ovary. Endocrinology 1997; 138: 3320-3329.

McGee EA and Hsueh AJW. Initial and cyclic recruitment of ovarian follicles. Endocrine Reviews 2000; 21: 200-214.

Miller WL. Steroidogenic acute regulatory protein (StAR), a novel mitochondrial cholesterol transporter. Biochimica et Biophysica Acta (1771) 2007; 663-676. Review.

Monks TJ, Xie R, Tikoo K, and Lau SS. Ros-induced histone modifications and their role in cell survival and cell death. Drug Metabolism Reviews 2006; 38: 755-767.

Nakamura Y, Yamamoto Y, Usui F, Mushika T, Ono T, Setioko AR, Takeda K, Nirasawa K, Kagami H, and Tagami T. Migration and proliferation of primordial germ cells in the early chicken embryo. Poultry Science 2007; 86: 2182-2193.

Nalbandov AV and Card LE. Effect and FSH and LH upon the ovaries of immature chicks and low-producing hens. Endocrinology 1946; 38: 71-8.

Navakanitworakul R, Hung WT, Gunewardena S, Davis JS, Chotigeat W, and Christenson LK. Characterization and Small RNA Content of Extracellular Vesicles in Follicular Fluid of Developing Bovine Antral Follicles. Scientific Reports 2016; 6: 25486.

Nilsson EE, Schindler R, Savenkova MI, and Skinner MK. Inhibitory actions of Anti-Müllerian Hormone (AMH) on ovarian primordial follicle assembly. PLoS One. 2011; 6(5):e20087.

Nitta H, Osawa Y, and Bahr JM. Immunolocalization of Steroidogenic Cells in Small Follicles of the Chicken Ovary: Anatomical Arrangement and Location of Steroidogenic Cells Change during Follicular Development. Domestic Animal Endocrinology 1991; 8(4): 587-594.

Nitta H, Mason JI, and Bahr JM. Localization of 3 beta-hydroxysteroid dehydrogenase in the chicken ovarian follicle shifts from the theca layer to granulosa layer with follicular maturation. Biology of Reproduction 1993; 48(1): 110-6.

Onagbesan OM, Metayer S, Tona K, Williams J, Decuypere E, and Bruggeman V. Effects of Genotype and Feed Allowance on Plasma Luteinizing Hormones, Follicle-Stimulating Hormones, Progesterone, Estradiol Levels, Follicle Differentiation, and Egg Production Rates of Broiler Breeder Hens. Poultry Science 2006; 85: 1245-1258.

Packer AI, Hsu YC, Besmer P, and Bachvarova RF. The ligand of the c-kit receptor promotes oocyte growth. Developmental Biology 1994; 161: 194–205.

Pangas SA. Regulation of the Ovarian Reserve by Members of the Transforming Growth Factor Beta Family. Molecular Reproduction and Development 2012; 79: 666–679. Review.

Parhar IS, Soga T, and Ogawa S. Editorial: Reproductive Neuroendocrinology and Social Behavior. Frontiers in Neuroscience 2016; 10: 124. Review.

Parrott JA and Skinner MK. Kit-ligand/stem cell factor induces primordial follicle development and initiates folliculogenesis. Endocrinology 1999; 140: 4262-4271.

Pearson G, Robinson F, Beers Gibson T, Xu BE, Karandikar M, Berman K, and Cobb MH. Mitogen-activated protein (MAP) kinase pathways: regulation and physiological functions. Endocrine Reviews 2001; 22(2): 153-83.

Peddie MJ, Onagbesan OM, and Williams J. Chicken granulosa cell proliferation and progesterone production in culture: effects of EGF and theca secretions. General and Comparative Endocrinology 1994; 94(3): 341-56.

Pepling ME. Follicular assembly: mechanisms of action. Reproduction 2012; 143: 139–149.

Perry MM, Waddington D, Gilbert AB, and Hardie MA. Growth rates of the small yolky follicles in the ovary of the domestic fowl. International Research Communications System Journal of Medical Science 1983; 11: 979-980.

Pisarska MD, Kuo F-T, Tang D, Zarrini P, Khan S, and Ketefian A. Expression of forkhead transcription factors in human granulosa cells. Fertility and Sterility 2009; 91(4) Supplement: 1392–1394.

Pishnamazi A, Renema RA, Zuidhof MJ, and Robinson FE. Effect of Initial Full Feeding of Broiler Breeder Pullets on Carcass Development and Body Weight Variation. Applied Poultry Research 2008; 17 (4): 505-514.

Pishnamazi A, Renema RA, Zuidhof MJ, and Robinson F. Effect of age at photostimulation on sexual maturation in broiler breeder pullets. Poultry Science 2014; 93(5): 1274-81.

Reddy PRK and Siegel PB. Selection for body weight at eight weeks of age.11. Ovulation and oviposition patterns. Poultry Science 1976; 55: 1518-1530.

Reddy P, Shen L, Ren C, Boman K, Lundin E, Ottander U, Lindgren P, Liu YX, Sun QY, and Liu K. Activation of Akt (PKB) and suppression of FKHRL1 in mouse and rat oocytes by stem cell

factor during follicular activation and development. Developmental Biology 2005; 281(2): 160-70.

Reddy P, Liu L, Adhikari D, Jagarlamudi K, Rajareddy S, Shen Y, Du C, Tang W, Hämäläinen T, Peng SL, Lan ZJ, Cooney AJ, Huhtaniemi I, Liu K. Oocyte-Specific Deletion of Pten Causes Premature Activation of the Primordial Follicle Pool. Science 2008; 319(5863): 611-3.

Reiter EO, Goldenberg RL, Vaitukaitis JL, and Ross GT. A role for endogenous estrogen in normal ovarian development in the neonatal rat. Endocrinology 1972; 91(6): 1537-9.

Renema RA and Robinson FE. Defining normal: comparison of feed restriction and full feeding of female broiler breeders. World's Poultry Science Journal 2004; 60: 508-522.

Renema RA, Robinson FE, and Zuidhof MJ. Reproductive Efficiency and Metabolism of Female Broiler Breeders as Affected by Genotype, Feed Allocation, and Age at Photostimulation. 2. Sexual Maturation. Poultry Science 2007; 86: 2267–2277.

Robinson FE and Etches RJ. Ovarian Steroidogenesis during Foillicular Maturation in the Domestic Fowl (Gallus domesticus). Biology of Reproduction 1986; 35: 1096-1105.

Rodgers RJ, van Wezel IL, Irving-Rodgers HF, Lavranos TC, Irvine CM, and Krupa M. Roles of extracellular matrix in follicular development. Journal of Reproduction and Fertility Supplement 1999; 54: 343-52. Review.

Rosas G, Ramirez MI, Linares R, Trujillo A, Dominguez R, and Morales-Ledesma L. Asymmetric steroidogenic response by the ovaries to the vasoactive intestinal peptide. Endocrine 2015; 48: 968-977.

Said SI and Mutt V. Polypeptide with broad biological activity: isolation from small intestine. Science 1970; 169: 1217-1218.

Said SI and Mutt V. Isolation from porcine-intestinal wall of a vasoactive octacosapeptide related to secretin and to glucagon. European Journal of Biochemistry 1972; 28: 199-204.

Saldanha CJ, Silverman AJ, and Silver R. Direct innervation of GnRH neurons by encephalic photoreceptors in birds. Biological Rhythms 2001; 16: 39–49.

Sanyal S and Van Tol HHM. Dopamine D4 Receptor-Mediated Inhibition of Cyclic Adenosine 3', 5'-Monophosphate Production Does Not Affect Prolactin Regulation. Endocrinology 1997; 138(5): 1871-1878.

Schaeffer JM and Hsueh AJ. Identification of gamma-aminobutyric acid and its binding sites in the rat ovary. Life Sciences 1982; 30(19): 1599-1604.

Schena M, Shalon D, Davis RW, and Brown PO. Quantitative monitoring of gene expression patterns with a complementary DNA microarray. Science 1995; 270(5235):467-70.

Schmierer B, Schuster MK, Shkumatava A, and Kuchler K. Activin A signaling induces Smad2, but not Smad3, requiring protein kinase A activity in granulosa cells from the avian ovary. Biological Chemistry 2003; 278: 21197-21203.

Schneider R, Bannister AJ, Myers FA, Thorne AW, Crane-Robinson C, and Kouzarides T. Histone H3 lysine 4 methylation patterns in higher eukaryotic genes. Nature Cell Biology 2004; 6 73-77.

Sharp PJ, Talbot RT, Main GM, Dunn IC, Fraser HM, and Huskisson NS. Physiological roles of chicken LHRH-I and -II in the control of gonadotrophin release in the domestic chicken. Endocrinology 1990; 124: 291–299.

Sharpe LJ, Howe V, Prabhu AV, Luu W, and Brown AJ. Navigating the Shallows and Rapids of Cholesterol Synthesis Downstream of HMGCR. Nutritional Science and Vitaminology 2015; 61: S154-S156. Review.

Siegel PB and Dunnington EA (1985). In W. G. Hill, J.M. Manson and D. Hewitt (Eds.) *Poultry Genetics and Breeding* (pp. 59-70). Longman Group, Harlow.

Sites CK, Kessel B, and LaBarbera AR. Adhesion proteins increase cellular attachment, follicle-stimulating hormone receptors, and progesterone production in cultured porcine granulosa cells. Proceedings of the Society for Experimental Biology and Medicine 1996; 212(1): 78-83.

Skinner M. Regulation of primordial follicle assembly and development. Human Reproduction Update 2005; 11(5): 461–471.

Smith CA and Sinclair AH. Sex determination: insights from the chicken. BioEssays 2004; 26(2): 120-32.

Soccio RE and Breslow JL, StAR-related lipid transfer (START) proteins: mediators of intracellular lipid metabolism. Biological Chemistry 2003; 278: 22183–22186.

Stocco DM, Wang XJ, Jo Y, and Manna PR. Multiple Signaling Pathways Regulating Steroidogenesis and Steroidogenic Acute Regulatory Protein Expression: More Complicated than We Thought. Molecular Endocrinology 2005; 19(11): 2647-2659. Review.

Sun T, Pepling ME, and Diaz FJ. Lats1 Deletion Causes Increased Germ Cell Apoptosis and Follicular Cysts in Mouse Ovaries. Biology of Reproduction 2015; 93 (1): 1-11.

Tagler D, Makanji Y, Tu T, Bernabé BP, Lee R, Zhu J, Kniazeva E, Hornick JE, Woodruff TK, and Shea LD. Promoting extracellular matrix remodeling via ascorbic acid enhances the survival of primary ovarian follicles encapsulated in alginate hydrogels. Biotechnology and Bioengineering 2014; 111(7): 1417-29.

Taussig R and Gilman AG. Mammalian Membrane-bound Adenylyl Cyclases. Journal of Biological Chemistry 1995; 270(1): 1-4.

Tian X, Halfhill AN, and Diaz FJ. Localization of phosphorylated SMAD proteins in granulosa cells, oocytes and oviduct of female mice. Gene Expression Patterns 2010; 10: 105-112.

Tilly JL, Kowalski KI, and Johnson AL. Stage of ovarian follicular development associated with the initiation of steroidogenic competence in avian granulosa cells. Biol Reprod 1991a ; 44: 305-314.

Tilly JL, Kowalski KI, Johnson AL, Hsueh AJW. Involvement of apoptosis in ovarian follicular atresia and postovulatory regression. Endocrinology 1991b; 129: 2799-2801.

Tilly JL, Kowalski KI, Li Z, Levorse JM, Johnson AL. 1992. Plasminogen activator activity and thymidine incorporation in avian granulosa cells during follicular development and the periovulatory period. Biol Reprod, 46:195-200.

Tischkau SA and Bahr JM. Avian germinal disc region secretes factors that stimulate proliferation and inhibit progesterone production by granulosa cells. Biology of Reproduction 1996; 54: 865-870.

Trojer P and Reinberg D. Facultative Heterochromatin: Is There a Distinctive Molecular Signature? Molecular Cell 2007; 28: 1-13

Trounson A, Anderiesz C, and Jones G. Maturation of human oocytes in vitro and their developmental competence. Reproduction 2001; 121(1): 51-75.

Ukeshima A and Fujimoto T. A fine morphological study of germ cells in asymmetrically developing right and left ovaries of the chick. Anatomical Record 1991; 230: 378-386.

Vaccari S, Latini S, Barberi M, Teti A, Stefanini M, and Canipari R. Characterization and expression of different pituitary adenylate cyclase-activating polypeptide/vasoactive intestinal polypeptide receptors in rat ovarian follicles. Endocrinology 2006; 191: 289-299.

Vaudry D, Gonzalez BJ, Basille M, Yon L, Fournier A, and Vaudry H. Pituitary adenylate cyclase-activating polypeptide and its receptors: from structure to functions. Pharmacological Reviews 2000; 52: 269-324. Review.

Vomhof-DeKrey EE, Sandy AR, Failing JJ, Hermann RJ, Hoselton SA, Schuh JM, Weldon AJ, Payne KJ, Dorsam GP. Radical reversal of vasoactive intestinal peptide (VIP) receptors during early lymphopoiesis. Peptides 2011; 32(10): 2058-66.

Waddington D and Walker MA. Distribution of follicular growth, atresia and ovulation in the ovary of the domestic hen (Gallus domesticus) at different ages. Journal of Reproduction and Fertility 1988; 84: 223-230.

Wang JY, Yaksh TL, Harty GJ, and Go VL. Neurotransmitter modulation of VIP release from cat cerebral cortex. American Journal of Physiology 1986; 250(1 Pt 2): R104-11.

Wang Y, Li J, Ying Wang C, Yan Kwok AH, and Leung FC. Epidermal growth factor (EGF) receptor ligands in the chicken ovary: I. Evidence for heparin-binding EGF-like growth factor (HB-EGF) as a potential oocyte-derived signal to control granulosa cell proliferation and HB-EGF and kit ligand expression. Endocrinology 2007; 148: 3426-3440.

Wang N, Luo LL, Xu JJ, Xu MY, Zhang XM, Zhou XL, Liu WJ, and Fu YC. Obesity accelerates ovarian follicle development and follicle loss in rats. Metabolism 2014; 63(1): 94-103.

Woods DC and Johnson AL. Regulation of Follicle-Stimulating Hormone-Receptor Messenger RNA in Hen Granulosa Cells Relative to Follicle Selection. Biology of Reproduction 2005; 72: 643-650.

Woods DC, Haugen MJ, Johnson AL. Opposing actions of TGFβ and MAP kinase signaling in undifferentiated hen granulosa cells. Biochemical and Biophysical Research Communications 2005; 336 (2): 450-457.

Woods DC, Haugen MJ, and Johnson AL. Actions of epidermal growth factor receptor/mitogen-activated protein kinase and protein kinase C signaling in granulosa cells from Gallus gallus are dependent upon stage of differentiation. Biology of Reproduction 2007; 77: 61-70.

Woods DC and Johnson AL . Phosphatase activation by epidermal growth factor family ligands regulates extracellular regulated kinase signaling in undifferentiated hen granulosa cells. Endocrinology 2006; 147: 4931-4940.

Wu Y, Zhang Z, Liao X, Qi L, Liu Y, and Wang Z. Effect of high-fat diet-induced obesity on the Akt/FoxO/Smad signaling pathway and the follicular development of the mouse ovary. Molecular Medicine Reports 2016; 14(4): 3894-900.

Yang XJ and Seto E. HATs and HDACs: from structure, function and regulation to novel strategies for therapy and prevention. Oncogene 2007; 26: 5310-5318.

Yao HHC and Bahr JM. Germinal disc-derived epidermal growth factor: a paracrine factor to stimulate proliferation of granulosa cells. Biology of Reproduction 2001; 64:390-395.

Yu MW, Robinson FE, and Robblee AR. Effect of feed allowance during rearing and breeding on female broiler breeders. 1. Growth and carcass characteristics. Poultry Science 1992a; 71: 1739-1749.

Yu MW, Robinson FE, Charles RG, and Weingardt R. Effect of Feed Allowance during Rearing and Breeding on Female Broiler Breeders. 2. Ovarian Morphology and Production. Poultry Science 1992b; 71: 1750-1761.

Yu M, Yu P, Leghari IH, Ge C, Mi Y, and Zhang C. RALDH2, the enzyme for retinoic acid synthesis, mediates meiosis initiation in germ cells of the female embryonic chickens. Amino Acids 2013; 44: 405-412.

Yui MA, Feng N, and Rothenberg EV. Fine-scale staging of T cell lineage commitment in adult mouse thymus. Journal of Immunology 2010; 185(1): 284-93.

Zhou R, Tsang AHK, Lau S-W, and Ge W. Pituitary Adenylate Cyclase-Activating Polypeptide (PACAP) and Its Receptors in the Zebrafish Ovary: Evidence for Potentially Dual Roles of PACAP in Controlling Final Oocyte Maturation. Biology of Reproduction 2011; 85: 615-625.

Zhou SS and Li P. Effects of NELL2 on the regulation of GnRH expression and puberty in female rats. Genetics and Molecular Research 2014; 13(3): 6672-6682.

Zuidhof MJ, Holm DE, Renema RA, Jalal MA, and Robinson FE. Effects of broiler breeder management on pullet body weight and carcass uniformity. Poultry Science 2015; 94(6): 1389-97.

APPENDIX

Edited Lists of Differentially Expressed Genes

Table 4.1. Edited list of 151 DEG with greater abundance in FF at 16 weeks. Pg 1 of 4

Probe Set ID	Gene Symbol	Transcript ID	Gene Name	Fold change
Gga.11339.1.S1_at	VIPR2	NM_001014970	vasoactive intestinal peptide receptor 2	6.653
GgaAffx.21361.1.S1_at	HOXC10	XM_001233805	homeobox C10	5.752
Gga.13143.1.S1_at	GDF9	NM_206988	growth differentiation factor 9	5.398
Gga.1644.1.S1_a_at	MGLL	NM_001277142	monoglyceride lipase	5.393
Gga.3225.1.S1_at	MYH11	NM_205274	myosin, heavy chain 11, smooth muscle	5.226
GgaAffx.11519.1.S1_at	RHOG	NM_001012536	ras homolog family member G	5.128
Gga.12800.1.S1_at	MMP10	NM_001278089	matrix metallopeptidase 10 (stromelysin 2)	5.088
Gga.595.1.S1_at	NELL2	NM_001030740	NEL-like 2	4.986
Gga.11229.1.S1_at	PPP1R3D	XM_417397	protein phosphatase 1, regulatory subunit 3D	4.785
Gga.3587.1.S1_at	MATN3	NM_205072	matrilin 3	4.306
Gga.596.1.S1_at	HSD3B2	NM_205118	hydroxy-delta-5-steroid dehydrogenase, 3 beta- and steroid delta-isomerase 2	4.118
Gga.7210.1.S1_at	ZP3	NM_204389	zona pellucida sperm-binding protein 3	3.834
Gga.8880.1.S1_at	MME	NM_001004412	membrane metallo-endopeptidase	3.754
Gga.2680.1.S1_at	AQP1	NM_001039453	aquaporin 1 (Colton blood group)	3.66
Gga.3108.1.S1_at	FHL2	XM_416924	four and a half LIM domains 2	3.644
GgaAffx.5451.1.S1_at	HDAC10	XM_415986	histone deacetylase 10	3.633
Gga.8352.1.S1_at	LAMA2	XM_419746	laminin, alpha 2	3.633
Gga.1128.2.S1_a_at	SOD3	XM_420760	superoxide dismutase 3, extracellular	3.593
GgaAffx.21669.1.S1_at	NR4A2	XM_422166	nuclear receptor subfamily 4, group A, member 2	3.539
Gga.12186.1.S1_at	LYVE1	NM_001199587	lymphatic vessel endothelial hyaluronan receptor 1	3.42
Gga.9293.1.S1_at	FN1	NM_001198712	fibronectin 1	3.274
Gga.6201.1.S1_at	ISG12-2	NM_001001296	ISG12-2 protein-like	3.239
Gga.13583.1.S1_at	CD36	NM_001030731	CD36 molecule (thrombospondin receptor)	3.177
GgaAffx.1288.1.S1_at	RSPO1	XM_417760	R-spondin 1	3.089
Gga.227.1.S1_at	STAR	NM_204686	steroidogenic acute regulatory protein	3.064
Gga.8977.1.S1_at	BROX	XM_419397	BRO1 domain and CAAX motif containing	3.057
Gga.14703.1.S1_at	SP8	NM_001198666	Sp8 transcription factor	3.05
GgaAffx.24185.1.S1_at	IL7R	NM_001080106	interleukin 7 receptor	2.999
Gga.2305.1.S1_at	CXCR4	NM_204617	chemokine (C-X-C motif) receptor 4	2.987
Gga.7528.1.S1_at	KLF2	XM_418264	Kruppel-like factor 2 (lung)	2.964
Gga.6303.1.S1_s_at	AGR2	XM_418698	anterior gradient homolog 2 (Xenopus laevis)	2.93
GgaAffx.6121.1.S1_s_at	ASNS	NM_001030977	asparagine synthetase (glutamine-hydrolyzing)	2.886
Gga.968.1.S1_at	COL20A1	NM_001004392	collagen, type XX, alpha 1	2.883
Gga.5505.1.S1_a_at	SOX9	NM_204281	SRY (sex determining region Y)-box 9	2.881
Gga.19199.1.S1_at	ABCC9	XM_003640404	ATP-binding cassette, sub-family C (CFTR/MRP), member 9	2.853
GgaAffx.20104.1.S1_s_at	POSTN	NM_001030541	periostin, osteoblast specific factor	2.848
Gga.19271.1.S1_at	NIM1	NM_001252130	serine/threonine-protein kinase NIM1	2.84
GgaAffx.21771.1.S1_at	COL6A1	NM_205107	collagen, type VI, alpha 1	2.827

Table 4.1. (con't) Edited list of 151 DEG with greater abundance FF at 16 weeks. 2 of 4

Probe Set ID	Gene Symbol	Transcript ID	Gene Name	Fold change
GgaAffx.21915.1.S1_at	IFIT5	XM_421662	interferon-induced protein with tetratricopeptide repeats 5	2.815
GgaAffx.3568.1.S1_at	CRISPLD2	XM_414180	cysteine-rich secretory protein LCCL domain containing 2	2.787
Gga.384.1.S1_at	HSD17B1	NM_204837	hydroxysteroid (17-beta) dehydrogenase 1	2.774
GgaAffx.11661.1.S1_at	XRCC3	NM_001006489	X-ray repair complementing defective repair in Chinese hamster cells 3	2.768
GgaAffx.9256.1.S1_s_at	C1S	NM_001030777	complement component 1, s subcomponent	2.758
Gga.4975.1.S1_a_at	TPM2	NM_205446	tropomyosin 2 (beta)	2.758
Gga.6296.1.S1_at	SAR1B	NM_001030621	SAR1 homolog B (S. cerevisiae)	2.689
Gga.5927.1.S1_at	GRP	NM_001277900	gastrin-releasing peptide	2.684
Gga.11838.1.S1_at	IGSF5	XM_416733	immunoglobulin superfamily, member 5	2.674
Gga.10874.1.S1_at	CNDP1	XM_419098	carnosine dipeptidase 1 (metallopeptidase M20 family)	2.672
Gga.893.1.S1_a_at	CYP24A1	NM_204979	cytochrome P450, family 24, subfamily A, polypeptide 1	2.664
GgaAffx.12895.1.S1_at	MRPS6	NM_001031486	mitochondrial ribosomal protein S6	2.646
Gga.2073.1.S1_at	COL1A1	XM_423116	collagen, type I, alpha 1	2.638
Gga.19191.1.S1_at	SEZ6L	XM_415197	seizure related 6 homolog (mouse)-like	2.636
Gga.12216.1.S1_at	CLRN1	XM_001233893	clarin 1	2.597
Gga.19474.1.S1_at	MAP7D3	XM_420230	MAP7 domain containing 3	2.577
GgaAffx.6945.1.S1_at	SERPINA5	XM_421344	serpin peptidase inhibitor, clade A (alpha-1 antiproteinase, antitrypsin), member 5	2.576
GgaAffx.20660.1.S1_at	SVOPL	XM_416339	SVOP-like	2.564
Gga.7386.1.S1_at	FBXO22	NM_001030545	F-box protein 22	2.563
Gga.918.1.S1_at	KCNMB1	NM_204602	potassium large conductance calcium-activated channel, subfamily M, beta member 1	2.561
Gga.238.1.S1_at	LRRC17	NM_001198600	leucine rich repeat containing 17	2.538
GgaAffx.9283.1.S1_at	KIAA0825	XM_003643061	KIAA0825	2.536
GgaAffx.23672.1.S1_at	LZTFL1	XM_418797	leucine zipper transcription factor-like 1	2.534
GgaAffx.7834.1.S1_at	NXPH2	XM_426606	neurexophilin 2	2.525
Gga.18351.1.A1_at	SULF1	XM_003640824	sulfatase 1	2.497
Gga.13146.1.S1_at	EPSTI1	XM_417033	epithelial stromal interaction 1 (breast)	2.495
Gga.16765.1.S1_at	LRRC58	XM_416555	leucine rich repeat containing 58	2.494
Gga.5111.1.S1_at	CCDC80	NM_204431	coiled-coil domain containing 80	2.49
Gga.3903.1.S1_at	CDH13	NM_001001760	cadherin 13, H-cadherin (heart)	2.485
GgaAffx.13010.1.S1_at	NUF2	NM_204478	NUF2, NDC80 kinetochore complex component, homolog (S. cerevisiae)	2.473
Gga.2129.1.S1_s_at	MAP1B	NM_205246	microtubule-associated protein 1B	2.466
Gga.11010.1.S1_at	SLC6A15	XM_416124	solute carrier family 6 (neutral amino acid transporter), member 15	2.463
Gga.1111.1.S1_a_at	USP18	XM_416398	ubiquitin specific peptidase 18	2.459
Gga.5092.1.S1_s_at	ANXA2	NM_205351	annexin A2	2.453
Gga.19950.1.S1_s_at	F13A1	NM_204685	coagulation factor XIII, A1 polypeptide	2.453
Gga.3908.1.S1_at	TAGLN	NM_205494	transgelin	2.453
GgaAffx.12935.1.S1_s_at	DHCR24	NM_001031288	24-dehydrocholesterol reductase	2.439
Gga.11876.1.S1_a_at	GLIPR2	XM_419085	GLI pathogenesis-related 2	2.439

Table 4.1. (con't) Edited list of 151 DEG with greater abundance in FF at 16 weeks. 3 of 4

Probe Set ID	Gene Symbol	Transcript ID	Gene Name	Fold change
Gga.9481.1.S1_s_at	KRT7	NM_204932	keratin 7	2.434
GgaAffx.12320.1.S1_at	STARD4	NM_001079742	StAR-related lipid transfer (START) domain containing 4	2.429
Gga.14273.1.S1_at	HAS2	NM_204806	hyaluronan synthase 2	2.41
Gga.16345.1.S1_at	SMAD2	NM_204561	SMAD family member 2	2.399
GgaAffx.12414.1.S1_s_at	HMGCR	NM_204485	3-hydroxy-3-methylglutaryl-CoA reductase	2.391
Gga.7813.1.S1_at	CFI	NM_001272018	complement factor I	2.375
Gga.9972.1.S1_at	RASD1	NM_001044636	RAS, dexamethasone-induced 1	2.361
Gga.15362.1.S1_at	RGS18	NM_001257327	Regulator of G-protein signaling 18	2.357
Gga.1035.1.S1_at	TGM2	NM_205448	transglutaminase 2 (C polypeptide, protein-glutamine-gamma-glutamyltransferase)	2.34
Gga.12310.1.S1_at	BBOX1	XM_424543	butyrobetaine (gamma), 2-oxoglutarate dioxygenase (gamma-butyrobetaine hydroxylase) 1	2.318
Gga.9630.1.S1_s_at	LDLR	NM_204452	low density lipoprotein receptor	2.309
GgaAffx.25118.1.S1_at	SLITRK6	XM_003640550	SLIT and NTRK-like family, member 6	2.302
Gga.888.1.S1_at	COL6A3	NM_205534	collagen, type VI, alpha 3	2.287
Gga.261.3.S1_a_at	PRLR	NM_204854	prolactin receptor	2.285
Gga.12111.1.S1_at	ANGPTL1	NM_001277665	angiopoietin-like 1	2.274
Gga.6358.1.S1_at	FAM189A2	XM_424828	family with sequence similarity 189, member A2	2.266
Gga.10208.1.S1_a_at	FHL5	NM_001277723	four and a half LIM domains 5	2.263
GgaAffx.21351.1.S1_s_at	CA4	XM_415893	carbonic anhydrase IV	2.257
Gga.46.1.S1_a_at	DPF3	NM_204639	D4, zinc and double PHD fingers, family 3	2.256
Gga.4091.1.S2_a_at	MYLK	NM_205459	myosin light chain kinase	2.255
Gga.4974.1.S2_at	VCAN	NM_204787	versican	2.253
Gga.6433.1.S1_at	CLDN2	NM_001277622	claudin 2	2.243
Gga.5396.1.S1_at	C1QB	ENSGALT00000007609	complement component 1, q subcomponent, B chain	2.236
GgaAffx.25534.1.S1_s_at	COL3A1	NM_205380	collagen, type III, alpha 1	2.231
Gga.16448.1.S1_at	HOXA9	XM_00364070	homeobox A9, homeobox protein Hox-A9-like, homeobox protein Hox-A9-like	2.23
Gga.666.1.S1_a_at	VIP	NM_001177309	vasoactive intestinal peptide	2.218
Gga.644.1.S1_at	ACTG2	NM_205172	actin, gamma 2, smooth muscle, enteric	2.217
Gga.8082.1.S1_at	RBM45	NM_001031252	RNA binding motif protein 45	2.207
Gga.620.1.S1_at	BMP5	NM_205148	bone morphogenetic protein 5	2.201
Gga.1763.1.S1_at	WFDC1	NM_204554	WAP four-disulfide core domain 1	2.186
Gga.6729.1.S1_at	DHX57	XM_424198	DEAH (Asp-Glu-Ala-Asp/His) box polypeptide 57	2.182
Gga.195.1.S1_at	GPR149	NM_204662	G protein-coupled receptor 149	2.179
GgaAffx.12155.1.S1_s_at	PGRMC1	NM_001271939	progesterone receptor membrane component 1	2.177
Gga.260.2.S1_a_at	DMRT1	NM_001101831	doublesex and mab-3 related transcription factor 1	2.175
Gga.4257.1.S1_at	COL6A2	NM_205348	collagen, type VI, alpha 2	2.172
Gga.3075.1.S1_at	ADAMTSL3	XM_413844	ADAMTS-like 3	2.166
Gga.7298.1.S1_at	C1QA	XM_417654	complement component 1, q subcomponent, A chain	2.16

Table 4.1. (con't) Edited list of 151 DEG with greater abundance in FF at 16 weeks. 4 of 4

Probe Set ID	Gene Symbol	Transcript ID	Gene Name	Fold change
GgaAffx.8303.1.S1_at	RERG	XM_416404	RAS-like, estrogen-regulated, growth inhibitor	2.16
Gga.90.1.S1_at	MEOX2	NM_001005427	mesenchyme homeobox 2	2.156
Gga.7708.1.S1_at	MAOA	NM_001030799	monoamine oxidase A	2.15
Gga.3378.1.S1_at	ODZ4	XM_425655	odz, odd Oz/ten-m homolog 4 (Drosophila)	2.147
Gga.175.1.S1_at	DEFB1	NM_204650	defensin, beta 1	2.145
Gga.13206.1.S1_at	PHTF2	NM_001006226	putative homeodomain transcription factor 2	2.139
GgaAffx.7511.2.S1_s_at	FAT4	XM_420617	FAT tumor suppressor homolog 4 (Drosophila)	2.126
Gga.4420.2.S1_at	RTN1	NM_001001466	reticulon 1	2.122
Gga.17632.1.S1_at	KCNJ8	XM_416431	potassium inwardly-rectifying channel, subfamily J, member 8	2.12
Gga.18298.1.S1_at	RAPGEF2	XM_420387	Rap guanine nucleotide exchange factor (GEF) 2	2.103
Gga.7044.3.S1_s_at	SEPP1	NM_001031609	selenoprotein P, plasma, 1	2.103
Gga.4510.1.S1_a_at	ALB	NM_205261	albumin	2.102
GgaAffx.9174.2.S1_at	CHD4	XM_003640441	chromodomain helicase DNA binding protein 4	2.09
Gga.9334.2.S1_a_at	SGK1	NM_204476	serum/glucocorticoid regulated kinase 1	2.085
GgaAffx.21816.1.S1_s_at	CYP19A1	NM_001001761	cytochrome P450, family 19, subfamily A, polypeptide 1	2.082
Gga.2558.1.S1_a_at	COL14A1	NM_205334	collagen, type XIV, alpha 1	2.081
Gga.14011.1.S1_at	ECSCR	XM_429401	endothelial cell surface expressed chemotaxis and apoptosis regulator	2.081
GgaAffx.22999.1.S1_s_at	COL1A2	NM_001079714	collagen, type I, alpha 2	2.08
Gga.11207.1.S1_s_at	ACSL4	XM_420317	acyl-CoA synthetase long-chain family member 4	2.068
Gga.7827.1.S1_at	MTHFS	NM_001277626	5,10-methenyltetrahydrofolate synthetase (5-formyltetrahydrofolate cyclo-ligase)	2.066
Gga.13093.1.S1_at	MCC	XM_413971	mutated in colorectal cancers	2.063
GgaAffx.4586.1.S1_at	MAP3K8	XM_418581	mitogen-activated protein kinase kinase kinase 8	2.055
Gga.3772.1.S1_a_at	T	NM_204940	T, brachyury homolog (mouse)	2.055
Gga.10521.1.S1_s_at	RALGAPA1	NM_001277447	Ral GTPase activating protein, alpha subunit 1 (catalytic)	2.051
Gga.3316.1.S1_s_at	HHEX	NM_205252	hematopoietically expressed homeobox	2.05
Gga.1364.1.S1_at	ARMC10	XM_415964	armadillo repeat containing 10	2.043
Gga.4446.1.S3_at	GIT2	NM_204206	G protein-coupled receptor kinase interactor 2	2.04
GgaAffx.20528.1.S1_at	PROS1	XM_416641	protein S (alpha)	2.035
Gga.6127.2.S1_a_at	ADCK3	NM_001199413	aarF domain containing kinase 3	2.03
GgaAffx.4808.1.S1_s_at	ARHGAP21	NM_001177357	Rho GTPase activating protein 21	2.027
Gga.8070.1.S1_at	USP35	XM_417222	ubiquitin specific peptidase 35	2.025
Gga.198.1.S1_at	MMP9	NM_204667	matrix metallopeptidase 9 (gelatinase B, 92kDa gelatinase, 92kDa type IV collagenase)	2.024
GgaAffx.7997.1.S1_at	BPIFCB	XM_001234742	BPI fold containing family C, member B	2.02
Gga.591.1.S1_s_at	CYP11A1	NM_001001756	cytochrome P450, family 11, subfamily A, polypeptide 1	2.009
Gga.12092.1.S1_at	FAM20C	XM_414753	family with sequence similarity 20, member C	2.007
GgaAffx.10417.7.S1_s_at	DST	XM_419901	dystonin	2.006
Gga.3104.1.S1_at	COL4A2	NM_001162390	collagen, type IV, alpha 2	2.003
Gga.6561.1.S1_at	KRT5	NM_001001195	keratin 5	2.002

Table 4.2. Edited list of 237 DEG with lesser abundance in FF at 16 weeks. Pg. 1 of 7

Probe Set ID	Gene Symbol	Transcript ID	Gene Title	Fold change
Gga.4225.1.S1_at	LECT2	NM_205478	leukocyte cell-derived chemotaxin 2	7.707
GgaAffx.10943.1.S1_at	MTUS2	XM_417117	microtubule associated tumor suppressor candidate 2	6.215
Gga.758.1.S1_at	LMX1B	NM_205358	LIM homeobox transcription factor 1, beta	5.643
Gga.919.1.S1_at	DLX5	NM_204159	distal-less homeobox 5	5.583
Gga.11262.1.S1_at	SLC35F3	XM_419560	solute carrier family 35, member F3	5.465
GgaAffx.21849.1.S1_s_at	CATHL3	NM_001001605	cathelicidin antimicrobial peptide	5.438
GgaAffx.22908.2.S1_s_at	CAPN8	XM_426117	calpain 8	4.779
GgaAffx.23292.1.S1_at	KIF26B	XM_003640984	kinesin family member 26B	4.573
GgaAffx.21842.1.S1_s_at	GAL7	NM_001001194	Gal 7	4.534
Gga.15599.1.S1_s_at	SPOCK1	XM_414622	sparc/osteonectin, cwcv and kazal-like domains proteoglycan (testican) 1	4.345
GgaAffx.22404.6.S1_s_at	CHL1	XM_414434	cell adhesion molecule with homology to L1CAM (close homolog of L1)	4.325
GgaAffx.23423.2.S1_s_at	KCNJ5	XM_417864	potassium inwardly-rectifying channel, subfamily J, member 5	4.305
Gga.2869.1.S1_at	KCNIP4	NM_204555	Kv channel interacting protein 4	4.293
Gga.10360.1.S1_at	DPP6	XM_418545	dipeptidyl-peptidase 6	4.253
Gga.5163.1.S1_at	NGF	XM_00364272	nerve growth factor (beta polypeptide)	4.21
Gga.12901.2.S1_a_at	SGCD	XM_414572	sarcoglycan, delta (35kDa dystrophin-associated glycoprotein)	4.094
Gga.4126.1.S1_at	RBP4	NM_205238	retinol binding protein 4, plasma	4.077
GgaAffx.3918.5.S1_s_at	TRPC7	XM_425214	transient receptor potential cation channel, subfamily C, member 7	3.951
Gga.12036.1.S1_at	EHF	NM_001277584	ets homologous factor	3.946
Gga.10124.2.S1_a_at	SETBP1	XM_001233853	SET binding protein 1	3.877
GgaAffx.8821.1.S1_at	MC2R	NM_001031515	melanocortin 2 receptor (adrenocorticotropic hormone)	3.766
GgaAffx.9053.2.S1_at	NSUN7	XM_420736	NOP2/Sun domain family, member 7	3.761
Gga.7801.1.S1_at	KYNU	XM_422147	kynureninase	3.75
GgaAffx.24539.1.S1_at	SLC35F1	XM_001233613	solute carrier family 35, member F1	3.734
Gga.8416.1.S1_at	GALNTL6	XM_420520	UDP-N-acetyl-alpha-D-galactosamine:polypeptide N-acetylgalactosaminyltransferase-like 6	3.68
Gga.12779.1.S1_at	VPS8	XM_003641729	thioredoxin domain-containing protein 6-like, vacuolar protein sorting 8 homolog (S. cerevisiae)	3.679
GgaAffx.22642.1.S1_s_at	SLC39A12	XM_418616	solute carrier family 39 (zinc transporter), member 12	3.654
GgaAffx.8356.1.S1_s_at	MOCOS	XM_419048	molybdenum cofactor sulfurase	3.632
Gga.2685.1.S2_at	FGF13	NM_001001743	fibroblast growth factor 13	3.621
GgaAffx.6024.1.S1_at	TMEM117	XM_416041	transmembrane protein 117	3.609
Gga.957.1.S1_at	HOXA11	NM_204619	homeobox A11, homeobox protein Hox-A11-like, homeobox protein Hox-A11-like	3.505
Gga.495.1.S1_at	GAL2	NM_001201399	gallinacin 2	3.482
GgaAffx.7313.1.S1_at	BCL2L14	XM_417285	BCL2-like 14 (apoptosis facilitator)	3.479
Gga.3047.2.S1_at	EPHA5	NM_205105	EPH receptor A5	3.473

Table 4.2. (con't)Edited list of 237 DEG with lesser abundance in FF at 16 weeks. 2 of 7

Probe Set ID	Gene Symbol	Transcript ID	Gene Title	Fold change
GgaAffx.6318.1.S1_at	LRFN2	XM_426127	leucine rich repeat and fibronectin type III domain containing 2	3.438
Gga.642.1.S1_a_at	BFSP2	NM_205218	beaded filament structural protein 2, phakinin	3.423
Gga.10684.1.S1_s_at	EFCAB7	XM_003641717	EF-hand calcium binding domain 7	3.37
Gga.952.1.S1_at	NKX2-1	NM_204616	NK2 homeobox 1	3.352
Gga.415.1.S1_at	SERPINB10	NM_204897	serpin peptidase inhibitor, clade B (ovalbumin), member 10	3.352
Gga.1428.2.S1_at	DPYSL4	NM_204197	dihydropyrimidinase-like 4	3.346
Gga.7638.2.S1_at	MAF	NM_001044671	v-maf musculoaponeurotic fibrosarcoma oncogene homolog (avian)	3.316
Gga.7758.1.S1_at	TCERG1L	XM_421827	transcription elongation regulator 1-like	3.244
Gga.11013.1.S1_at	MEGF11	XM_413915	multiple EGF-like-domains 11	3.22
Gga.153.1.S2_at	ZIC1	NM_204254	Zic family member 1	3.213
GgaAffx.10704.1.S1_at	FAM176A	XM_420070	family with sequence similarity 176, member A	3.196
GgaAffx.8403.1.S1_at	GABBR2	XM_419066	gamma-aminobutyric acid (GABA) B receptor, 2	3.192
GgaAffx.6816.2.S1_s_at	DGKB	XM_001235515	diacylglycerol kinase, beta 90kDa	3.151
Gga.10538.1.S1_at	PIEZO2	ENSGALT00000022620	piezo-type mechanosensitive ion channel component 2	3.144
Gga.1814.1.S1_at	IGDCC3	XM_413904	immunoglobulin superfamily, DCC subclass, member 3	3.139
Gga.4053.1.S1_at	EEF1A2	NM_001032398	eukaryotic translation elongation factor 1 alpha 2	3.132
Gga.10474.1.S1_at	SNTG1	XM_419197	syntrophin, gamma 1	3.129
GgaAffx.8148.1.S1_at	SERPINB5	XM_418986	serpin peptidase inhibitor, clade B (ovalbumin), member 5	3.116
GgaAffx.20140.1.S1_at	DLX6	NM_001080890	distal-less homeobox 6	3.06
GgaAffx.1786.1.S1_at	TMEM132B	XM_415101	transmembrane protein 132B	3.034
GgaAffx.21953.2.S1_at	GRIP2	XM_414383	glutamate receptor interacting protein 2	3.03
GgaAffx.7341.1.S1_s_at	SLC22A3	XM_419620	solute carrier family 22 (extraneuronal monoamine transporter), member 3	3.023
GgaAffx.22897.1.S1_at	RGS6	NM_001199452	regulator of G-protein signaling 6	3.008
Gga.738.1.S1_at	GSC	NM_205331	goosecoid homeobox	2.955
Gga.18653.1.S1_at	FAM179A	NM_001277797	family with sequence similarity 179, member A	2.947
GgaAffx.22016.1.S1_at	BRSK2	NM_001199596	BR serine/threonine kinase 2	2.926
GgaAffx.20670.1.S1_at	RNF150	XM_003641153	ring finger protein 150	2.921
Gga.9647.1.S1_at	DPYS	NM_001277426	dihydropyrimidinase	2.913
GgaAffx.7323.1.S1_at	PARK2	XM_419615	parkinson protein 2, E3 ubiquitin protein ligase (parkin)	2.904
Gga.12772.1.S1_s_at	PDCL2	XM_420702	phosducin-like 2	2.9
Gga.13959.1.S1_at	ZNF385B	XM_421977	zinc finger protein 385B	2.889
Gga.1821.1.S1_at	ASMT	NM_205343	acetylserotonin O-methyltransferase	2.886
Gga.729.1.S1_at	AVD	NM_205320	avidin	2.883
Gga.8917.1.S1_at	MEP1A	NM_001277721	meprin A, alpha (PABA peptide hydrolase)	2.883

Table 4.2. (con't) Edited list of 237 DEG with lesser abundance in FF at 16 weeks. 3 of 7

Probe Set ID	Gene Symbol	Transcript ID	Gene Title	Fold change
Gga.11798.1.S1_s_at	NOX4	NM_001101829	NADPH oxidase 4	2.877
GgaAffx.5095.1.S1_at	SATB2	NM_001199110	SATB homeobox 2	2.869
Gga.16205.1.S1_at	B-G	NM_001030670	MHC B-G antigen	2.862
GgaAffx.9053.2.S1_s_at	NSUN7	XM_420736	NOP2/Sun domain family, member 7	2.86
Gga.10569.1.S1_at	MXI1	NM_001012911	MAX interactor 1	2.847
GgaAffx.20085.1.S1_s_at	SOX5	NM_001004385	SRY (sex determining region Y)-box 5	2.843
Gga.11052.1.S1_at	SORBS2	XM_420674	sorbin and SH3 domain containing 2	2.84
Gga.2896.1.S1_at	CBR1	NM_001030795	carbonyl reductase 1	2.832
Gga.12129.1.S1_at	SLC25A21	XM_001233199	solute carrier family 25 (mitochondrial oxoadipate carrier), member 21	2.829
Gga.19488.1.S1_at	TPH2	NM_001001301	tryptophan hydroxylase 2	2.782
Gga.6921.1.S1_a_at	CDO1	XM_424964	cysteine dioxygenase, type I	2.775
Gga.18352.1.S1_at	HOXB1	NM_001080859	homeobox B1	2.771
Gga.10828.1.S1_at	SMYD3	XM_419536	SET and MYND domain containing 3	2.759
GgaAffx.10689.2.S1_s_at	SUPT3H	NM_001031102	suppressor of Ty 3 homolog (S. cerevisiae)	2.758
Gga.12522.1.S1_a_at	FHIT	NM_001277802	fragile histidine triad	2.753
GgaAffx.23310.1.S1_at	GLIS1	XM_422485	GLIS family zinc finger 1	2.747
Gga.23.1.S1_s_at	EPHA6	XM_416644	EPH receptor A6	2.728
Gga.10531.1.S1_at	TEAD1	NM_001199405	TEA domain family member 1 (SV40 transcriptional enhancer factor)	2.728
Gga.1546.1.S1_at	PRRX1	NM_001007821	paired related homeobox 1	2.727
GgaAffx.5596.4.S1_s_at	ABCB1LA	XM_418636	ATP-binding cassette, sub-family B (MDR/TAP), member 1-like A	2.726
GgaAffx.1062.1.S1_at	CAMKK1	XM_001234324	calcium/calmodulin-dependent protein kinase kinase 1, alpha	2.722
GgaAffx.4551.1.S1_at	GABRA3	XM_420268	gamma-aminobutyric acid (GABA) A receptor, alpha 3	2.708
Gga.14368.1.S1_at	GNAZ	XM_001232444	guanine nucleotide binding protein (G protein), alpha z polypeptide	2.694
Gga.11325.1.S1_at	GCM1	NM_206980	glial cells missing homolog 1 (Drosophila)	2.674
Gga.14911.1.S1_at	OXTR	NM_001031569	oxytocin receptor	2.646
GgaAffx.2955.1.S1_at	KCNB1	XM_425704	potassium voltage-gated channel, Shab-related subfamily, member 1	2.643
GgaAffx.4203.1.S1_s_at	XYLT1	XM_414904	xylosyltransferase I	2.643
Gga.19935.1.S1_s_at	ARSJ	XM_420639	arylsulfatase family, member J	2.622
Gga.16926.1.S1_at	OFCC1	XM_418951	orofacial cleft 1 candidate 1	2.621
GgaAffx.3394.1.S1_at	CACNA2D3	XM_414338	calcium channel, voltage-dependent, alpha 2/delta subunit 3	2.61
GgaAffx.9855.1.S1_at	CD80	NM_001079739	CD80 molecule	2.61
Gga.967.1.S1_at	CDX2	NM_204311	caudal type homeobox 2	2.6
Gga.10018.1.S1_at	RIN3	XM_421327	Ras and Rab interactor 3	2.596
Gga.10595.2.S1_at	REEP1	XM_001235010	receptor accessory protein 1	2.591
Gga.352.1.S1_at	RGS20	NM_204842	regulator of G-protein signaling 20	2.588

Table 4.2. (con't) Edited list of 237 DEG with lesser abundance in FF at 16 weeks. 4 of 7

Probe Set ID	Gene Symbol	Transcript ID	Gene Title	Fold change
GgaAffx.10481.1.S1_at	TPO	XM_001235672	thyroid peroxidase	2.576
Gga.10867.1.S1_at	ACTBL2	XM_422898	actin, beta-like 2	2.575
GgaAffx.9996.1.S1_s_at	SUSD1	XM_424913	sushi domain containing 1	2.55
Gga.3461.1.S1_at	LRP8	NM_205186	low density lipoprotein receptor-related protein 8, apolipoprotein e receptor	2.549
Gga.7476.1.S1_at	TMEM108	XM_418792	transmembrane protein 108	2.549
GgaAffx.23346.2.S1_s_at	HDAC9	NM_001030981	histone deacetylase 9	2.535
Gga.18770.1.S1_at	NEIL3	XM_426306	nei endonuclease VIII-like 3 (E. coli)	2.534
GgaAffx.6199.1.S1_at	DIEXF	NM_001031051	digestive organ expansion factor homolog (zebrafish)	2.531
Gga.9289.1.S1_at	TFAP2B	NM_204895	transcription factor AP-2 beta (activating enhancer binding protein 2 beta)	2.527
Gga.3781.1.S1_at	ACE	NM_001167732	angiotensin I converting enzyme (peptidyl-dipeptidase A) 1	2.519
GgaAffx.4104.1.S1_at	CLDN18	XM_0036417301	claudin 18	2.496
Gga.10566.1.S1_at	CHRM5	NM_001031550	cholinergic receptor, muscarinic 5	2.488
GgaAffx.22707.1.S1_at	LPHN2	NM_001190477	latrophilin 2	2.487
GgaAffx.4776.1.S1_s_at	MYO3A	XM_418597	myosin IIIA	2.482
GgaAffx.2166.2.S1_s_at	ZMAT4	XM_424398	zinc finger, matrin-type 4	2.479
Gga.14433.1.S2_at	IL12B	NM_213571	interleukin 12B (natural killer cell stimulatory factor 2, cytotoxic lymphocyte maturation factor 2, p40)	2.475
Gga.1714.1.S1_at	A2M, A2ML3	XM_00364314	alpha-2-macroglobulin, alpha-2-macroglobulin-like 3, alpha-2-macroglobulin-like	2.463
GgaAffx.6280.1.S1_at	AKAP6	XM_003641359	A kinase (PRKA) anchor protein 6	2.46
Gga.2006.1.S1_at	CD109	XM_419879	CD109 molecule	2.451
Gga.12716.1.S1_at	MGMT	XM_421823	O-6-methylguanine-DNA methyltransferase	2.449
GgaAffx.4283.1.S1_at	EFCAB4B	XM_001234653	EF-hand calcium binding domain 4B, ras-related protein Rab-44-like	2.441
Gga.18576.1.S1_at	SPTLC3	XM_001231525	serine palmitoyltransferase, long chain base subunit 3	2.438
GgaAffx.21842.2.S1_s_at	GAL6	NM_001001193	Gal 6	2.431
Gga.1363.1.S1_at	CD38	NM_001201388	CD38 molecule	2.422
GgaAffx.7969.2.S1_s_at	LARGE	NM_001004383	like-glycosyltransferase	2.422
Gga.5755.1.S1_at	TSPAN4	XM_421038	tetraspanin 4	2.422
Gga.18126.1.S1_at	HDGFRP3	XM_413841	hepatoma-derived growth factor, related protein 3	2.421
GgaAffx.1237.1.S1_at	GRID1	XM_426488	glutamate receptor, ionotropic, delta 1	2.42
Gga.13448.1.S1_at	OSTN	NM_001098608	osteocrin	2.42
GgaAffx.7793.4.S1_s_at	GRM1	XM_419652	glutamate receptor, metabotropic 1	2.418
Gga.4046.1.S1_at	MEIS2	NM_204803	Meis homeobox 2	2.416
GgaAffx.8254.1.S1_at	CACNA1C	ENSGALT00000021261	calcium channel, voltage-dependent, L type, alpha 1C subunit	2.41
Gga.5419.1.S1_at	CLDN11	XM_422797	claudin 11	2.403
Gga.5620.2.S1_a_at	PACRG	XM_419614	PARK2 co-regulated	2.397
GgaAffx.6869.1.S1_at	MACC1	XM_418705	metastasis associated in colon cancer 1	2.396

Table 4.2. (con't) Edited list of 237 DEG with lesser abundance in FF at 16 weeks. 5 of 7

Probe Set ID	Gene Symbol	Transcript ID	Gene Title	Fold change
GgaAffx.2551.1.S1_at	TRPM8	NM_001007082	transient receptor potential cation channel, subfamily M, member 8	2.395
GgaAffx.6552.2.S1_s_at	ESRRB	XM_001235146	estrogen-related receptor beta	2.387
GgaAffx.7275.2.S1_s_at	RPS6KA2	XM_419611	ribosomal protein S6 kinase, 90kDa, polypeptide 2	2.381
Gga.190.1.S1_at	GBX1	NM_204659	gastrulation brain homeobox 1	2.373
GgaAffx.4960.3.S1_at	IQCH	XM_413925	IQ motif containing H	2.366
Gga.19493.2.S1_s_at	ST8SIA2	NM_001001604	ST8 alpha-N-acetyl-neuraminide alpha-2,8-sialyltransferase 2	2.355
Gga.15188.1.S1_at	CNTN4	XM_414435	contactin 4	2.349
Gga.18109.1.S1_at	CNOT2	NM_001012808	CCR4-NOT transcription complex, subunit 2	2.346
Gga.12773.1.S1_at	SYNDIG1	XM_415014	synapse differentiation inducing 1	2.338
GgaAffx.9020.1.S1_at	KCTD8	XM_001233939	potassium channel tetramerisation domain containing 8	2.331
Gga.16665.1.S1_at	EEPD1	NM_205190	ret proto-oncogene	2.324
Gga.19162.1.S1_at	RET	XM_418838	endonuclease/exonuclease/phosphatase family domain containing 1	2.324
Gga.3667.1.S1_at	PDLIM4	NM_204839	PDZ and LIM domain 4	2.315
Gga.540.1.S1_at	MGP	NM_205044	matrix Gla protein	2.313
Gga.17997.1.S1_s_at	SPATA13	XM_417134	spermatogenesis associated 13	2.307
Gga.2645.1.S1_at	TGFBR2	NM_205428	transforming growth factor, beta receptor II (70/80kDa)	2.302
GgaAffx.9678.1.S1_s_at	DTNA	XM_419187	dystrobrevin, alpha	2.297
GgaAffx.7583.1.S1_at	MYRIP	XM_426015	myosin VIIA and Rab interacting protein	2.291
Gga.3178.1.S1_at	DACH2	NM_204795	dachshund homolog 2 (Drosophila)	2.284
GgaAffx.4980.1.S1_at	LRRC4C	XM_426419	leucine rich repeat containing 4C	2.283
GgaAffx.26351.2.S1_s_at	SLC24A5	NM_001038497	solute carrier family 24, member 5	2.278
Gga.539.1.S1_at	CD247	NM_206879	CD247 molecule	2.276
Gga.488.1.S1_at	ASCL1	NM_204412	achaete-scute complex homolog 1 (Drosophila)	2.274
GgaAffx.3186.1.S1_at	DRD4	NM_001142849	dopamine receptor D4	2.269
GgaAffx.15.1.S1_at	CUZD1	ENSGALT00000038694	CUB and zona pellucida-like domains 1	2.262
Gga.169.1.S1_at	DCX	NM_204335	doublecortin	2.248
Gga.11270.1.S1_at	GPR160	NM_001277472	G protein-coupled receptor 160	2.245
Gga.19869.1.S1_at	OXSR1	XM_418527	oxidative-stress responsive 1	2.242
GgaAffx.8186.2.S1_s_at	BICD1	XM_425492	bicaudal D homolog 1 (Drosophila)	2.233
Gga.651.1.S1_at	EFNA5	NM_205184	ephrin-A5	2.227
Gga.588.1.S1_at	GFRA1	NM_205102	GDNF family receptor alpha 1	2.225
Gga.16538.1.S1_at	AP2B1	XM_415772	adaptor-related protein complex 2, beta 1 subunit	2.224
GgaAffx.24064.1.S1_at	FBXL7	XM_426048	F-box and leucine-rich repeat protein 7	2.222
Gga.6437.1.S1_at	IL12A	NM_213588	interleukin 12A (natural killer cell stimulatory factor 1, cytotoxic lymphocyte maturation factor 1, p35)	2.217
GgaAffx.5903.1.S1_at	RAPGEF4	XM_426579	Rap guanine nucleotide exchange factor (GEF) 4	2.217

Table 4.2. (con't) Edited list of 237 DEG with lesser abundance in FF at 16 weeks. 6 of 7

Probe Set ID	Gene Symbol	Transcript ID	Gene Title	Fold change
GgaAffx.8988.1.S1_s_at	SCUBE1	XM_416453	signal peptide, CUB domain, EGF-like 1	2.211
Gga.7769.1.S1_at	FGD5	XM_414463	FYVE, RhoGEF and PH domain containing 5	2.207
GgaAffx.10623.1.S1_at	ARHGAP6	XM_416840	Rho GTPase activating protein 6	2.204
Gga.10.1.S1_at	OTX2	NM_204520	orthodenticle homeobox 2	2.204
Gga.316.1.S1_at	NHLH2	NM_204797	nescient helix loop helix 2	2.202
Gga.351.2.S1_s_at	RGS7	NM_001198598	regulator of G-protein signalling 7, regulator of G-protein signaling 7	2.188
GgaAffx.24657.1.S1_at	ZPLD1	XM_001232730	zona pellucida-like domain containing 1	2.187
Gga.18181.1.S1_at	SUFU	NM_204264	suppressor of fused homolog (Drosophila)	2.182
Gga.7877.1.S1_at	PIGL	XM_415845	phosphatidylinositol glycan anchor biosynthesis, class L	2.177
GgaAffx.23330.1.S1_at	PPAP2B	NM_001130488	phosphatidic acid phosphatase type 2B	2.172
GgaAffx.21536.1.S1_at	INPP4B	XM_420420	inositol polyphosphate-4-phosphatase, type II, 105kDa	2.168
GgaAffx.2958.1.S1_at	SCG3	XM_413807	secretogranin III	2.167
Gga.6203.1.S1_at	BTBD11	XM_001234770	BTB (POZ) domain containing 11	2.157
Gga.4134.1.S2_at	CHRNA1	NM_204816	cholinergic receptor, nicotinic, alpha 1 (muscle)	2.156
GgaAffx.1020.1.S1_s_at	C5	XM_415405	complement component 5	2.153
GgaAffx.20776.1.S1_at	AKT3	XM_419544	v-akt murine thymoma viral oncogene homolog 3 (protein kinase B, gamma)	2.15
GgaAffx.24188.1.S1_at	B3GNTL1	XM_415599	UDP-GlcNAc:betaGal beta-1,3-N-acetylglucosaminyltransferase-like 1	2.139
Gga.5148.1.S1_at	TNFRSF1B	NM_204439	tumor necrosis factor receptor superfamily, member 1B	2.136
GgaAffx.1950.1.S1_at	CBFA2T2	NM_001011689	core-binding factor, runt domain, alpha subunit 2; translocated to, 2	2.126
Gga.2839.1.S1_at	COL2A1	NM_204426	collagen, type II, alpha 1	2.124
GgaAffx.4564.1.S1_at	DSCAML1	XM_003642612	Down syndrome cell adhesion molecule like 1	2.124
Gga.2584.1.S1_s_at	CPNE2	NM_001012773	copine II	2.12
GgaAffx.26497.2.S1_s_at	ERC2	XM_001232639	ELKS/RAB6-interacting/CAST family member 2	2.12
Gga.2533.1.S1_s_at	GSTA3	NM_001001777	glutathione S-transferase alpha 3	2.119
Gga.10214.1.S1_s_at	MAPK12	XM_001233061	mitogen-activated protein kinase 12	2.114
Gga.14109.1.S1_s_at	TMEM132D	XM_415097	transmembrane protein 132D	2.113
Gga.3238.2.S1_a_at	NEGR1	NM_204856	neuronal growth regulator 1	2.11
GgaAffx.9195.1.S1_at	FAM184B	XM_003641223	family with sequence similarity 184, member B	2.107
GgaAffx.21143.1.S1_s_at	GPR89B	NM_001030791	G protein-coupled receptor 89B	2.105
Gga.265.1.S1_at	MARCO	NM_204736	macrophage receptor with collagenous structure	2.098
Gga.15901.1.S1_at	NME7	XM_003640457	NME/NM23 family member 7	2.094
GgaAffx.12680.1.S1_at	NDUFS1	NM_001006518	NADH dehydrogenase (ubiquinone) Fe-S protein 1, 75kDa (NADH-coenzyme Q reductase)	2.086
GgaAffx.9380.1.S1_at	LAMA2	XM_419746	laminin, alpha 2	2.083
Gga.15912.1.S1_at	CLUAP1	NM_001277591	clusterin associated protein 1	2.078
GgaAffx.10717.1.S1_at	GABRA5	XM_416880	gamma-aminobutyric acid (GABA) A receptor, alpha 5	2.075

Table 4.2. (con't) Edited list of 237 DEG with lesser abundance in FF at 16 weeks. 7 of 7

Probe Set ID	Gene Symbol	Transcript ID	Gene Title	Fold change
GgaAffx.9882.2.S1_s_at	ROBO2	XM_416674	roundabout, axon guidance receptor, homolog 2 (Drosophila)	2.073
GgaAffx.3027.1.S1_at	SLC6A11	XM_414302	solute carrier family 6 (neurotransmitter transporter, GABA), member 11	2.072
Gga.256.1.S2_at	TPD52L1	NM_204215	tumor protein D52-like 1	2.071
GgaAffx.2745.1.S1_at	LUZP2	NM_001199521	leucine zipper protein 2	2.066
GgaAffx.8709.1.S1_at	ZNF407	XM_419097	zinc finger protein 407	2.061
GgaAffx.6820.1.S1_at	AGMO	XM_001235520	alkylglycerol monooxygenase	2.06
Gga.5751.1.S1_at	ANKRD1	NM_204405	ankyrin repeat domain 1 (cardiac muscle)	2.058
GgaAffx.8825.1.S1_at	MATN2	XM_424219	matrilin 2	2.057
Gga.13499.1.S1_at	ZPBP	NM_001030380	zona pellucida binding protein	2.057
Gga.6096.1.S1_at	EPB41L5	XM_422083	erythrocyte membrane protein band 4.1 like 5	2.05
Gga.276.1.S1_at	EBF1	NM_204752	early B-cell factor 1	2.048
Gga.3035.1.S1_at	EPAS1	NM_204807	endothelial PAS domain protein 1	2.045
Gga.695.1.S1_at	HOXD12	NM_205249	homeobox D12	2.043
Gga.2408.1.S1_at	BCAT1	XM_416424	branched chain amino-acid transaminase 1, cytosolic	2.041
GgaAffx.11898.1.S1_at	FBXO22	NM_001030545	F-box protein 22	2.032
GgaAffx.5951.1.S1_s_at	MECOM	XM_422804	MDS1 and EVI1 complex locus	2.028
GgaAffx.9214.1.S1_at	CTNND2	XM_003640780	catenin (cadherin-associated protein), delta 2 (neural plakophilin-related arm-repeat protein)	2.027
GgaAffx.6654.1.S1_at	NRXN3	NM_001271923	neurexin 3	2.024
Gga.10988.1.S1_a_at	EFCAB1	XM_418657	EF-hand calcium binding domain 1	2.019
Gga.1166.1.S1_at	SERPIND1	XM_001232766	serpin peptidase inhibitor, clade D (heparin cofactor), member 1	2.018
Gga.10094.1.S1_s_at	NLGN1	NM_001081502	neuroligin 1	2.016
Gga.4868.1.S1_a_at	PNLIP	NM_001277382	pancreatic lipase	2.016
GgaAffx.21817.1.S1_s_at	CDH13	NM_001001760	cadherin 13, H-cadherin (heart)	2.015
Gga.6177.1.S1_at	SIL1	XM_414514	SIL1 homolog, endoplasmic reticulum chaperone (S. cerevisiae)	2.013
GgaAffx.5735.1.S1_at	NAALADL2	XM_426711	N-acetylated alpha-linked acidic dipeptidase-like 2	2.012
Gga.3474.1.S1_at	FANCA	NM_001134359	Fanconi anemia, complementation group A	2.01
Gga.4798.1.S1_s_at	GPM6A	NM_001012579	glycoprotein M6A	2.01
Gga.7230.1.S1_at	MGARP	XM_001234187	mitochondria-localized glutamic acid-rich protein	2.001
GgaAffx.1144.1.S1_at	MGAT5B	XM_003642334	mannosyl (alpha-1,6-)-glycoprotein beta-1,6-N-acetyl-glucosaminyltransferase, isozyme B	2.001